



TOXICOLOGICAL REVIEW OF FORMALDEHYDE INHALATION TOXICITY

(CAS No. 50-00-0)

**In Support of Summary Information on the
Integrated Risk Information System (IRIS)**

VOLUME IV of IV

Appendices

March 17, 2010

NOTICE

This document is an *Inter-Agency Science Consultation draft*. This information is distributed solely for the purpose of pre-dissemination peer review under applicable information quality guidelines. It has not been formally disseminated by EPA. It does not represent and should not be construed to represent any Agency determination or policy. It is being circulated for review of its technical accuracy and science policy implications.

U.S. Environmental Protection Agency
Washington, DC

DISCLAIMER

This document is a preliminary draft for review purposes only. This information is distributed solely for the purpose of pre-dissemination peer review under applicable information quality guidelines. It has not been formally disseminated by EPA. It does not represent and should not be construed to represent any Agency determination or policy. Mention of trade names or commercial products does not constitute endorsement or recommendation for use.

This document is a draft for review purposes only and does not constitute Agency policy.

IV-ii **DRAFT—DO NOT CITE OR QUOTE**

**CONTENTS—TOXICOLOGICAL REVIEW OF FORMALDEHYDE
(CAS No. 50-00-0)**

LIST OF TABLES	xi
LIST OF FIGURES	xx
LIST OF ABBREVIATIONS AND ACRONYMS.....	xxv
FOREWORD	xxxii
AUTHORS, CONTRIBUTORS, AND REVIEWERS.....	xxxiii

VOLUME I

1. INTRODUCTION	1-1
2. BACKGROUND	2-1
2.1. PHYSICOCHEMICAL PROPERTIES OF FORMALDEHYDE.....	2-1
2.2. PRODUCTION, USES, AND SOURCES OF FORMALDEHYDE	2-1
2.3. ENVIRONMENTAL LEVELS AND HUMAN EXPOSURE.....	2-4
2.3.1. Inhalation.....	2-5
2.3.2. Ingestion	2-10
2.3.3. Dermal Contact.....	2-11
3. TOXICOKINETICS	3-1
3.1. CHEMICAL PROPERTIES AND REACTIVITY	3-1
3.1.1. Binding of Formaldehyde to Proteins	3-1
3.1.2. Endogenous Sources of Formaldehyde	3-3
3.1.2.1. Normal Cellular Metabolism (Enzymatic)	3-3
3.1.2.2. Normal Metabolism (Non-Enzymatic).....	3-5
3.1.2.3. Exogenous Sources of Formaldehyde Production.....	3-5
3.1.2.4. FA-GSH Conjugate as a Method of Systemic Distribution	3-6
3.1.2.5. Metabolic Products of FA Metabolism (e.g., Formic Acid).....	3-6
3.1.2.6. Levels of Endogenous Formaldehyde in Animal and Human Tissues	3-6
3.2. ABSORPTION	3-9
3.2.1. Oral	3-9
3.2.2. Dermal	3-9
3.2.3. Inhalation.....	3-9
3.2.3.1. Formaldehyde Uptake Can be Affected by Effects at the Portal of Entry	3-10
3.2.3.2. Variability in the Nasal Dosimetry of Formaldehyde in Adults and Children.....	3-12
3.3. DISTRIBUTION	3-13
3.3.1. Levels in Blood	3-13
3.3.2. Levels in Various Tissues.....	3-15
3.3.2.1. Disposition of Formaldehyde: Differentiating Covalent Binding and Metabolic Incorporation	3-16

This document is a draft for review purposes only and does not constitute Agency policy.

CONTENTS (continued)

3.4. METABOLISM.....	3-20
3.4.1. In Vitro and In Vivo Characterization of Formaldehyde Metabolism	3-20
3.4.2. Formaldehyde Exposure and Perturbation of Metabolic Pathways	3-23
3.4.3. Evidence for Susceptibility in Formaldehyde Metabolism	3-24
3.5. EXCRETION.....	3-25
3.5.1. Formaldehyde Excretion in Rodents	3-26
3.5.2. Formaldehyde Excretion in Exhaled Human Breath.....	3-27
3.5.3. Formaldehyde Excretion in Human Urine	3-31
3.6. MODELING THE TOXICOKINETICS OF FORMALDEHYDE AND DPX	3-32
3.6.1. Motivation	3-32
3.6.2. Species Differences in Anatomy: Consequences for Gas Transport and Risk.....	3-34
3.6.3. Modeling Formaldehyde Uptake in Nasal Passages	3-40
3.6.3.1. Flux Bins	3-41
3.6.3.2. Flux Estimates	3-41
3.6.3.3. Mass Balance Errors.....	3-42
3.6.4. Modeling Formaldehyde Uptake in the Lower Respiratory Tract	3-42
3.6.5. Uncertainties in Formaldehyde Dosimetry Modeling	3-44
3.6.5.1. Verification of Predicted Flow Profiles.....	3-44
3.6.5.2. Level of Confidence in Formaldehyde Uptake Simulations	3-45
3.6.6. PBPK Modeling of DNA Protein Cross-Links (DPXs) Formed by Formaldehyde.....	3-48
3.6.6.1. PBPK Models for DPXs.....	3-48
3.6.6.2. A PBPK Model for DPXs in the F344 Rat and Rhesus Monkey that uses Local Tissue Dose of Formaldehyde.....	3-50
3.6.6.3. Uncertainties in Modeling the Rat and Rhesus DPX Data.....	3-51
3.6.7. Uncertainty in Prediction of Human DPX Concentrations	3-53

VOLUME II

4. HAZARD CHARACTERIZATION.....	4-1
4.1. HUMAN STUDIES.....	4-1
4.1.1. Noncancer Health Effects.....	4-1
4.1.1.1. Sensory Irritation (Eye, Nose, Throat Irritation).....	4-1
4.1.1.2. Pulmonary Function	4-11
4.1.1.3. Asthma.....	4-19
4.1.1.4. Respiratory Tract Pathology.....	4-26
4.1.1.5. Immunologic Effects	4-30
4.1.1.6. Neurological/Behavioral.....	4-42
4.1.1.7. Developmental and Reproductive Toxicity.....	4-45
4.1.1.8. Oral Exposure Effects on the Gastrointestinal Tract.....	4-56
4.1.1.9. Summary: Noncarcinogenic Hazard in Humans	4-56

This document is a draft for review purposes only and does not constitute Agency policy.

CONTENTS (continued)

4.1.2. Cancer Health Effects..... 4-57
 4.1.2.1. Respiratory Tract Cancer..... 4-57
 4.1.2.2. Non-Respiratory Tract Cancer 4-84
 4.1.2.3. Summary: Carcinogenic Hazard in Humans 4-107
4.2. ANIMAL STUDIES..... 4-109
 4.2.1. Noncancer Health Effects..... 4-110
 4.2.1.1. Reflex Bradypnea 4-110
 4.2.1.2. Respiratory Tract Pathology..... 4-120
 4.2.1.3. Gastrointestinal Tract and Systemic Toxicity 4-201
 4.2.1.4. Immune Function..... 4-216
 4.2.1.5. Hypersensitivity and Atopic Reactions 4-225
 4.2.1.6. Neurological and Neurobehavioral Function 4-250
 4.2.1.7. Reproductive and Developmental Toxicity..... 4-285
 4.2.2. Carcinogenic Potential: Animal Bioassays 4-324
 4.2.2.1. Respiratory Tract..... 4-324
 4.2.2.2. Gastrointestinal Tract 4-326
 4.2.2.3. Lymphohematopoietic Cancer..... 4-328
 4.2.2.4. Summary..... 4-335
4.3. GENOTOXICITY 4-335
 4.3.1. Formaldehyde-DNA Reactions 4-335
 4.3.1.1. DNA-Protein Cross-Links (DPXs)..... 4-336
 4.3.1.2. DNA Adducts 4-341
 4.3.1.3. DNA-DNA Cross-Links (DDXs)..... 4-343
 4.3.1.4. Single Strand Breaks 4-344
 4.3.1.5. Other Genetic Effects of Formaldehyde in Mammalian Cells 4-345
 4.3.2. In Vitro Clastogenicity 4-345
 4.3.3. In Vitro Mutagenicity..... 4-347
 4.3.3.1. Mutagenicity in Bacterial Systems..... 4-347
 4.3.3.2. Mutagenicity in Non-mammalian Cell Systems..... 4-353
 4.3.3.3. Mutagenicity in Mammalian Cell Systems 4-353
 4.3.4. In Vivo Mammalian Genotoxicity 4-360
 4.3.4.1. Genotoxicity in Laboratory Animals..... 4-360
 4.3.4.2. Genotoxicity in Humans..... 4-362
 4.3.5. Summary of Genotoxicity 4-370
4.4. SYNTHESIS AND MAJOR EVALUATION OF NONCARCINOGENIC EFFECTS 4-371
 4.4.1. Sensory Irritation..... 4-376
 4.4.2. Pulmonary Function 4-379
 4.4.3. Hypersensitivity and Atopic Reactions 4-382
 4.4.4. Upper Respiratory Tract Histopathology 4-383
 4.4.5. Toxicogenomic and Molecular Data that May Inform MOAs..... 4-385
 4.4.6. Noncancer Modes of Actions 4-387
 4.4.7. Immunotoxicity 4-389

This document is a draft for review purposes only and does not constitute Agency policy.

CONTENTS (continued)

4.4.8. Effects on the Nervous System	4-390
4.4.8.1. Irritant Threshold Detection	4-390
4.4.8.2. Behavioral Effects	4-391
4.4.8.3. Neurochemistry, Neuropathology, and Mechanistic Studies	4-392
4.4.8.4. Summary.....	4-392
4.4.8.5. Data Gaps	4-393
4.4.9. Reproductive and Developmental Toxicity.....	4-393
4.4.9.1. Spontaneous Abortion and Fetal Death.....	4-393
4.4.9.2. Congenital Malformations.....	4-396
4.4.9.3. Low Birth Weight and Growth Retardation	4-396
4.4.9.4. Functional Development Outcomes (Developmental Neurotoxicity)	4-397
4.4.9.5. Male Reproductive Toxicity.....	4-398
4.4.9.6. Female Reproductive Toxicity	4-399
4.4.9.7. Mode of Action.....	4-400
4.4.9.8. Data Gaps	4-402
4.5. SYNTHESIS AND EVALUATION OF CARCINOGENICITY	4-402
4.5.1. Cancers of the Respiratory Tract.....	4-402
4.5.2. Lymphohematopoietic Malignancies	4-408
4.5.2.1. Background.....	4-408
4.5.2.2. All LHP Malignancies.....	4-410
4.5.2.3. All Leukemia	4-414
4.5.2.4. Subtype Analysis	4-418
4.5.2.5. Myeloid Leukemia.....	4-419
4.5.2.6. Solid Tumors of Lymphoid Origin.....	4-421
4.5.2.7. Supporting Evidence from Animal Bio-Assays for Formaldehyde-Induced Lymphohematopoietic Malignancies	4-423
4.5.3. Carcinogenic Mode(s) of Action.....	4-427
4.5.3.1. Mechanistic Data for Formaldehyde	4-428
4.5.3.2. Mode of Action Evaluation for Upper Respiratory Tract Cancer (Nasopharyngeal Cancer, Sino-Nasal).....	4-439
4.5.3.3. Mode(s) of Action for Lymphohematopoietic Malignancies.....	4-446
4.5.4. Hazard Characterization for Formaldehyde Carcinogenicity	4-453
4.6. SUSCEPTIBLE POPULATIONS	4-454
4.6.1. Life Stages.....	4-454
4.6.1.1. Early Life Stages	4-455
4.6.1.2. Later Life Stages.....	4-459
4.6.1.3. Conclusions on Life-Stage Susceptibility	4-459
4.6.2. Health/Disease Status	4-460
4.6.3. Nutritional Status.....	4-461
4.6.4. Gender Differences.....	4-462
4.6.5. Genetic Differences.....	4-462

This document is a draft for review purposes only and does not constitute Agency policy.

CONTENTS (continued)

4.6.6. Co-Exposures 4-464
 4.6.6.1. Cumulative Risk 4-464
 4.6.6.2. Aggregate Exposure 4-465
4.6.7. Uncertainties of Database..... 4-465
 4.6.7.1. Uncertainties of Exposure 4-465
 4.6.7.2. Uncertainties of Effect..... 4-466
4.6.8. Summary of Potential Susceptibility 4-467

VOLUME III

5. QUANTITATIVE ASSESSMENT: INHALATION EXPOSURE..... 5-1
 5.1. INHALATION REFERENCE CONCENTRATION (RfC) 5-2
 5.1.1. Candidate Critical Effects by Health Effect Category 5-3
 5.1.1.1. Sensory Irritation of the Eyes, Nose, and Throat 5-3
 5.1.1.2. Upper Respiratory Tract Pathology 5-5
 5.1.1.3. Pulmonary Function Effects 5-6
 5.1.1.4. Asthma and Allergic Sensitization (Atopy) 5-10
 5.1.1.5. Immune Function..... 5-16
 5.1.1.6. Neurological and Behavioral Toxicity 5-17
 5.1.1.7. Developmental and Reproductive Toxicity 5-25
 5.1.2. Summary of Critical Effects and Candidate RfCs..... 5-33
 5.1.2.1. Selection of Studies for Candidate RfC Derivation 5-33
 5.1.2.2. Derivation of Candidate RfCs from Key Studies 5-40
 5.1.2.3. Evaluation of the Study-Specific Candidate RfC 5-66
 5.1.3. Database Uncertainties in the RfC Derivation 5-69
 5.1.4. Uncertainties in the RfC Derivation..... 5-72
 5.1.5. Previous Inhalation Assessment..... 5-74
 5.2. QUANTITATIVE CANCER ASSESSMENT BASED ON THE NATIONAL
 CANCER INSTITUTE COHORT STUDY..... 5-74
 5.2.1. Choice of Epidemiology Study 5-75
 5.2.2. Nasopharyngeal Cancer..... 5-76
 5.2.2.1. Exposure-Response Modeling of the National Cancer
 Institute Cohort..... 5-76
 5.2.2.2. Prediction of Lifetime Extra Risk of Nasopharyngeal Cancer
 Mortality 5-79
 5.2.2.3. Prediction of Lifetime Extra Risk of Nasopharyngeal Cancer
 Incidence 5-81
 5.2.2.4. Sources of Uncertainty 5-83
 5.2.3. Lymphohematopoietic Cancer 5-88
 5.2.3.1. Exposure-Response Modeling of the National Cancer
 Institute Cohort..... 5-88

This document is a draft for review purposes only and does not constitute Agency policy.

CONTENTS (continued)

- 5.2.3.2. Prediction of Lifetime Extra Risks for Hodgkin Lymphoma and Leukemia Mortality 5-91
- 5.2.3.3. Prediction of Lifetime Extra Risks for Hodgkin Lymphoma and Leukemia Incidence..... 5-93
- 5.2.3.4. Sources of Uncertainty 5-95
- 5.2.4. Conclusions on Cancer Unit Risk Estimates Based on Human Data..... 5-99
- 5.3. DOSE-RESPONSE MODELING OF RISK OF SQUAMOUS CELL CARCINOMA IN THE RESPIRATORY TRACT USING ANIMAL DATA 5-102
 - 5.3.1. Long-Term Bioassays in Laboratory Animals 5-104
 - 5.3.1.1. Nasal Tumor Incidence Data 5-104
 - 5.3.1.2. Mechanistic Data 5-105
 - 5.3.2. The CIIT Biologically Based Dose-Response Modeling 5-106
 - 5.3.2.1. Major Results of the CIIT Modeling Effort 5-111
 - 5.3.3. This Assessment’s Conclusions from Evaluation of Dose-Response Models of DPX Cell-Replication and Genomics Data, and of BBDR Models for Risk Estimation..... 5-111
 - 5.3.4. Benchmark Dose Approaches to Rat Nasal Tumor Data 5-118
 - 5.3.4.1. Benchmark Dose Derived from BBDR Rat Model and Flux as Dosimeter 5-118
 - 5.3.4.2. Comparison with Other Benchmark Dose Modeling Efforts 5-125
 - 5.3.4.3. Kaplan-Meier Adjustment 5-128
 - 5.3.4.4. EPA Time-to-Tumor Statistical Modeling 5-129
- 5.4. CONCLUSIONS FROM THE QUANTITATIVE ASSESSMENT OF CANCER RISK FROM FORMALDEHYDE EXPOSURE BY INHALATION .. 5-133
 - 5.4.1. Inhalation Unit Risk Estimates Based on Human Data..... 5-133
 - 5.4.2. Inhalation Unit Risk Estimates Based on Rodent Data..... 5-133
 - 5.4.3. Summary of Inhalation Unit Risk Estimates 5-135
 - 5.4.4. Application of Age-Dependent Adjustment Factors (ADAFs)..... 5-136
 - 5.4.5. Conclusions: Cancer Inhalation Unit Risk Estimates 5-137
- 6. MAJOR CONCLUSIONS IN THE CHARACTERIZATION OF HAZARD AND DOSE-RESPONSE..... 6-1
 - 6.1. SUMMARY OF HUMAN HAZARD POTENTIAL 6-1
 - 6.1.1. Exposure 6-1
 - 6.1.2. Absorption, Distribution, Metabolism, and Excretion 6-1
 - 6.1.3. Noncancer Health Effects in Humans and Laboratory Animals 6-4
 - 6.1.3.1. Sensory Irritation 6-4
 - 6.1.3.2. Respiratory Tract Pathology 6-5
 - 6.1.3.3. Effects on Pulmonary Function 6-8
 - 6.1.3.4. Asthmatic Responses and Increased Atopic Symptoms 6-9
 - 6.1.3.5. Effects on the Immune System 6-10
 - 6.1.3.6. Neurological Effects 6-11
 - 6.1.3.7. Reproductive and Developmental Effects 6-12

This document is a draft for review purposes only and does not constitute Agency policy.

CONTENTS (continued)

6.1.3.8. Effects on General Systemic Toxicity 6-13
6.1.3.9. Summary..... 6-14
6.1.4. Carcinogenicity in Human and Laboratory Animals 6-14
6.1.4.1. Carcinogenicity in Humans 6-14
6.1.4.2. Carcinogenicity in Laboratory Animals 6-20
6.1.4.3. Carcinogenic Mode(s) of Action 6-21
6.1.5. Cancer Hazard Characterization..... 6-24
6.2. DOSE-RESPONSE CHARACTERIZATION 6-25
6.2.1. Noncancer Toxicity: Reference Concentration (RfC)..... 6-25
6.2.1.1. Assessment Approach Employed 6-25
6.2.1.2. Derivation of Candidate Reference Concentrations 6-25
6.2.1.3. Adequacy of Overall Data Base for RfC Derivation..... 6-26
6.2.1.4. Uncertainties in the Reference Concentration (RfC) 6-29
6.2.1.5. Conclusions 6-32
6.2.2. Cancer Risk Estimates..... 6-32
6.2.2.1. Choice of Data 6-32
6.2.2.2. Analysis of Epidemiologic Data..... 6-33
6.2.2.3. Analysis of Laboratory Animal Data 6-36
6.2.2.4. Extrapolation Approaches 6-37
6.2.2.5. Inhalation Unit Risk Estimates for Cancer 6-41
6.2.2.6. Early-Life Susceptibility 6-41
6.2.2.7. Uncertainties in the Quantitative Risk Estimates 6-42
6.2.2.8. Conclusions 6-45
6.3. SUMMARY AND CONCLUSIONS 6-45
REFERENCESR-1

VOLUME IV

APPENDIX A: SUMMARY OF EXTERNAL PEER REVIEW AND PUBLIC
COMMENTS AND DISPOSITIONS A-1
APPENDIX B: SIMULATIONS OF INTERINDIVIDUAL AND ADULT-TO-CHILD
VARIABILITY IN REACTIVE GAS UPTAKE IN A SMALL SAMPLE
OF PEOPLE (Garcia et al., 2009).....B-1
APPENDIX C: LIFETABLE ANALYSISC-1
APPENDIX D: MODEL STRUCTURE & CALIBRATION IN CONOLLY ET AL.
(2003, 2004)..... D-1
APPENDIX E: EVALUATION OF BBDR MODELING OF NASAL CANCER IN THE
F344 RAT: CONOLLY ET AL. (2003) AND ALTERNATIVE
IMPLEMENTATIONS.....E-1
APPENDIX F: SENSITIVITY ANALYSIS OF BBDR MODEL FOR FORMALDEHYDE
INDUCED RESPIRATORY CANCER IN HUMANS..... F-1

This document is a draft for review purposes only and does not constitute Agency policy.

CONTENTS (continued)

- APPENDIX G: EVALUATION OF THE CANCER DOSE-RESPONSE MODELING
OF GENOMIC DATA FOR FORMALDEHYDE RISK ASSESSMENT G-1
- APPENDIX H: EXPERT PANEL CONSULTATION ON QUANTITATIVE
EVALUATION OF ANIMAL TOXICOLOGY DATA FOR
ANALYZING CANCER RISK DUE TO INHALED FORMALDEHYDE .. H-1

This document is a draft for review purposes only and does not constitute Agency policy.

IV-x DRAFT—DO NOT CITE OR QUOTE

LIST OF TABLES

Table 2-1. Physicochemical properties of formaldehyde	2-2
Table 2-2. Ambient air levels by land use category	2-6
Table 2-3. Studies on residential indoor air levels of formaldehyde (non-occupational)	2-8
Table 3-1. Endogenous formaldehyde levels in animal and human tissues and body fluids	3-8
Table 3-2. Formaldehyde kinetics in human and rat tissue samples	3-21
Table 3-3. Allelic frequencies of ADH3 in human populations	3-25
Table 3-4. Percent distribution of airborne [¹⁴ C]-formaldehyde in F344 rats	3-26
Table 3-5. Apparent formaldehyde levels in exhaled breath of individuals attending a health fair, adjusted for methanol and ethanol levels which contribute to the detection of the protonated species with a mass to charge ratio of 31 reported as formaldehyde (<i>m/z</i> = 31).....	3-29
Table 3-6. Measurements of exhaled formaldehyde concentrations in the mouth and nose, and in the oral cavity after breath holding in three healthy male laboratory workers	3-30
Table 3-7. Extrapolation of parameters for enzymatic metabolism to the human.....	3-53
Table 4-1. Cohort and case-control studies of formaldehyde cancer and NPC.....	4-59
Table 4-2. Case-control studies of formaldehyde and nasal and paranasal cancer.....	4-71
Table 4-3. Epidemiologic studies of formaldehyde and pharyngeal cancer (includes nasopharyngeal cancer)	4-78
Table 4-4. Epidemiologic studies of formaldehyde and lymphohematopoietic cancers	4-98
Table 4-5. Respiratory effects of formaldehyde-induced reflex bradypnea in various strains of mice	4-112
Table 4-6. Respiratory effects of formaldehyde-induced reflex bradypnea in various strains of rats	4-113
Table 4-7. Inhaled dose of formaldehyde to nasal mucosa of F344 rats and B6C3F1 mice exposed to 15 ppm.....	4-116

This document is a draft for review purposes only and does not constitute Agency policy.

LIST OF TABLES (continued)

Table 4-8. Exposure regimen for cross-tolerance study 4-117

Table 4-9. Summary of formaldehyde effects on mucociliary function in the upper respiratory tract 4-127

Table 4-10. Concentration regimens for ultrastructural evaluation of male CDF rat nasoturbinates 4-129

Table 4-11. Enzymatic activities in nasal respiratory epithelium of male Wistar rats exposed to formaldehyde, ozone, or both..... 4-130

Table 4-12. Lipid analysis of lung tissue and lung gavage from male F344 rats exposed to 0, 15, or 145.6 ppm formaldehyde for 6 hours..... 4-138

Table 4-13. Formaldehyde effects on biochemical parameters in nasal mucosa and lung tissue homogenates from male F344 rats exposed to 0, 15, or 145.6 ppm formaldehyde for 6 hours 4-139

Table 4-14. Mast cell degranulation and neutrophil infiltration in the lung of rats exposed to formaldehyde via inhalation..... 4-140

Table 4-15. Summary of respiratory tract pathology from inhalation exposures to formaldehyde—short term studies 4-143

Table 4-16. Location and incidence of respiratory tract lesions in B6C3F1 mice exposed to formaldehyde..... 4-146

Table 4-17. Formaldehyde effects (incidence and severity) on histopathologic changes in the noses and larynxes of male and female albino SPF Wistar rats exposed to formaldehyde 6 hours/day for 13 weeks 4-148

Table 4-18. Formaldehyde-induced nonneoplastic histopathologic changes in male albino SPF Wistar rats exposed to 0, 10, or 20 ppm formaldehyde and examined at the end of 130 weeks inclusive of exposure..... 4-149

Table 4-19. Formaldehyde-induced nasal tumors in male albino SPF Wistar rats exposed to formaldehyde (6 hours/day, 5 days/week for 13 weeks) and examined at the end of 130 weeks inclusive of exposure 4-150

Table 4-20. Formaldehyde effects on nasal epithelium for various concentration-by-time products in male albino Wistar rats 4-153

This document is a draft for review purposes only and does not constitute Agency policy.

LIST OF TABLES (continued)

Table 4-21. Rhinitis observed in formaldehyde-treated animals; data pooled for male and female animals 4-154

Table 4-22. Epithelial lesions found in the middle region of nasoturbinates of formaldehyde-treated and control animals; data pooled for males and females..... 4-155

Table 4-23. Cellular and molecular changes in nasal tissues of F344 rats exposed to formaldehyde..... 4-156

Table 4-24. Percent body weight gain and concentrations of iron, zinc, and copper in cerebral cortex of male Wistar rats exposed to formaldehyde via inhalation for 4 and 13 weeks..... 4-158

Table 4-25. Zinc, copper, and iron content of lung tissue from formaldehyde-treated male Wistar rats..... 4-158

Table 4-26. Total lung cytochrome P450 measurements of control and formaldehyde-treated male Sprague-Dawley rats..... 4-159

Table 4-27. Cytochrome P450 levels in formaldehyde-treated rats 4-160

Table 4-28. Summary of respiratory tract pathology from inhalation exposures to formaldehyde, subchronic studies 4-162

Table 4-29. Histopathologic findings and severity scores in the naso- and maxilloturbinates of female Sprague-Dawley rats exposed to inhaled formaldehyde and wood dust for 104 weeks..... 4-166

Table 4-30. Histopathologic changes (including tumors) in nasal cavities of male Sprague-Dawley rats exposed to inhaled formaldehyde or HCl alone and in combination for a lifetime 4-170

Table 4-31. Summary of neoplastic lesions in the nasal cavity of f344 rats exposed to inhaled formaldehyde for 2 years..... 4-173

Table 4-32. Apparent sites of origin for the SCCs in the nasal cavity of F344 rats exposed to 14.3 ppm of formaldehyde gas in the Kerns et al. (1983) bioassay 4-174

Table 4-33. Incidence and location of nasal squamous cell carcinoma in male F344 rats exposed to inhaled formaldehyde for 2 years..... 4-175

Table 4-34. Summary of respiratory tract pathology from chronic inhalation exposures to formaldehyde..... 4-183

This document is a draft for review purposes only and does not constitute Agency policy.

LIST OF TABLES (continued)

Table 4-35. Cell proliferation in nasal mucosa, trachea, and free lung cells isolated from male Wistar rats after inhalation exposures to formaldehyde 4-194

Table 4-36. The effect of repeated formaldehyde inhalation exposures for 3 months on cell count, basal membrane length, proliferation cells, and two measures of cell proliferation, LI and ULLI, in male F344 rats..... 4-196

Table 4-37. Formaldehyde-induced changes in cell proliferation and (ULLI) in the nasal passages of male F344 rats exposed 6 hours/day 4-198

Table 4-38. Cell population and surface area estimates in untreated male F344 rats and regional site location of squamous cell carcinomas in formaldehyde exposed rats for correlation to cell proliferation rates..... 4-199

Table 4-39. Summary of formaldehyde effects on cell proliferation in the upper respiratory tract 4-202

Table 4-40. Summary of lesions observed in the gastrointestinal tracts of Wistar rats after drinking-water exposure to formaldehyde for 4 weeks 4-206

Table 4-41. Incidence of lesions observed in the gastrointestinal tracts of Wistar rats after drinking-water exposure to formaldehyde for 2 years 4-209

Table 4-42. Effect of formaldehyde on gastroduodenal carcinogenesis initiated by MNNG and NaCl in male Wistar rats exposed to formaldehyde (0.5% formalin) in drinking water for 8 weeks..... 4-212

Table 4-43. Summary of benign and malignant gastrointestinal tract neoplasia reported in male and female Sprague-Dawley rats exposed to formaldehyde in drinking water at different ages 4-214

Table 4-44. Incidence of hemolymphoreticular neoplasia reported in male and female Sprague-Dawley rats exposed to formaldehyde in drinking water from 7 weeks old for up to 2 years (experiment BT 7001) 4-215

Table 4-45. Battery of immune parameters and functional tests assessed in female B6C3F1 mice after a 3 week, 15-ppm formaldehyde exposure 4-218

Table 4-46. Summary of the effects of formaldehyde inhalation on the mononuclear phagocyte system (MPS) in female B6C3F1 mice after a 3-week, 15 ppm formaldehyde exposure (6 hours/day, 5 days/week) 4-219

Table 4-47. Formaldehyde exposure regimens for determining the effects of formaldehyde exposure on pulmonary *S. aureus* infection 4-221

This document is a draft for review purposes only and does not constitute Agency policy.

LIST OF TABLES (continued)

Table 4-48. Summary of immune function changes due to inhaled formaldehyde exposure in experimental animals 4-226

Table 4-49. Study design for guinea pigs exposed to formaldehyde through different routes of exposure: inhalation, dermal, and injection 4-232

Table 4-50. Sensitization response of guinea pigs exposed to formaldehyde through inhalation, topical application, or footpad injection..... 4-233

Table 4-51. Cytokine and chemokine levels in lung tissue homogenate supernatants in formaldehyde-exposed male ICR mice with and without Der f sensitization..... 4-240

Table 4-52. Correlation coefficients among ear swelling responses and skin mRNA levels in contact hypersensitivity to formaldehyde in mice 4-249

Table 4-53. Summary of sensitization and atopy studies by inhalation or dermal sensitization due to formaldehyde in experimental animals 4-251

Table 4-54. Fluctuation of behavioral responses when male AB mice inhaled formaldehyde in a single 2-hour exposure: effects after 2 hours 4-259

Table 4-55. Fluctuation of behavioral responses when male AB mice inhaled formaldehyde in a single 2-hour exposure: effects after 24 hours 4-259

Table 4-56. Effects of formaldehyde exposure on completion of the labyrinth test by male and female LEW.1K rats 4-263

Table 4-57. Summary of neurological and neurobehavioral studies in inhaled formaldehyde in experimental animals 4-279

Table 4-58. Effects of formaldehyde on body and organ weights in rat pups from dams exposed via inhalation from mating through gestation..... 4-289

Table 4-59. Formaldehyde effects on Leydig cell quantity and nuclear damage in adult male Wistar rats..... 4-298

Table 4-60. Formaldehyde effects on adult male albino Wistar rats 4-299

Table 4-61. Formaldehyde effects on testosterone levels and seminiferous tubule diameters in Wistar rats following 91 days of exposure 4-300

Table 4-62. Effects of formaldehyde exposure on seminiferous tubule diameter and epithelial height in Wistar rats following 18 weeks of exposure 4-302

This document is a draft for review purposes only and does not constitute Agency policy.

LIST OF TABLES (continued)

Table 4-63. Incidence of sperm abnormalities and dominant lethal effects in formaldehyde-treated mice..... 4-302

Table 4-64. Body weights of pups born to beagles exposed to formaldehyde during gestation..... 4-303

Table 4-65. Testicular weights, sperm head counts, and percentage incidence of abnormal sperm after oral administration of formaldehyde to male Wistar rats..... 4-305

Table 4-66. Effect of formaldehyde on spermatogenic parameters in male Wistar rats exposed intraperitoneally 4-306

Table 4-67. Incidence of sperm head abnormalities in formaldehyde-treated rats..... 4-307

Table 4-68. Dominant lethal mutations after exposure of male rats to formaldehyde 4-308

Table 4-69. Summary of reported developmental effects in formaldehyde inhalation exposure studies 4-311

Table 4-70. Summary of reported developmental effects in formaldehyde oral exposure studies 4-317

Table 4-71. Summary of reported developmental effects in formaldehyde dermal exposure studies 4-318

Table 4-72. Summary of reported reproductive effects in formaldehyde inhalation studies..... 4-319

Table 4-73. Summary of reported reproductive effects in formaldehyde oral studies 4-322

Table 4-74. Summary of reported reproductive effects in formaldehyde intraperitoneal studies..... 4-323

Table 4-75. Summary of chronic bioassays which address rodent leukemia and lymphoma..... 4-329

Table 4-76. Formaldehyde-DNA reactions (DPX formation)..... 4-340

Table 4-77. Formaldehyde-DNA reactions (DNA adduct formation)..... 4-343

Table 4-78. Formaldehyde-DNA interactions (single stranded breaks)..... 4-344

Table 4-79. Other genetic effects of formaldehyde in mammalian cells..... 4-346

Table 4-80. In vitro clastogenicity of formaldehyde 4-348

This document is a draft for review purposes only and does not constitute Agency policy.

LIST OF TABLES (continued)

Table 4-81. Summary of mutagenicity of formaldehyde in bacterial systems 4-350

Table 4-82. Mutagenicity in mammalian cell systems 4-355

Table 4-83. Genotoxicity in laboratory animals 4-361

Table 4-84. MN frequencies in buccal mucosa cells of volunteers exposed to formaldehyde..... 4-364

Table 4-85. MN and SCE formation in mortuary science students exposed to formaldehyde for 85 days..... 4-364

Table 4-86. Incidence of MN formation in mortuary students exposed to formaldehyde for 90 days 4-365

Table 4-87. Multivariate regression models linking genomic instability/occupational exposures to selected endpoints from the MN assay..... 4-369

Table 4-88. Genotoxicity measures in pathological anatomy laboratory workers and controls 4-370

Table 4-89. Summary of human cytogenetic studies..... 4-372

Table 4-90. Summary of cohort and case-control studies which evaluated the incidence of all LHP cancers in formaldehyde-exposed populations (ICD-8 Codes: 200-209) and all leukemias (ICD-8 Codes: 204-207) 4-412

Table 4-91. Secondary analysis of published mortality statistics to explore alternative disease groupings within the broad category of all lymphohematopoietic malignancies 4-419

Table 4-92. Summary of studies which provide mortality statistics for myeloid leukemia sub-types 4-420

Table 4-93. Summary of mortality statistics for Hodgkin’s lymphoma, lymphoma and multiple myeloma from cohort analyses of formaldehyde exposed workers..... 4-422

Table 4-94. Summary of chronic bioassays which address rodent leukemia and lymphoma 4-424

Table 4-95. Incidence of lymphoblastic leukemia and lymphosarcoma orally dosed in Sprague-Dawley rats 4-425

Table 4-96. Available evidence for susceptibility factors of concern for formaldehyde exposure..... 4-469

This document is a draft for review purposes only and does not constitute Agency policy.

LIST OF TABLES (continued)

Table 5-1. Points of departure (POD) for nervous system toxicity in key human and animal studies 5-19

Table 5-2. Effects of formaldehyde exposure on completion of the labyrinth test by male and female LEW.1K rats 5-23

Table 5-3. Developmental and reproductive toxicity PODs including duration adjustments – key human study..... 5-31

Table 5-4. Summary of candidate studies for formaldehyde RfC development by health endpoint category 5-36

Table 5-5. Adjustment for nonoccupational exposures to formaldehyde 5-64

Table 5-6. Summary of reference concentration (RfC) derivation from critical study and supporting studies..... 5-68

Table 5-7. Relative risk estimates for mortality from nasopharyngeal malignancies (ICD-8 code 147) by level of formaldehyde exposure for different exposure metrics..... 5-78

Table 5-8. Regression coefficients from NCI log-linear trend test models for NPC mortality from cumulative exposure to formaldehyde 5-79

Table 5-9. Extra risk estimates for NPC mortality from various levels of continuous exposure to formaldehyde 5-80

Table 5-10. EC₀₀₀₅, LEC₀₀₀₅, and inhalation unit risk estimates for NPC mortality from formaldehyde exposure based on the Hauptmann et al. (2004) log-linear trend analyses for cumulative exposure 5-81

Table 5-11. EC₀₀₀₅, LEC₀₀₀₅, and inhalation unit risk estimates for NPC incidence from formaldehyde exposure based on the Hauptmann et al. (2004) trend analyses for cumulative exposure..... 5-82

Table 5-12. Relative risk estimates for mortality from Hodgkin lymphoma (ICD-8 code 201) and leukemia (ICD-8 codes 204–207) by level of formaldehyde exposure for different exposure metrics..... 5-90

Table 5-13. Regression coefficients for Hodgkin lymphoma and leukemia mortality from NCI trend test models 5-90

Table 5-14. Extra risk estimates for Hodgkin lymphoma mortality from various levels of continuous exposure to formaldehyde 5-91

This document is a draft for review purposes only and does not constitute Agency policy.

LIST OF TABLES (continued)

Table 5-15. Extra risk estimates for leukemia mortality from various levels of continuous exposure to formaldehyde..... 5-91

Table 5-16. EC₀₀₀₅, LEC₀₀₀₅, and inhalation unit risk estimates for Hodgkin lymphoma mortality from formaldehyde exposure based on Beane Freeman et al. (2009) log-linear trend analyses for cumulative exposure 5-93

Table 5-17. EC₀₀₅, LEC₀₀₅, and inhalation unit risk estimates for leukemia mortality from formaldehyde exposure based on Beane Freeman et al. (2009) log-linear trend analyses for cumulative exposure..... 5-93

Table 5-18. EC₀₀₀₅, LEC₀₀₀₅, and inhalation unit risk estimates for Hodgkin lymphoma incidence from formaldehyde exposure, based on Beane Freeman et al. (2009) log-linear trend analyses for cumulative exposure 5-94

Table 5-19. EC₀₀₅, LEC₀₀₅, and inhalation unit risk estimates for leukemia incidence from formaldehyde exposure based on Beane Freeman et al. (2009) log-linear trend analyses for cumulative exposure..... 5-94

Table 5-20. Calculation of combined cancer mortality unit risk estimate at 0.1 ppm..... 5-100

Table 5-21. Calculation of combined cancer incidence unit risk estimate at 0.1 ppm 5-100

Table 5-22. Summary of tumor incidence in long-term bioassays on F344 rats 5-105

Table 5-23. BMD modeling of unit risk of SCC in the human respiratory tract 5-125

Table 5-24. Formaldehyde-induced rat tumor incidences 5-128

Table 5-25. Human benchmark extrapolations of nasal tumors in rats using formaldehyde flux and DPX..... 5-135

Table 5-26. Summary of inhalation unit risk estimates 5-136

Table 5-27. Total cancer risk from exposure to a constant formaldehyde exposure level of 1 µg/m³ from ages 0–70 years 5-137

Table 6-1. Summary of candidate Reference Concentrations (RfC) for co-critical studies 6-27

Table 6-2. Effective concentrations (lifetime continuous exposure levels) predicted for specified extra cancer risk levels for selected formaldehyde-related cancers 6-36

Table 6-3. Inhalation unit risk estimates based on epidemiological and experimental animal data..... 6-42

This document is a draft for review purposes only and does not constitute Agency policy.

LIST OF FIGURES

Figure 2-1. Chemical structure of formaldehyde.....	2-1
Figure 2-2. Locations of hazardous air pollutant monitors.....	2-5
Figure 2-3. Modeled ambient air concentrations based on 1999 emissions	2-7
Figure 2-4. Range of formaldehyde air concentrations (ppb) in different environments	2-9
Figure 3-1. Formaldehyde-mediated protein modifications	3-2
Figure 3-2. $^3\text{H}/^{14}\text{C}$ ratios in macromolecular extracts from rat tissues following exposure to ^{14}C and ^3H -labeled formaldehyde (0.3, 2, 6, 10, 15 ppm).....	3-18
Figure 3-3. Formaldehyde clearance by ALDH2 (GSH-independent) and ADH3 (GSH-dependent).....	3-20
Figure 3-4. Metabolism of formate.....	3-22
Figure 3-5. Scatter plot of formaldehyde concentrations measured in ppb in direct breath exhalations (x axis) and exhaled breath condensate headspace (y axis).....	3-31
Figure 3-6. Reconstructed nasal passages of F344 rat, rhesus monkey, and human	3-36
Figure 3-7. Illustration of interspecies differences in airflow and verification of CFD simulations with water-dye studies	3-37
Figure 3-8. Lateral view of nasal wall mass flux of inhaled formaldehyde simulated in the F344 rat, rhesus monkey, and human	3-38
Figure 3-9. CFD simulations of formaldehyde flux to human nasal lining at different inspiratory flow rates.....	3-39
Figure 3-10. Single-path model simulations of surface flux per ppm of formaldehyde exposure concentration in an adult male human	3-43
Figure 3-11. Pressure drop vs. volumetric airflow rate predicted by the CIIT CFD model compared with pressure drop measurements made in two hollow molds (C1 and C2) of the rat nasal passage (Cheng et al., 1990) or in rats in vivo.....	3-45
Figure 3-12. Formaldehyde-DPX dosimetry in the F344 rat.....	3-47
Figure 4-1. Delayed asthmatic reaction following the inhalation of formaldehyde after “painting” 100% formalin for 20 minutes	4-20

This document is a draft for review purposes only and does not constitute Agency policy.

LIST OF FIGURES (continued)

Figure 4-2. Formaldehyde effects on minute volume in naïve and formaldehyde-pretreated male B6C3F1 mice and F344 rats	4-115
Figure 4-3. Sagittal view of the rat nose (nares oriented to the left)	4-121
Figure 4-4. Main components of the nasal respiratory epithelium.....	4-122
Figure 4-5. Decreased mucus clearance and ciliary beat in isolated frog palates exposed to formaldehyde after 3 days in culture.....	4-126
Figure 4-6. Diagram of nasal passages showing section levels chosen for morphometry and autoradiography in male rhesus monkeys exposed to formaldehyde	4-135
Figure 4-7. Formaldehyde-induced cell proliferation in male rhesus monkeys exposed to formaldehyde.....	4-136
Figure 4-8. Formaldehyde-induced lesions in male rhesus monkeys exposed to formaldehyde	4-137
Figure 4-9. Frequency and location by cross-section level of squamous metaplasia in the nasal cavity of F344 rats exposed to formaldehyde via inhalation	4-172
Figure 4-10. Effect of formaldehyde exposure on cell proliferation of the respiratory mucosa of rats and mice	4-190
Figure 4-11. Alveolar MP Fc-mediated phagocytosis from mice exposed to 5 ppm formaldehyde, 10 mg/m ³ carbon black, or both	4-223
Figure 4-12. Compressed air in milliliters as parameter for airway obstruction following formaldehyde exposure in guinea pigs after OVA sensitization and OVA challenge	4-235
Figure 4-13. OVA-specific IgG1 (1B) in formaldehyde-treated sensitized guinea pigs prior to OVA challenge	4-235
Figure 4-14. Anti-OVA titers in female Balb/C mice exposed to 6.63 ppm formaldehyde for 10 consecutive days, or once a week for 7 weeks	4-236
Figure 4-15. Vascular permeability in the tracheae and bronchi of male Wistar rats after 10 minutes of formaldehyde inhalation	4-238
Figure 4-16. Effect of select receptor antagonists on formaldehyde-induced vascular permeability in the trachea and bronchi of male Wistar rats.....	4-239

This document is a draft for review purposes only and does not constitute Agency policy.

LIST OF FIGURES (continued)

- Figure 4-17. The effects of formaldehyde inhalation exposures on eosinophil infiltration (Panel A) and goblet cell proliferation (Panel B) after Der f challenge in the nasal mucosa of male ICR mice after sensitization and challenge..... 4-241
- Figure 4-18. NGF in BAL fluid from formaldehyde-exposed female C3H/He mice with and without OA sensitization 4-243
- Figure 4-19. Plasma Substance P levels in formaldehyde-exposed female C3H/He mice with and without OVA sensitization 4-244
- Figure 4-20. Motor activity in male and female rats 2 hours after exposure to formaldehyde expressed as mean number of crossed quadrants \pm SEM 4-256
- Figure 4-21. Habituation of motor activity was observed in control rats during the second observation period (day 2, 24 hours after formaldehyde exposure)..... 4-257
- Figure 4-22. Motor activity was reduced in male and female LEW.1K rats 2 hours after termination of 10-minute formaldehyde exposure..... 4-258
- Figure 4-23. The effects of the acute formaldehyde (FA) exposures on the ambulatory and vertical components of SLMA 4-260
- Figure 4-24. Effects of formaldehyde exposure on the error rate of female LEW.1K rats performing the water labyrinth learning test 4-264
- Figure 4-25. Basal and stress-induced trunk blood corticosterone levels in male LEW.1K rats after formaldehyde inhalation exposures 4-269
- Figure 4-26. NGF production in the brains of formaldehyde-exposed mice..... 4-274
- Figure 4-27. Mortality corrected cumulative incidences of nasal carcinomas in the indicated exposure groups 4-325
- Figure 4-28. Leukemia incidence in Sprague-Dawley rats exposed to formaldehyde in drinking water for 2 years 4-330
- Figure 4-29. Unscheduled deaths in female F344 rats exposed to formaldehyde for 24 months 4-332
- Figure 4-30. Cumulative leukemia incidence in female F344 rats exposed to formaldehyde for 24 months 4-333
- Figure 4-31. Cumulative incidence or tumor bearing animals for lymphoma in female mice exposed to formaldehyde for 24 months..... 4-334

This document is a draft for review purposes only and does not constitute Agency policy.

LIST OF FIGURES (continued)

Figure 4-32. DNA-protein cross-links (DPX) and thymidine kinase (<i>tk</i>) mutants in TK6 human lymphoblasts exposed to formaldehyde for 2 hours	4-357
Figure 4-33. Developmental origins for cancers of the lymphohematopoietic system	4-409
Figure 4-34A. Association between peak formaldehyde exposure and the risk of lymphohematopoietic malignancy	4-415
Figure 4-34B. Association between average intensity of formaldehyde exposure and the risk of lymphohematopoietic malignancy	4-416
Figure 4-35. Effect of various doses of formaldehyde on cell number in (A) HT-29 human colon carcinoma cells and in (B) human umbilical vein epithelial cells (HUVEC)	4-433
Figure 4-36. Integrated MOA scheme for respiratory tract tumors	4-446
Figure 4-37. Location of intra-epithelial lymphocytes along side epithelial cells in the human adenoid.....	4-450
Figure 5-1. Change in number of additions made in 10 minutes following formaldehyde exposure at 32, 170, 390, or 890 ppb	5-21
Figure 5-2. Effects of formaldehyde exposure on the error rate of female LEW.1K rats performing the water labyrinth learning test	5-24
Figure 5-3. Fecundity density ratio among women exposed to formaldehyde in the high exposure index category with 8-hour time weighted average formaldehyde exposure concentration of 219 ppb	5-27
Figure 5-4. Estimated reduction in peak expiratory flow rate (PEFR) in children in relation to indoor residential formaldehyde concentrations.....	5-41
Figure 5.5. Odds ratios for physician-diagnosed asthma in children associated with in-home formaldehyde levels in air	5-45
Figure 5-6. Prevalence of asthma and respiratory symptom scores in children associated with in-home formaldehyde levels.....	5-48
Figure 5-7. Prevalence and severity of allergic sensitization in children associated with in-home formaldehyde levels	5-49
Figure 5-8. Positive exposure-response relationships reported for in-home formaldehyde exposures and sensory irritation (eye irritation)	5-53

This document is a draft for review purposes only and does not constitute Agency policy.

LIST OF FIGURES (continued)

Figure 5-9. Positive exposure-response relationships reported for in-home formaldehyde exposures and sensory irritation (burning eyes) 5-54

Figure 5-10. Age-specific mortality and incidence rates for myeloid, lymphoid, and all leukemia 5-98

Figure 5-11. Schematic of integration of pharmacokinetic and pharmacodynamic components in the CIIT model 5-110

Figure 5-12. Fit to the rat tumor incidence data using the model and assumptions in Conolly et al. (2003)..... 5-112

Figure 5-13. Spatial distribution of formaldehyde over the nasal lining, as characterized by partitioning the nasal surface by formaldehyde flux to the tissue per ppm of exposure concentration, resulting in 20 flux bins 5-120

Figure 5-14. Distribution of cells at risk across flux bins in the F344 rat nasal lining..... 5-120

Figure 5-15. MLE and upper bound (UB) added risk of SCC in the human nose for two BBDR models..... 5-124

Figure 5-16. Replot of log-probit fit of the combined Kerns et al. (1983) and Monticello et al. (1996) data on tumor incidence showing BMC_{10} and $BMCL_{10}$ 5-127

Figure 5-17. EPA multistate Weibull modeling: nasal tumor dose response 5-131

Figure 5-18. Multistage Weibull model fit 5-132

Figure 5-19. Multistage Weibull model fit of tumor incidence data compared with KM estimates of spontaneous tumor incidence..... 5-132

LIST OF ABBREVIATIONS AND ACRONYMS

ACGIH	American Conference of Governmental Industrial Hygienists
ADAF	age-dependent adjustment factors
ADH	alcohol dehydrogenase
ADS	anterior dorsal septum
AIC	Akaike Information Criterion
AIE	average intensity of exposure
AIHA	American Industrial Hygiene Association
ALB	albumin
ALDH	aldehyde dehydrogenase
ALL	acute lymphocytic leukemia
ALM	anterior lateral meatus
ALP	alkaline phosphatase
ALS	amyotrophic lateral sclerosis
ALT	alanine aminotransferase
AML	acute myelogenous leukemia
AMM	anterior medial maxilloturbinate
AMPase	adenosine monophosphatase
AMS	anterior medial septum
ANAE	alpha-naphthylacetate esterase
ANOVA	analysis of variance
APA	American Psychiatric Association
ARB	Air Resources Board
AST	aspartate aminotransferase
ATCM	airborne toxic control measure
ATP	adenosine triphosphate
ATPase	adenosine triphosphatase
ATS	American Thoracic Society
ATSDR	Agency for Toxic Substances and Disease Registry
AUC	area under the curve
BAL	bronchoalveolar lavage
BALT	bronchus associated lymphoid tissue
BBDR	biologically based dose response
BC	bronchial constriction
BCME	bis(chloromethyl)ether
BDNF	brain-derived neurotrophic factor
BEIR	biologic effects of ionizing radiation
BfR	German Federal Institute for Risk Assessment
BHR	bronchial hyperresponsiveness
BMC	benchmark concentration
BMCL	95% lower bound on the benchmark concentration
BMCR	binucleated micronucleated cell ratefluoresce
BMD	benchmark dose
BMDL	95% lower bound on the benchmark dose

This document is a draft for review purposes only and does not constitute Agency policy.

LIST OF ABBREVIATIONS AND ACRONYMS (continued)

BMR	benchmark response
BN	Brown-Norway
BrdU	bromodeoxyuridine
BUN	blood urea nitrogen
BW	body weight
CA	chromosomal aberrations
CalEPA	California Environmental Protection Agency
CAP	College of American Pathologists
CASRN	Chemical Abstracts Service Registry Number
CAT	catalase
CBMA	cytokinesis-blocked micronucleus assay
CBMN	cytokinesis-blocked micronucleus
CDC	U.S. Centers for Disease Control and Prevention
CDHS	California Department of Health Services
CFD	computational fluid dynamics
CGM	clonal growth model
CHO	Chinese hamster ovary
CI	confidence interval
CIIT	Chemical Industry Institute of Toxicology
CLL	chronic lymphocytic leukemia
CML	chronic myelogenous leukemia
CNS	central nervous system
CO ₂	carbon dioxide
COEHHA	California Office of Environmental Health Hazard Assessment
CREB	cyclic AMP responsive element binding proteins
CS	conditioned stimulus
C × t	concentration times time
DA	Daltons
DAF	dosimetric adjustment factor
DDX	DNA-DNA cross-links
DEI	daily exposure index
DEN	diethylnitrosamine
Der f	common dust mite allergen
DMG	dimethylglycine
DMGDH	dimethylglycine dehydrogenase
DNA	deoxyribonucleic acid
DOPAC	3,4-dihydroxyphenylacetic acid
DPC / DPX	DNA-protein cross-links
EBV	Epstein-Barr virus
EC	effective concentration
ED	effective dose
EHC	Environmental Health Committee
ELISA	enzyme-linked immunosorbent assay

This document is a draft for review purposes only and does not constitute Agency policy.

LIST OF ABBREVIATIONS AND ACRONYMS (continued)

EPA	U.S. Environmental Protection Agency
ERPG	emergency response planning guideline
ET	ethmoid turbinates
FALDH	formaldehyde dehydrogenase
FDA	U.S. Food and Drug Administration
FDR	fecundability density ratio
FEF	forced expiratory flow
FEMA	Federal Emergency Management Agency
FEV1	forced expiratory volume in 1 second
FISH	fluorescent in situ hybridization
FSH	follicle-stimulating hormone
FVC	forced vital capacity
GALT	gut-associated lymphoid tissue
GC-MS	gas chromatography-mass spectrometry
GD	gestation day
GI	gastrointestinal
GO	gene ontology
G6PDH	glucose-6-phosphate dehydrogenase
GPX	glutathione peroxidase
GR	glutathione reductase
GM-CSF	granulocyte macrophage-colony-stimulating factor
GSH	reduced glutathione
GSNO	S-nitrosoglutathione
GST	glutathione S-transferase
HAP	hazardous air pollutant
Hb	hemoglobin
HCl	hydrochloric acid
HCT	hematocrit
HEC	human equivalent concentration
5-HIAA	5-hydroxyindoleacetic acid
hm	hydroxymethyl
HMGSH	S-hydroxymethylglutathione
HPA	hypothalamic-pituitary adrenal
HPG	hypothalamo-pituitary-gonadal
HPLC	high-performance liquid chromatography
HPRT	hypoxanthine-guanine phosphoribosyl transferase
HR	high responders
HSA	human serum albumin
HSDB	Hazardous Substances Data Bank
Hsp	heat shock protein
HWE	healthy worker effect
I cell	initiated cell
IARC	International Agency for Research on Cancer

This document is a draft for review purposes only and does not constitute Agency policy.

LIST OF ABBREVIATIONS AND ACRONYMS (continued)

ICD	International Classification of Diseases
IF	interfacial
IFN	interferon
Ig	immunoglobulin
IL	interleukin
I.P.	intraperitoneal
IPCS	International Programme on Chemical Safety
IRIS	Integrated Risk Information System
K_m	Michaelis-Menton constant
KM	Kaplan-Meier
LD ₅₀	median lethal dose
LDH	lactate dehydrogenase
LEC	95% lower bound on the effective concentration
LED	95% lower bound on the effective dose
LHP	lymphohematopoietic
LI	labeling index
LM	Listeria monocytogenes
LMS	linearized multistage
LLNA	local lymph node assay
LOAEL	lowest-observed-adverse-effect level
LPS	lipopolysaccharide
LR	low responders
LRT	lower respiratory tract
MA	methylamine
MALT	mucus-associated lymph tissues
MCH	mean corpuscular hemoglobin
MCHC	mean corpuscular hemoglobin concentration
MCS	multiple chemical sensitivity
MCV	mean corpuscular volume
MDA	malondialdehyde
MEF	maximal expiratory flow
ML	myeloid leukemia
MLE	maximum likelihood estimate
MMS	methyl methane sulfonate
MMT	medial maxilloturbinate
MN	micronucleus, micronuclei
MNNG	N-methyl-N-nitro-N-nitrosoguanidine
MOA	mode of action
MoDC	monocyte-derived dendritic cell
MP	macrophage
MPD	multistage polynomial degree
MPS	mononuclear phagocyte system
MRL	minimum risk level

This document is a draft for review purposes only and does not constitute Agency policy.

LIST OF ABBREVIATIONS AND ACRONYMS (continued)

mRNA	messenger ribonucleic acid
MVE-2	Murray Valley encephalitis virus
MVK	Moolgavkar, Venzon, and Knudson
N cell	normal cell
NaCl	sodium chloride
NAD+	nicotinamide adenine dinucleotide
NADH	reduced nicotinamide adenine dinucleotide
NALT	nasally associated lymphoid tissue
NATA	National-Scale Air Toxics Assessment
NCEA	National Center for Environmental Assessment
NCHS	National Center for Health Statistics
NCI	National Cancer Institute
NEG	Nordic Expert Group
NER	nucleotide excision repair
NGF	nerve growth factor
NHL	non-Hodgkin's lymphoma
NHMRC/ARMCANZ	National Health and Medical Research Council/Agriculture and Resource Management Council of Australia and New Zealand
NNK	nitrosamine nitrosamine 4-(methylnitrosamino)-1-(3-pyridyl)-butanone
N ⁶ -hmdA	N ⁶ -hydroxymethyldeoxyadenosine
N ⁴ -hmdC	N ⁴ -hydroxymethylcytidine
N ² -hmdG	N ² -hydroxymethyldeoxyguanosine
NICNAS	National Industrial Chemicals Notification and Assessment Scheme
NIOSH	National Institute for Occupational Safety and Health
NLM	National Library of Medicine
NMDA	N-methyl-D-aspartate
NO	nitric oxide
NOAEL	no-observed-adverse-effect level
NPC	nasopharyngeal cancer
NRBA	neutrophil respiratory burst activity
NRC	National Research Council
NTP	National Toxicology Program
OR	odds ratio
OSHA	Occupational Safety and Health Administration
OTS	Office of Toxic Substances
OVA	ovalbumin
PBPK	physiologically based pharmacokinetic
PC	Philadelphia chromosome
PCA	passive cutaneous anaphylaxis
PCMR	proportionate cancer mortality ratio
PCNA	proliferating cell nuclear antigen
PCR	polymerase chain reaction
PCV	packed cell volume

This document is a draft for review purposes only and does not constitute Agency policy.

LIST OF ABBREVIATIONS AND ACRONYMS (continued)

PECAM	platelet endothelial cell adhesion molecule
PEF	peak expiratory flow
PEFR	peak expiratory flow rates
PEL	permissible exposure limit
PFC	plaque-forming cell
PG	periglomerular
PHA	phytohemagglutinin
PLA2	phospholipase A2
PI	phagocytic index
PLM	posterior lateral meatus
PMA	phorbol 12-myristate 13-acetate
PMR	proportionate mortality ratio
PMS	posterior medial septum
PND	postnatal day
POD	point of departure
POE	portal of entry
PTZ	pentilenetetrazole
PUFA	polyunsaturated fatty acids
PWULLI	population weighted unit length labeling index
RA	reflex apnea
RANTES	regulated upon activation, normal T-cell expressed and secreted
RB	reflex bradypnea
RBC	red blood cells
RD ₅₀	exposure concentration that results in a 50% reduction in respiratory rate
REL	recommended exposure limit
RfC	reference concentration
RfD	reference dose
RGD	regional gas dose
RGDR	regional gas dose ratio
RR	relative risk
RT	reverse transcriptase
SAB	Science Advisory Board
SCC	squamous cell carcinoma
SCE	sister chromatid exchange
SCG	sodium cromoglycate
SD	standard deviation
SDH	succinate dehydrogenase; sarcosine dehydrogenase
SEER	Surveillance, Epidemiology, and End Results
SEM	standard error of the mean
SEN	sensitizer
SH	sulfhydryl
SHE	Syrian hamster embryo
SLMA	spontaneous locomotor activity

This document is a draft for review purposes only and does not constitute Agency policy.

LIST OF ABBREVIATIONS AND ACRONYMS (continued)

SMR	standardized mortality ratio
SNP	single nucleotide polymorphism
SOD	superoxide dismutase
SOMedA	N ⁶ -sulfomethyldeoxyadenosine
Sp1	specificity protein
SPIR	standardized proportionate incidence ratio
SSAO	semicarbazole-sensitive amine oxidase
SSB	single strand breaks
STEL	short-term exposure limit
TBA	tumor bearing animal
TH	T-lymphocyte helper
THF	tetrahydrofolate
TK	toxicokinetics
TL	tail length
TLV	threshold limit value
TNF	tumor necrosis factor
TP	total protein
TRI	Toxic Release Inventory
TRPV	transient receptor potential vanilloid
TWA	time-weighted average
TZCA	thiazolidine-4-carboxylate
UCL	upper confidence limit
UDS	unscheduled DNA synthesis
UF	uncertainty factor
UFFI	urea formaldehyde foam insulation
ULLI	unit length labeling index
URT	upper respiratory tract
USDA	U.S. Department of Agriculture
VC	vital capacity
VOC	volatile organic compound
WBC	white blood cell
WDS	wet dog shake
WHO	World Health Organization
WHOROE	World Health Organization Regional Office for Europe

This document is a draft for review purposes only and does not constitute Agency policy.

This page intentionally left blank.

Appendix A

APPENDIX A

**SUMMARY OF EXTERNAL PEER REVIEW
AND PUBLIC COMMENTS AND DISPOSITIONS**

1
2
3
4
5
6
7
8
9
10
11
12
13
14
15
16

[NOTE: This is a placeholder for Appendix A which will be drafted following External Peer review and receipt of public comments.]

Appendix B

1
2
3 **APPENDIX B**

4 **SIMULATIONS OF INTERINDIVIDUAL AND ADULT-TO-CHILD VARIABILITY IN**
5 **REACTIVE GAS UPTAKE IN A SMALL SAMPLE OF PEOPLE (Garcia et al., 2009)**

6 Garcia et al. (2009) used computational fluid dynamics to study human variability in the
7 nasal dosimetry of reactive, water-soluble gases in 5 adults and 2 children, aged 7 and 8 years
8 old. They considered two model categories of gases, corresponding to maximal and moderate
9 absorption at the nasal lining. The nasal airway (including the nasopharynx) geometries of these
10 individuals were mapped out using magnetic resonance imaging or computed tomography scans.
11 The scans chosen for the analysis were from individuals who had normal nasal anatomies with
12 no pathology (as per a review carried out by a ear-nose-throat surgeon). The minute volumes of
13 these individuals were estimated to range from 6.8 to 9.0 L/min (adults) and 5.5 to 5.8 L/min
14 (children). The sample size in this study is too small to consider the results representative of the
15 population as a whole (as also recognized by the authors). Nonetheless, various comparisons
16 with the characteristics of other study populations add to the strength of this study. The range of
17 adult minute volumes in this study is reported by the authors to be in good agreement with that
18 obtained in many other studies in the literature; minute volumes for the children in the study
19 were found to be similar to the average minute volume of 6.1 ± 1.7 L/min obtained by Bennett
20 and Zeman (2004) in a study of 36 children aged 6 to 13 years; the range of nasal surface area
21 values for the adults agreed well with that obtained by Guilmette et al. (1997) for 45 adults; and
22 the range of values for the surface area to volume ratio is in good agreement with that obtained
23 for 40 adult Caucasians studied by Yokley (2006). The surface area to volume ratio is useful for
24 comparing the rate of diffusional transport of a gas out of different cavities; however in the case
25 of the highly non-homogenously shaped nasal lumen, this might at best be considered a gross
26 indicator.

27 We focus here only on the “maximum uptake” simulations in Garcia et al. (2009). In this
28 case, the gas was considered so highly reactive and soluble that it was reasonable to assume an
29 infinitely fast reaction of the absorbed gas with compounds in the airway lining. Although such a
30 gas could be reasonably considered to represent formaldehyde, these results cannot be fully
31 utilized to inform quantitative estimates of formaldehyde dosimetry (and that does not appear to
32 have been the intent of the authors either). This is because the same boundary condition
33 corresponding to maximal uptake was applied on the vestibular section as well as on the
34 transitional and transitional epithelial lining of the nasal cavity. This is not appropriate for
35 formaldehyde as the lining on the nasal vestibule is made of keratinized epithelium which is
36 considerably less absorbing than the transitional or respiratory epithelium (Kimbell et al. 2001).

This document is a draft for review purposes only and does not constitute Agency policy.

1 Table B-1 provides results obtained by Garcia et al. (2009) for five adults and two
 2 children for uptake for the maximal uptake scenario. Although the nasal cavities of the children
 3 were smaller in surface area, volume and length, the surface-area-to-volume ratios were similar
 4 in the two age groups. Overall uptake efficiency, average flux (rate of gas absorbed per unit
 5 surface area of the nasal lining) and maximum flux levels over the entire nasal lining did not
 6 vary substantially between adults (1.6-fold difference in average flux and much less in maximum
 7 flux), and the mean values of these quantities were comparable between adults and children.
 8 These results are in agreement with conclusions reached by Ginsberg et al. (2005) that overall
 9 extrathoracic absorption of highly and moderately reactive and soluble gases (corresponding to
 10 category 1 and 2 reactive gases as per the scheme in USEPA [1994]) is similar in adults and
 11 children. However, none of these three quantities should be considered as reasonable indicators
 12 of variability in the interaction of the gas with the nasal lining. For a very reactive and soluble
 13 gas, regional absorption of the gas is highly nonhomogenously distributed; therefore
 14 interindividual variability in this distribution will be washed out when averaged over the whole
 15 nose. Estimates of maximum gas flux, on the other hand, correspond to extremely small
 16 localized regions of hot spots (see chapter 3), and thus may not be a proper measure of inter-
 17 individual variability in flux distribution patterns over the whole nose. Furthermore, numerical
 18 error in the calculation (such as mass balance and irregularly shaped elements of the finite-
 19 element mesh) is likely to be most pronounced when estimates are considered over extremely
 20 small regions.

21
 22 **Table B-1: Variations in overall nasal uptake, whole nose flux, and key parameters**
 23

	% nasal uptake	MV (L)	SA/V (1/mm)	Avg flux 10^{-8} kg/(s.m ²)		Maximum flux 10^{-8} kg/(s.m ²)	
				left cavity	right cavity	left cavity	right cavity
adult1	93.5	9	1.12	1.8	1.5	10.8	10.0
adult1	92.4	6.8	1.09	1.5	1.5	10.8	10.4
adult1	93.1	9	0.88	1.6	1.3	11	10.6
adult1	89.2	7.1	0.87	1.2	1.2	10.6	10.2
adult1	91.5	6.9	0.95	1.4	1.5	10.8	10.0
child1	92	5.5	1.13	1.9	1.5	11.8	11.0
child2	88.2	5.8	0.95	1.6	1.5	12.3	11.6

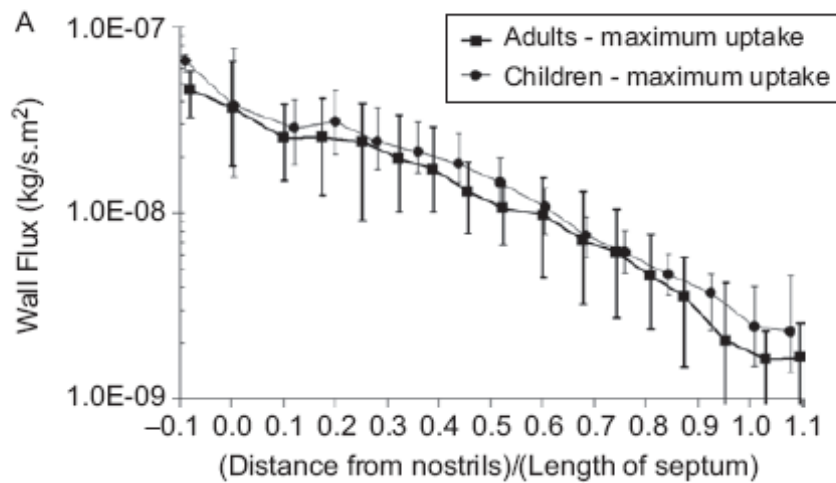
24 MV = minute volume, SA=nasal surface area, V=nasal volume
 25 Source: Garcia et al. (2009).
 26
 27

1 On the other hand, Figure 6A of Garcia et al. (2009), reproduced here as Figure B-1,
2 shows significant interhuman variability in flux values at specific points on the nasal walls. The
3 local flux of formaldehyde varies among individuals by a factor of 3 to 5 at various distances
4 along the septal axis of the nose. However, interpretation of the values in this plot is problematic
5 for reasons explained in the paper¹:

6 The greater variability among individuals seen for wall fluxes at specific sites of the nasal
7 passages (Figure 6) in comparison to the minimal variability in total uptake
8 (Table 2) and whole-nose dose (Tables 3 and Tables 4) indicates that fluxes of equal
9 magnitude do not exactly overlay the same anatomical regions of the nasal cavity in each
10 individual. This implies that specific anatomical regions subtended by maximum flux
11 could be offset from one individual to another.

12 Notwithstanding this difficulty in interpretation, we believe the quantities plotted in Figure B-1
13 provide a better perspective of the inter-individual (adult) variability in local flux than the
14 variation in whole nose average or in maximum flux presented in Table B-1.

15



16

17 **Figure B-1: Gas flux across the nasal lining for the case of a “maximum**
18 **uptake” gas in Garcia et al. (2009) as a function of axial distance from the**
19 **nostril.** The vertical bars show range of variation. See the paper for further
20 details. Figure is reproduced from Garcia et al. (2009).
21

22

23

24 Clearly, multiple measures of variability in dose can be developed depending on the
25 adverse response. The advantage of models such as that developed by Garcia et al. is that they
make it possible to carry out these calculations. For example, if deficit in pulmonary function is

1 The Figures and Tables in the cited text refer those in Garcia et al. (2009)

This document is a draft for review purposes only and does not constitute Agency policy.

1 the adverse response, then variation in average whole nose flux or overall nasal uptake efficiency
2 would be most useful since one is then interested in inter-individual variability in the overall
3 dose delivered to the lung. It is possible to conceive of allergic or irritation responses being
4 triggered by some threshold value of local flux. In such a case it may be preferable to calculate
5 the variability associated with the net surface area receiving flux values greater than that
6 threshold. On the other hand, the probability of developing a tumor at a nasal site may be non-
7 linearly related to the flux at that site and linearly related to the number of cells at that site. In
8 this case, the appropriate metric may be the nasal surface area associated with some intermediate
9 levels of local flux (see Appendix in Subramaniam et al. 2008).

10 Various caveats presented by the authors as limitations of their study should be noted:
11 Possible nonuniform distribution of epithelial types, enzymes, glands and other cellular
12 metabolic or clearance machinery were not considered in the model; only effects pertaining to
13 resting breathing were considered; the study sample size was small; children younger than 7
14 years old were not studied; and, the model assumed a rigid nasal geometry.

15
16 Garcia et al. (2009) conclude their paper as follows:

17 “..., our simulations predicted no differences in the nasal dosimetry of reactive, water-
18 soluble gases between children and adults, suggesting that the risk factor of 10 typically
19 used to accommodate inter-human variability is adequate.”

20
21 In addition to the obvious caveat already recognized by the authors in regards extrapolating from
22 a study involving just two children, this conclusion needs further qualification. Firstly, the safety
23 factor of 10 that is typically applied for interhuman variability does not specifically include
24 children. Instead, EPA practice is that unless there is reasonable evidence that childhood forms a
25 more susceptible lifestage, no additional factors are applied for this population. Second, it is
26 important not to confuse dosimetric differences across lifestages—which actually contribute to
27 intra-individual differences—with inter-individual differences that may contribute towards the 10-
28 fold uncertainty factor. This interhuman variability in susceptibility—for a given life-stage—may
29 be considered to arise from both pharmacokinetic and pharmacodynamic factors, and the practice
30 in the US has been to split these into factors of 3.3 each. Then, the roughly 3 to 5 -fold variation
31 estimated for adults (and also between the two children) in Figure B-1 suggest that a factor of 10
32 may not be adequate to accommodate inter-human variability for those formaldehyde-induced
33 adverse responses for which the localized nature of formaldehyde flux, and therefore the inter-
34 individual differences in regional dosimetry, play a role.

This page intentionally left blank.

Appendix C

1
2
3
4
5
6
7
8

APPENDIX C

LIFETABLE ANALYSIS

A spreadsheet illustrating the extra-risk calculation for the derivation of the lower 95% bound on the effective concentration associated with a 0.05% extra risk (LEC_{0005}) for nasopharyngeal carcinoma (NPC) incidence is presented in Table C-1.

Table C-1. Extra-risk calculation^a for environmental exposure to 0.0461 ppm formaldehyde (the LEC₀₀₀₅ for NPC incidence)^b using a log-linear exposure-response model based on the cumulative exposure trend results of Hauptmann et al. (2004), as described in Section 5.2.2.

A	B	C	D	E	F	G	H	I	J	K	L	M	N	O	P	
Interval number (i)	Age interval	All cause mortality ($\times 10^5/\text{yr}$)	NPC incidence ($\times 10^5/\text{yr}$)	All cause hazard rate (h*)	Prob of surviving interval (q)	Prob of surviving up to interval (S)	NPC cancer hazard rate (h)	Cond prob of NPC incidence in interval (Ro)	Exp duration mid interval (xtime)	Cum exp mid interval (xdose)	Exposed NPC hazard rate (hx)	Exposed all cause hazard rate (h*x)	Exposed prob of surviving interval (qx)	Exposed prob of surviving up to interval (Sx)	Exposed cond prob of NPC in interval (Rx)	
1	<1	728.7	0	0.0073	0.9927	1.0000	0.00000	0.000000	0	0.0000	0.0000	0.0073	0.9927	1.0000	0.00000	
2	1-4	32.9	0.05	0.0013	0.9987	0.9927	0.00000	0.000002	0	0.0000	0.0000	0.0013	0.9987	0.9927	0.00000	
3	5-9	16.4	0.03	0.0008	0.9992	0.9914	0.00000	0.000001	0	0.0000	0.0000	0.0008	0.9992	0.9914	0.00000	
4	10-14	20.9	0.09	0.0010	0.9990	0.9906	0.00000	0.000004	0	0.0000	0.0000	0.0010	0.9990	0.9906	0.00000	
5	15-19	68.2	0.12	0.0034	0.9966	0.9896	0.00001	0.000006	2.5	0.3506	0.0000	0.0034	0.9966	0.9896	0.00001	
6	20-24	96	0.16	0.0048	0.9952	0.9862	0.00001	0.000008	7.5	1.0517	0.0000	0.0048	0.9952	0.9862	0.00001	
7	25-29	99	0.23	0.0050	0.9951	0.9815	0.00001	0.000011	12.5	1.7528	0.0000	0.0050	0.9951	0.9815	0.00001	
8	30-34	116.3	0.48	0.0058	0.9942	0.9766	0.00002	0.000023	17.5	2.4539	0.0000	0.0058	0.9942	0.9766	0.00003	
9	35-39	162.2	0.55	0.0081	0.9919	0.9710	0.00003	0.000027	22.5	3.1550	0.0000	0.0081	0.9919	0.9710	0.00003	
10	40-44	237.3	1.14	0.0119	0.9882	0.9631	0.00006	0.000055	27.5	3.8561	0.0001	0.0119	0.9882	0.9631	0.00008	
11	45-49	356	1.3	0.0178	0.9824	0.9518	0.00007	0.000061	32.5	4.5572	0.0001	0.0178	0.9823	0.9517	0.00009	
12	50-54	518.6	1.72	0.0259	0.9744	0.9350	0.00009	0.000079	37.5	5.2583	0.0001	0.0260	0.9744	0.9349	0.00012	
13	55-59	801.8	1.69	0.0401	0.9607	0.9111	0.00008	0.000075	42.5	5.9594	0.0001	0.0401	0.9607	0.9110	0.00012	
14	60-64	1257.9	1.9	0.0629	0.9390	0.8753	0.00010	0.000081	47.5	6.6605	0.0002	0.0630	0.9390	0.8751	0.00014	
15	65-69	1928.2	2.87	0.0964	0.9081	0.8219	0.00014	0.000112	52.5	7.3616	0.0003	0.0965	0.9080	0.8217	0.00021	
16	70-74	2968.1	2.1	0.1484	0.8621	0.7464	0.00011	0.000073	57.5	8.0627	0.0002	0.1485	0.8620	0.7461	0.00014	
17	75-79	4556.6	2.19	0.2278	0.7963	0.6434	0.00011	0.000063	62.5	8.7638	0.0002	0.2279	0.7962	0.6431	0.00013	
18	80-84	7399.6	1.98	0.3700	0.6907	0.5123	0.00010	0.000042	67.5	9.4649	0.0002	0.3701	0.6907	0.5120	0.00009	
							Ro =	0.000725							Rx =	0.001225
Extra Risk = (Rx-Ro)/(1-Ro) = 0.0005																

- Column A: interval index number (i).
- Column B: 5-year age interval (except <1 and 1–4) up to age 85.
- Column C: all-cause mortality rate for interval i ($\times 10^5/\text{year}$) (2000 data from NCHS).
- Column D: NPC incidence rate for interval i ($\times 10^5/\text{year}$) (1996-2000 SEER data).
- Column E: all-cause hazard rate for interval i (h^*_i) (= all-cause mortality rate \times number of years in age interval).^c
- Column F: probability of surviving interval i without being diagnosed with NPC (q_i) (= $\exp(-h^*_i)$).
- Column G: probability of surviving up to interval i without having been diagnosed with NPC (S_i) ($S_1 = 1$; $S_i = S_{i-1} \times q_{i-1}$, for $i > 1$).
- Column H: NPC incidence hazard rate for interval i (h_i) (= NPC incidence rate \times number of years in interval).
- Column I: conditional probability of being diagnosed with NPC in interval i (= $(h_i/h^*_i) \times S_i \times (1-q_i)$), i.e., conditional upon surviving up to interval i without having been diagnosed with NPC [Ro, the background lifetime probability of being diagnosed with NPC = the sum of the conditional probabilities across the intervals].
- Column J: exposure duration (in years) at mid-interval (xtime).
- Column K: cumulative exposure mid-interval (xdose) (= exposure level (i.e., 0.0461 ppm) \times 365/240 \times 20/10 \times xtime) [365/240 \times 20/10 converts continuous environmental exposures to corresponding occupational exposures].
- Column L: NPC incidence hazard rate in exposed people for interval i (hx_i) (= $h_i \times (1 + \beta \times \text{xdose})$, where $\beta = 0.05183 + (1.645 \times 0.01915) = 0.08333$) [0.05183 per ppm \times year is the regression coefficient obtained, along with its SE of 0.01915, from Dr. Hauptmann (see Section 5.2.2.1). To estimate the LEC_{0005} , i.e., the 95% lower bound on the continuous exposure giving an extra risk of 0.05%, the 95% upper bound on the regression coefficient is used, i.e., $MLE + 1.645 \times SE$].
- Column M: all-cause hazard rate in exposed people for interval i (h^*x_i) (= $h^*_i + (hx_i - h_i)$).
- Column N: probability of surviving interval i without being diagnosed with NPC for exposed people (qx_i) (= $\exp(-h^*x_i)$).
- Column O: probability of surviving up to interval i without having been diagnosed with NPC for exposed people (Sx_i) ($Sx_1 = 1$; $Sx_i = Sx_{i-1} \times qx_{i-1}$, for $i > 1$).
- Column P: conditional probability of being diagnosed with NPC in interval i for exposed people (= $(hx_i/h^*x_i) \times Sx_i \times (1-qx_i)$) [Rx, the lifetime probability of being diagnosed with NPC for exposed people = the sum of the conditional probabilities across the intervals].

^a Using the methodology of BEIR IV (1988).

^b The estimated 95% lower bound on the continuous exposure level of TCE that gives a 0.05% extra lifetime risk of NPC.

^c For the cancer incidence calculation, the all-cause hazard rate for interval i should technically be the rate of either dying of any cause or being diagnosed with the specific cancer during the interval, i.e., (the all-cause mortality rate for the interval + the cancer-specific incidence rate for the interval—the cancer-specific mortality rate for the interval [so that a cancer case isn't counted twice, i.e., upon diagnosis and upon death]) \times number of years in interval. This adjustment was ignored here because the NPC incidence rates are small compared with the all-cause mortality rates.

MLE = maximum likelihood estimate, SE = standard error

Appendix D

1 **APPENDIX D**

2 **MODEL STRUCTURE & CALIBRATION IN CONOLLY ET AL. (2003, 2004)**

3
4
5 The various studies indicated in Section 5.4.1 were followed by the development of a
6 biologically motivated dose-response model for formaldehyde-induced cancer as represented in a
7 series of papers and in a health assessment report (CIIT model) (Conolly et al., 2004, 2003,
8 2000; Conolly, 2002; Kimbell et al., 2001a, b; Overton et al., 2001; CIIT, 1999). EPA’s cancer
9 guidelines (U.S. EPA, 2005a) suggest using a BBDR model for extrapolation when data permits
10 since it facilitates the incorporation of MOA in risk assessment. The CIIT modeling and
11 available data were evaluated in a series of peer-reviewed papers (Klein et al., 2009; Crump et
12 al., 2008; Subramaniam et al., 2008, 2007) and debated further in the literature (Conolly et al.,
13 2009; Crump et al., 2009). In addition, alternatives to the CIIT biological modeling (but based
14 on that original model) are further explored and evaluated here.

15 In Conolly et al. (2003), tumor incidence data in the above long-term bioassays were
16 modeled by using an approximation of the two-stage clonal growth model (Moolgavkar et al.,
17 1988) and allowing formaldehyde to have directly mutagenic action. Conolly et al. (2003)
18 combined these data with historical control data on 7,684 animals obtained from National
19 Toxicology Program (NTP) bioassays. These models are based on the Moolgavkar, Venzon, and
20 Knudson (MVK) stochastic two-stage model of cancer (Moolgavkar et al., 1988; Moolgavkar
21 and Knudson, 1981; Moolgavkar and Venzon, 1979), which accounts for growth of a pool of
22 normal cells, mutation of normal cells to initiated cells, clonal expansion and death of initiated
23 cells, and mutation of initiated cells to fully malignant cells.

24 The MVK model for formaldehyde accounted for two MOAs that may be relevant to
25 formaldehyde carcinogenicity:

- 26
- 27 ○ An indirect MOA in which the regenerative cell proliferation in response to formaldehyde
28 cytotoxicity increased the probability of errors in DNA replication. This MOA was modeled
29 by using labeling data on normal cells in nasal mucosa of rats exposed to formaldehyde.
 - 30 ○ A possible direct mutagenic MOA, based on information indicating that formaldehyde is
31 mutagenic (Speit and Merk, 2002; Heck et al., 1990; Grafstrom et al., 1985), was modeled by
32 using rat data on formaldehyde production of DPXs (Monticello et al., 1996, 1991).
- 33

34 The human model for formaldehyde carcinogenicity (Conolly et al., 2004) is
35 conceptually very similar to the rat model. The model uses, as input, results from a dosimetry
36 model for an anatomically realistic representation of the human upper airways and an idealized

1 representation of the lower airways. However, the model does not incorporate any data on
2 human responses to formaldehyde exposure. The rat and human formaldehyde models are
3 detailed further below.

4
5 The following notations are used in the rest of this chapter:

6 N cell, normal cell

7 I cell, initiated cell

8 LI, labeling index (number of labeled cells/(number labeled + unlabeled cells))

9 ULLI, unit length labeling index (number labeled cells/length of basement membrane)

10 N, number of normal cells that are eligible for progression to malignancy

11 α_N , division rate of normal cells (hours⁻¹)

12 μ_N , rate at which an initiated cell is formed by mutation of a normal cell (per cell division
13 of normal cells)

14 α_I , division rate of an initiated cell (hours⁻¹)

15 β_I , death rate of an initiated cell (hours⁻¹)

16 μ_I , rate at which a malignant cell is formed by mutation of an initiated cell (per cell
17 division of initiated cells)

18
19 A novel contribution of the CIIT model is that cell replication rates and DPX
20 concentrations are driven by local dose, which is formaldehyde flux to each region of nasal
21 tissue expressed as pmol/mm²-hour. This dosimetry is predicted by computational fluid
22 dynamics (CFD) modeling using anatomically accurate representations of the nasal passages (see
23 Chapter 3). Such a feature is important to incorporating site-specific toxicity in the case of a
24 highly reactive gas like formaldehyde, for which uptake patterns are spatially localized and
25 significantly different across species (see Chapter 3). In the CIIT model, each of these
26 parameters is characterized by local flux. The inputs to the two-stage cancer modeling consisted
27 of results from other model predictions as well as empirical data as follows:

- 28
- 29 • Regional uptake of formaldehyde in the respiratory tract predicted by using CFD
30 modeling in the F344 rat and human (Kimbell et al., 2001a, b; Overton et al., 2001;
31 Subramaniam et al., 1998)
 - 32 • Concentrations of DPXs predicted by a PBPK model (Conolly et al., 2000) calibrated to
33 fit the DPX data in F344 rat and rhesus monkey (Casanova et al., 1994, 1991) and
34 subsequently scaled up to humans

This document is a draft for review purposes only and does not constitute Agency policy.

- α_N inferred from LI data on rats exposed to formaldehyde (Monticello et al., 1996, 1991, 1990)

D.1. DPX AND MUTATIONAL ACTION

Formaldehyde interacts with DNA to form DPXs. These cross-links are considered to induce mutagenic as well as clastogenic effects. Casanova et al. (1994, 1989) carried out two studies of DPX measurements in F344 rats. In the first study, rats were exposed to concentrations of 0.3, 0.7, 2, 6, and 10 ppm for 6 hours and DPX measurements were made over the whole respiratory mucosa of the rat, while, in the second study, the exposure was to 0.7, 2, 6, or 15 ppm formaldehyde for 3 hours and measurements were made at “high” and “low” tumor sites. Overall, these studies showed statistically significantly elevated levels of DPXs at concentrations ≥ 2 ppm, with the trend also indicating elevated DPXs at 0.7 ppm. In Conolly et al. (2003), DPX formation is considered proportional to the intracellular dose that induces mutations. Conolly et al. (2000) used data from the second study to develop a PBPK model that predicted the time course of DPX concentrations as a function of regional formaldehyde flux (estimated in the CFD modeling and expressed as $\text{pmol}/\text{mm}^2\text{-hour}$). In Conolly et al. (2003), this PBPK model was then used to predict regional DPX concentrations (that is, as a function of regional formaldehyde flux) (Figure 5-11, Chapter 5). These data were incorporated into the two-stage clonal expansion model by defining the mutation rate of normal and initiated cells as the same linear function of DPX concentration as follows:

$$\mu_N = \mu_I = \mu_{N\text{basal}} + \text{KMU} \times \text{DPX} \quad (1)$$

The unknown constants $\mu_{N\text{basal}}$ and KMU were estimated by fitting model predictions to the tumor bioassay data.

D.2. CALIBRATION OF MODEL

The rat model in Conolly et al. (2003) involved six unknown statistical parameters that were estimated by fitting the model to the rat formaldehyde bioassay data shown in Table 5-24 in Chapter 5 (Monticello et al., 1996; Kerns et al., 1983) plus data from several thousand control animals from all the rat bioassays conducted by the NTP. These NTP bioassays were conducted from 1976 through 1999 and included 7,684 animals with an incidence of 13 SCCs (i.e., 0.17% incidence). The resulting model predicts the probability of a nasal SCC in the F344 rat as a function of age and exposure to formaldehyde. The fit to the tumor incidence data is shown in Figure 5-12, Chapter 5. (Note: This figure also shows the fit to the data obtained by the

1 implementation of this model in Subramaniam et al. [2007], which is discussed later in this
2 chapter.)

3

4 **D.3. FLUX BINS**

5 The spatial distribution of formaldehyde over the nasal lining was characterized by
6 partitioning the nasal surface by formaldehyde flux to the tissue, resulting in 20 “flux bins”
7 (Figure 5-13, Chapter 5). Each bin is comprised of elements (not necessarily contiguous) of the
8 nasal surface that receive a particular interval of formaldehyde flux per ppm of exposure
9 concentration (Kimbell et al., 2001a). The spatial coordinates of elements comprising a
10 particular flux bin are fixed for all exposure concentrations, with formaldehyde flux in a bin
11 scaling linearly with exposure concentration (ppm). The number of cells at risk varies across the
12 bins, as shown in Figure 5-14, Chapter 5.

13

14 **D.4. USE OF LABELING DATA**

15 Cell replication rates in Conolly et al. (2003) were obtained by pooling labeling data
16 from two phases of a labeling study in which male F344 rats were exposed to formaldehyde gas
17 at similar concentrations (0, 0.7, 2.0, 6.0, 10.0, or 15.0 ppm). The first phase employed injection
18 labeling with a 2-hour pulse labeling time, and animals were exposed to formaldehyde for early
19 exposure periods of 1, 4, and 9 days and 6 weeks (Monticello et al., 1991). The second phase
20 used osmotic minipumps for labeling with a 120-hour labeling time to quantify labeling in
21 animals exposed for 13, 26, 52, and 78 weeks (Monticello et al., 1996). The combined pulse and
22 continuous labeling data were expressed as one exposure TWA over all sites for each exposure
23 concentration. α_N was calculated from these labeling data by using an approximation from
24 Moolgavkar and Luebeck (1992). A dose-response curve for normal cell replication rates (i.e.,
25 α_N as a function of formaldehyde flux) was then calculated as shown in Figure D-1. These steps
26 are carefully detailed and evaluated in Subramaniam et al. (2008), and discussion of the data will
27 continue in the section on uncertainties in characterizing cell replication rates.

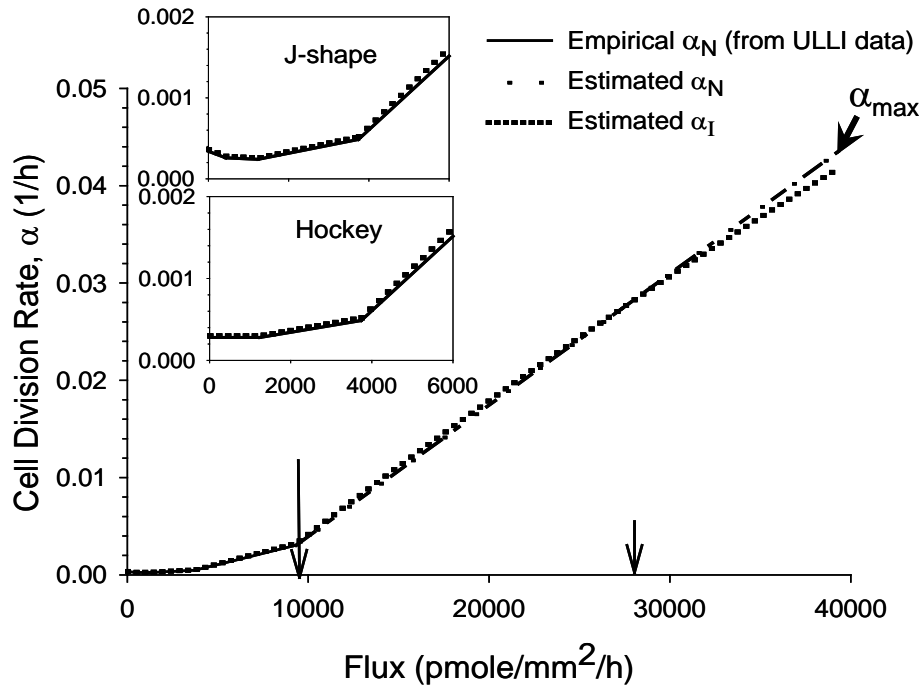
28

29 **D.5. UPWARD EXTRAPOLATION OF NORMAL CELL DIVISION RATE**

30 The extensive labeling data collected by Monticello et al. (1996, 1991) present an
31 opportunity to use precursor data in assessing cancer risk. However, these empirical data could
32 be used to determine $\alpha_N(\text{flux})$ only for the lower flux range, 0–9,340 pmol/mm²-hour (see
33 Subramaniam et al. [2008] for the reasons), as shown by the solid line in Figure D-1, whereas the
34 highest computed flux at 15.0 ppm exposure was 39,300 pmol/mm²-hour. Therefore Conolly et
35 al. (2003) introduced an adjustable parameter, α_{max} , that represented the value of $\alpha_N(\text{flux})$ at the

This document is a draft for review purposes only and does not constitute Agency policy.

1 maximum flux of 39,300 pmol/mm²-hour. α_{\max} was estimated by maximizing the likelihood of
 2 the two-stage model fit to the tumor incidence data. For $9,340 < \text{flux} \leq 39,300$ pmol/mm²-
 3 hour, $\alpha_N(\text{flux})$ was determined by linear interpolation from $\alpha_N(9,340)$ to α_{\max} , as shown by the
 4 dashed line in Figure D-1.
 5



6
 7
 8 **Figure D-1. Dose response of normal (α_N) and initiated (α_I) cell division rate**
 9 **in Conolly et al. (2003).**

10
 11 Note: Empirically derived values of α_N (TWA over six sites) from Table 1 in
 12 Conolly et al. (2003) and optimized parameter values from their Table 4 were
 13 used. The main panel is for the J-shape dose response. Insets show J-shape and
 14 hockey-stick shape representations at the low end of the flux range. The long
 15 arrow denotes the upper end of the flux range for which the empirical unit-length
 16 labeling data are available for use in the clonal growth model. α_{\max} is the value of
 17 α_N at the maximum formaldehyde flux delivered at 15 ppm exposure and
 18 estimated by optimizing against the tumor incidence data. $\alpha_I < \alpha_N$ for flux greater
 19 than the value indicated by the small vertical arrow. Conolly et al. (2004, 2003)
 20 assumed $\beta_I = \alpha_N$ at all flux values.

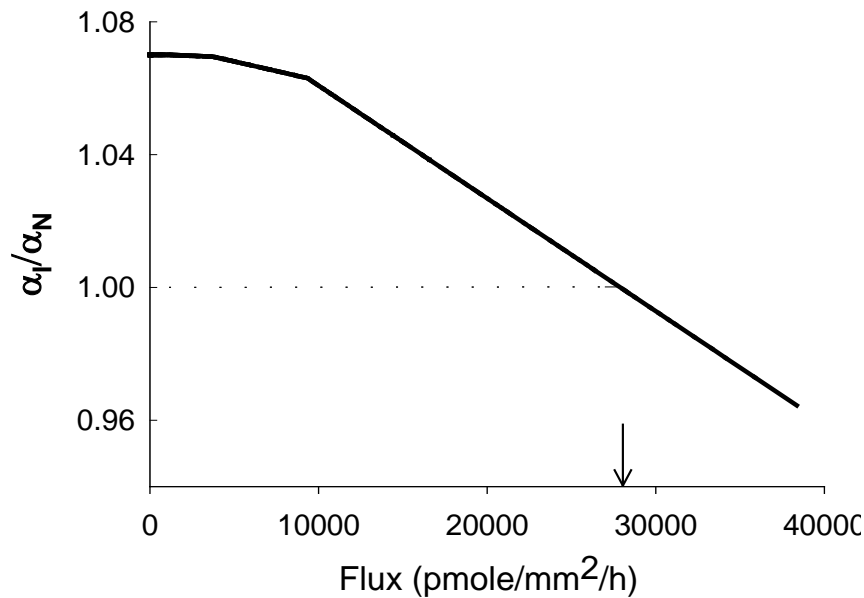
21
 22 Source: Subramaniam et al. (2008).
 23

1 **D.6. INITIATED CELL DIVISION AND DEATH RATES**

2 The pool of cells used for obtaining the LI data in Monticello et al. (1996, 1991) consists
 3 of largely normal cells with perhaps increasing numbers of initiated cells at higher exposure
 4 concentrations. Since the division rates of initiated cells in the nasal epithelium, either
 5 background or formaldehyde exposed, could not be inferred from the available empirical data,
 6 Conolly et al. (2003) made what they perceived to be a biologically reasonable assumption for
 7 α_I , assuming α_I to be linked to α_N via a two-parameter function:

8
 9
$$\alpha_I = \alpha_N \times \{multb - multc \times \max[\alpha_N - \alpha_{N(basal)}, 0]\} \tag{2}$$

10 where $\alpha_N \equiv \alpha_N(\text{flux})$, $\alpha_{N(basal)}$ is the estimated average cell division rate in unexposed normal
 11 cells, and multb and multc are unknown parameters estimated by likelihood optimization against
 12 the tumor data.² The value of $\alpha_{N(basal)}$ was equal to 3.39×10^{-4} hours⁻¹ as determined by Conolly
 13 et al. (2003) from the raw averaged LI data. The ratio α_I/α_N is plotted against flux in Figure D-2,
 14 and $\alpha_I(\text{flux})$ is shown by the dotted line in Figure D-1.
 15



16
 17
 18 **Figure D-2. Flux dependence of ratio of initiated and normal cell replication**
 19 **rates (α_I/α_N) in CIIT model.**

20 Note: Cell replication rate of initiated cells is less than normal cell replication rate
 21 at flux exceeding the value denoted by the arrow. By assumption, the y-axis also
 22 represents (α_I/β_I) .

23 Source: Subramaniam et al. (2008).
 24

2 multb and multc were equal to 1.072 and 2.583, respectively (J-shaped α_N), and 1.070 and 2.515, respectively (hockey-stick shaped α_N).

This document is a draft for review purposes only and does not constitute Agency policy.

1 Death rates of initiated cells (β_I) are assumed to equal the division rates of normal cells
2 for all formaldehyde flux values, that is

$$\beta_I(\text{flux}) = \alpha_N(\text{flux}) \quad (3)$$

3
4
5
6 Conolly et al. (2003) stated that this formulation for α_I and β_I provided the best fit of the
7 model to the tumor data.

8 9 **D.7. STRUCTURE OF THE CIIT HUMAN MODEL**

10 Subsequent to the BBDR model for modeling rat cancer, Conolly et al. (2004) developed
11 a corresponding model for humans for the purpose of extrapolating the risk to humans estimated
12 by the rat model. Also, rather than considering only nasal tumors, it is used to predict the risk of
13 all human respiratory tumors. DPXs observed at proximal portions of the rhesus monkey LRT
14 (Casanova et al., 1991) suggested that the LRT may be at risk in addition to the URT. In
15 addition, some epidemiologic studies (Gardner et al., 1993; Blair et al., 1990, 1986) reported an
16 increase in lung cancer associated with formaldehyde exposure, while others reported no such
17 increases (Collins et al., 1997; Stayner et al., 1988). The human model for formaldehyde
18 carcinogenicity (Conolly et al., 2004) is conceptually very similar to the rat model and follows
19 the schematic in Figure 5-11, Chapter 5. The following points need to be noted:

- 20
- 21 • The model does not incorporate any data on human responses to formaldehyde exposure.
 - 22 • The model is based on an anatomically realistic representation of the human nasal
23 passages (in a single individual) and an idealized representation of the LRT. Local
24 formaldehyde flux to respiratory tissue is estimated by a CFD model for humans
25 (Subramaniam et al., 1998; Kimbell et al., 2001a; Overton et al., 2001).
 - 26 • Rates of cell division and cell death are, with a minor modification, assumed to be the
27 same in humans as in rats.
 - 28 • The concentration of formaldehyde-induced DPXs in humans is estimated by scaling up
29 from values obtained from experiments in the F344 rat and rhesus monkey. This scaling
30 up was discussed in chapter 3.
 - 31 • The statistical parameters for the human model are either estimated by fitting the model
32 to the human background data, assumed to have the same value as obtained in the rat
33 model, or, in one case, fixed at a value suggested by the epidemiologic literature. The
34 delay, D , is fixed at 3.5 years, based on a fit to the incidence of lung cancer in a cohort of
35 British doctors (Doll and Peto, 1978). The two other parameters in the rat model that

This document is a draft for review purposes only and does not constitute Agency policy.

1 affect the background rate of cancer (multb and μ_{basal}) are estimated by fitting to U.S.
2 cancer incidence or mortality data. These parameters affect the baseline values for the
3 human α_I , μ_N , and μ_I . Since α_{max} , multfc , and KMU do not affect the background cancer
4 rate, they cannot be estimated from the (baseline) U.S. cancer incidence rates. Therefore,
5 in Conolly et al. (2004, 2003), α_{max} and multfc are assumed to have the same values in
6 humans as in rats, and the human value for KMU is obtained by assuming that the ratio
7 $\text{KMU}/\mu_{\text{basal}}$ is invariant across species. Thus,
8

$$9 \quad \text{KMU}_{(\text{human})} = \text{KMU}_{(\text{rat})} \times \frac{\mu_{\text{Nbasal}(\text{human})}}{\mu_{\text{Nbasal}(\text{rat})}} \quad (4)$$

This page intentionally left blank.

Appendix E

APPENDIX E

EVALUATION OF BBDR MODELING OF NASAL CANCER IN THE F344 RAT: CONOLLY ET AL. (2003) AND ALTERNATIVE IMPLEMENTATIONS

A biologically based dose-response model for formaldehyde-induced cancer was in a series of papers and in a health assessment report (CIIT model) (Conolly et al., 2004, 2003, 2000; Conolly, 2002; Kimbell et al., 2001a, b; Overton et al., 2001; CIIT, 1999). The model structure, notations, and calibration have been described in Appendix D. In Chapter 5, an evaluation of the uncertainties of this model and alternative approaches based on its conceptual framework was presented in a summary form. This Appendix provides the relevant details of that evaluation and presents a range of dose-response curves for tumor risk in the rat. It is divided into the following major sections. First, an overview of all the issues evaluated is provided in tabular form. The rest of the Appendix then presents only those issues which have a significant impact on model predictions. These issues pertain to the use of history controls, the uncertainty and variability in the dose-response for normal cell-replication rates, and sensitivity of model results to uncertainty in the kinetics of initiated cells. The issues have significant impact on mode of action inferences, and this is discussed in some detail.

E.1. TABULATION OF ALL ISSUES EVALUATED IN THE RAT MODELS

Table E-1 summarizes model uncertainties and their impact as evaluated by EPA. The key uncertainties are discussed in considerably more detail in additional sections in this Appendix and in published manuscripts as denoted in the tables.

E.2. Statistical Methods Used in Evaluation

Parameters of the alternate models shown here were estimated by maximizing the likelihood function defined by the data (Cox and Hinkley, 1974). Such estimates are referred to as maximum likelihood estimates (MLEs). Statistical confidence bounds were computed by using the profile likelihood method (Crump, 2002; Cox and Oakes, 1984; Cox and Hinkley, 1974). In this approach, an asymptotic $100(1 - \alpha)\%$ upper (lower) statistical confidence bound for a parameter, β , in the animal cancer model is calculated as the largest (smallest) value of β that satisfies

$$2[L_{max} - L^*(\beta)] = \chi_{1-2\alpha} \quad (5)$$

This document is a draft for review purposes only and does not constitute Agency policy.

Table E-1. Evaluation of assumptions and uncertainties in the CIIT model for nasal tumors in the F344 rat

Assumptions, approach, and characterization of input data	Rationale	EPA evaluation	Further elaboration^a
Hoogenveen et al. (1999) solution method, which is valid only for time-independent parameters, is accurate enough.	Errors due to this assumption thought to be significant only at high concentration and not at human exposures.	EPA implemented a solution method valid for time-dependent parameters. Results did not differ significantly from those obtained assuming Hoogenveen et al.(1999) solutions. Caveat: Impact not evaluated for the case where cell replication rates vary in time.	Crump et al. (2006); Subramaniam et al. (2007)
All SCC tumors are rapidly fatal; no incidental tumors.	Death is expected to occur typically within 1–2 weeks of observed tumor (personal communication with R. Conolly).	1) Overall, assumption does not impact model calibration or prediction. 2) However, since 57 animals were observed to have tumors at interim sacrifice times, EPA implementation distinguished between incidental and fatal tumors. Time lag between observable tumor and time of death was significant compared to time lag between first malignant cell and observable tumor.	Subramaniam et al. (2007)
Historical controls from entire NTP database were lumped with concurrent controls in studies.	Data is on control animals, and number is large (7,684). Therefore, intercurrent mortality was not expected to be substantial.	1) Tumor incidence in “all NTP” 10-fold higher than in “all inhalation NTP” controls. Including all NTP controls is considered inappropriate. 2) Low-dose response curve sensitive to use of historical controls. 3) Model inference on relevance of formaldehyde’s mutagenic potential to its carcinogenicity varies from “insignificant” to “highly significant,” depending on controls used. (See Appendix F for impact on human risk.)	Table E-2; Subramaniam et al. (2007); Sec E.3.1
LI was derived from experimentally measured ULLI.	Derived from correlating ULLI to LI measured in same experiment.	Significant variation in number of cells per unit length of basement membrane. Spread in ULLI/LI ~25%. Impact on risk not evaluated.	Subramaniam et al. (2008);

Table E-1. Evaluation of assumptions and uncertainties in the CIIT model for nasal tumors in the F344 rat

Assumptions, approach, and characterization of input data	Rationale	EPA evaluation	Further elaboration^a
Pulse and continuous labeling data combined in deriving α_N from LI.	Continuous LI normalized by ratio of pulse to continuous values for control data.	Formula used for deriving α_N from LI is not applicable for pulse labeling data. Pulse labeling is measure of number of cells in S-phase, not of their recruitment rate into S-phase; not enough information to derive α_N from pulse data. Impact on risk predictions could not be evaluated.	Subramaniam et al. (2008); Sec E.3.2.2
To construct dose response for α_N , labeling data were weighted by exposure time (t) and averaged over all nasal sites (TWA). Flux at an exposure concentration was averaged over all nasal sites.	Site-to-site variation in LI large and did not vary consistently with flux. No reasonable approach available for incorporating time variation in labeling in interspecies extrapolation.	<ol style="list-style-type: none"> 1) TWA assigns low weight to early time LI, but α_N for early t is very important to the cancer process. Since pulse ULLI was used for $t < 13$ weeks, impact of these ULLIs on risk could not be evaluated. 2) Time dependence in α_N derived from continuous ULLI does not significantly impact model predictions. 3) Site-to-site variation of α_N at least 10-fold and has major impact on model calibration. 10-fold variation in tumor incidence data across sites. 4) Large differences in number of cells across nasal sites (Table E-3), so averaging over sites is problematic. 5) Histologic changes, thickening of epithelium and metaplasia occur at later times for the higher dose and would affect replication rate. 	Figures E-1, E-2, E-3; Subramaniam et al. (2008); Sec E.3.2.3

Table E-1. Evaluation of assumptions and uncertainties in the CIIT model for nasal tumors in the F344 rat

Assumptions, approach, and characterization of input data	Rationale	EPA evaluation	Further elaboration^a
Steady-state flux estimates not affected by airway and tissue reconfiguration due to long-term dosing.	Histopathologic changes not likely to be rate-limiting factors in dosimetry.	1) Thickening of epithelium and squamous metaplasia occurring at later times for the higher dose will reduce tissue flux. Not incorporated in model. 2) These effects will push regions of higher flux to more posterior regions of respiratory tract. Likely to affect calibration of rat model. Uncertainty not evaluated quantitatively. 3) Calibration of PBPK model for DPXs seen to be highly sensitive to tissue thickness.	Kimbell et al (1997); Subramaniam et al. (2008)
TWA $\alpha_N(\text{flux})$ rises above baseline levels only at cytolethal dose. Above such dose, $\alpha_N(\text{flux})$ rises sharply due to regenerative proliferation.	Variability in $\alpha_N(\text{flux})$ rate is represented by also considering hockey-stick (threshold in dose) when TWA indicates J-shape (inhibition of cell division) description of $\alpha_N(\text{flux})$.	1) Uncertainty and variability in α_N quantitatively evaluated to be large. In addition, several qualitative uncertainties in characterization of $\alpha_N(\text{flux})$ from LI. 2) Several dose-response shapes, including a monotonic increasing curve without a threshold, were considered in order to adequately describe highly dispersed cell replication data. Substantial impact on low dose risk, including negative added risk.	Figures E-1, E-2, E-3, E-4, E-5; Subramaniam et al. (2008); Sec E.3.2

Table E-1. Evaluation of assumptions and uncertainties in the CIIT model for nasal tumors in the F344 rat

Assumptions, approach, and characterization of input data	Rationale	EPA evaluation	Further elaboration^a
<p>Dose response for α_I was obtained from α_N, assuming ratio (α_I/α_N) to be a two-parameter function of flux (see Figures 5-7, 5-9). Parameters were estimated by optimizing model predictions against tumor incidence data.</p>	<p>(α_I/α_N) was >1.0 in line with the notion of I cells possessing a growth advantage over N cells. Satisfies Occam's razor principle (Conolly et al., 2009).</p>	<p>1) Estimated (α_I/α_N) in CIIT modeling is <1.0 (growth disadvantage) for higher flux values and is >1.0 only at lower end of flux range in model (see Figure 5-9). 2) Since there are no data to inform α_I, sensitivity of risk estimates to various functional forms was evaluated. Risk estimates for the rat were extremely sensitive to alternate biologically plausible assumptions for α_I(flux) and varied by many orders of magnitude at ≤ 1 ppm, including negative risk. All these models described tumor incidence data and cell replication and DPX data equally well.</p>	<p>Figures D-2, E-5, E-6; Subramaniam et al. (2008); Crump et al. (2009, 2008); Sec E.3.3</p>
<p>Death rate of I cells β_I(flux) assumed = division rate of N cells α_N(flux).</p>	<p>Based on homeostasis ($\alpha_N = \beta_N$) and assumption that formaldehyde is equally cytotoxic to N cells and I cells. Satisfies Occam's Razor principle (Conolly et al., 2009).</p>	<p>1) In general, data indicate I cells are more resistant to cytolethality and that ADH3 clearance capacity is greater in transformed cells. Therefore, plausibility of assumption ($\beta_I = \alpha_N$) is tenuous. 2) Alternate assumption, β_I proportional to α_I, was examined. Risk estimates extremely sensitive to assumptions on β_I (see Figure 5-12).</p>	<p>Subramaniam et al. (2008); Crump et al. (2009, 2008); Sec E.3.3</p>
<p>DPX is dose surrogate for formaldehyde mutagenic potential. DPX clearance is rapid and complete in 18 hours.</p>	<p>Casanova et al. (1994).</p>	<p>Half-life for DPX clearance in in vitro experiments on transformed cell lines was sevenfold longer than estimated by Conolly et al. (2004, 2003) and perhaps 14-fold longer with normal (non-transformed) human cells. Some DPX accumulation therefore likely. However, model calibration and dose response in rat is insensitive to this uncertainty.</p>	<p>Quievryn and Zhitkovich, (2000); Subramaniam et al. (2007); Chap 3</p>

Table E-1. Evaluation of assumptions and uncertainties in the CIIT model for nasal tumors in the F344 rat

Assumptions, approach, and characterization of input data	Rationale	EPA evaluation	Further elaboration^a
Formaldehyde mutagenic action takes place only while DPXs are in place.		DNA lesions remain after DPX removal. DPX induces further DNA and protein damage. Potential for formaldehyde-induced mutation after DPX clearance. Thus, formaldehyde mutagenicity may be underrepresented. Could not quantitatively evaluate uncertainty (no data on clearance of secondary lesions).	Barker et al. (2005); Speit and Schmid (2006); Subramaniam et al. (2008); Chap 4

^aReferences stated here are in addition to Conolly et al. (2004, 2003).

Note: Risk estimates discussed in this table are for the F344 rat.

1 where L indicates the likelihood of the rat bioassay data, L_{max} is its maximum value, $L^*(\beta)$ is, for
2 a fixed value of β , the maximum value of the log-likelihood with respect to all of the remaining
3 parameters, and $x_{1-2\alpha}$ is the 100(1-2 α) percentage point of the chi-square distribution with one
4 degree of freedom. The required bound for a parameter, β , was determined via a numerical
5 search for a value of β that satisfies this equation.

6 The additional risk is defined as the probability of an animal dying from an SCC by the
7 age of 790 days, in the absence of other competing risks of death, while exposed throughout life
8 to a prescribed constant air concentration of formaldehyde, minus the corresponding probability
9 in an animal not exposed to formaldehyde. The MLE of additional risk is the additional risk
10 computed using MLEs of the model parameters.

11 The method described above for computing profile likelihood confidence bounds cannot
12 be used with additional risk because additional risk is not a parameter in the cancer model.
13 Instead, an asymptotic 100(1 - α)% upper (lower) statistical confidence bound for additional risk
14 was computed by finding the parameter values that presented the largest (smallest) value of
15 additional risk, subject to the inequality

$$16 \quad 2[L_{max} - L] \leq x_{1-2\alpha} \quad (6)$$

17
18 being satisfied, with the resulting value of additional risk being the required bound. This
19 procedure was implemented through use of penalty functions (Smith and Coit, 1995). For
20 example, the profile upper bound on additional risk was computed by maximizing the “penalized
21 added risk,” defined as (*additional risk - penalty*), where

$$22 \quad penalty = W \times \{[(L_{max} - L) - x_{1-2\alpha}/2]^+\}^2 \quad (7)$$

23
24 and $[]^+$ equals the quantity in the brackets whenever it is positive and zero otherwise. The
25 multiplicative weight, W , was selected by trial and error so that the final solution satisfied the
26 following equation sufficiently well.

$$27 \quad 2(L_{max} - L) = x_{1-2\alpha} \quad (8)$$

28
29
30
31
32 The computer code was written in Microsoft Excel® 2002 SP3 Visual Basic. Either the
33 regular Excel Solver or the Frontline Systems Premium Solver® was used to make the required
34 function optimizations. Computation of confidence bounds was highly computationally
35 intensive, and, consequently, confidence bounds were computed only for selected parameters in

This document is a draft for review purposes only and does not constitute Agency policy.

1 selected runs. For select cases, the bootstrap method was also used to calculate confidence
2 bounds in order to confirm their accuracy. Values so calculated were found to be in agreement
3 with those calculated by using the likelihood method.

4 5 **E.3. PRIMARY UNCERTAINTIES IN BBDR MODELING OF THE F344 RAT DATA**

6 The evaluation of the CIIT model and alternatives to this model that were implemented
7 for the F344 rat will be discussed first. Of the issues tabulated above, the following uncertainties
8 in the modeling of the F344 rat data will be discussed in considerably more detail: use of
9 historical controls, uncertainty and variability in characterizing cell replication rates from the
10 labeling data, and uncertainty in model specification of initiated cell kinetics.

11 In their evaluation, Subramaniam et al. (2007) first attempted to reproduce the Conolly et
12 al. (2003) results under similar conditions and assumptions as employed in their paper, which
13 included the assumption that tumors were rapidly fatal. Figure 5-12 in Chapter 5 shows the
14 results for this case. The predicted probabilities shown in this figure were obtained by
15 Subramaniam et al. (2007) by using the source code made available by Dr. Conolly. These are
16 compared with the best-fitting model and plotted against the Kaplan-Meier (KM) probabilities.
17 Although the results are largely similar, there are some differences (Subramaniam et al., 2007).

18 Given the scope of issues to examine for the uncertainty analyses, the evaluation
19 proceeded in stages. First, the Hoogenveen et al. (1999) solution was replaced by one that is
20 valid for a model with time varying parameters (first entry in Table E-1), and tumors found at
21 scheduled sacrifices were assumed to be incidental rather than fatal (second entry in Table E-1).
22 Second, weekly averaged solutions for DPX concentration levels were used instead of hourly
23 varying solutions (predicted by a PBPK model). The log-likelihood values and tumor
24 probabilities remained essentially unchanged. Upon quantitative evaluation, these factors,
25 although important from a methodological point of view, were not found to be major
26 determinants of either calibration or prediction of the model for the F344 rat data (Subramaniam
27 et al., 2007).

28 Subramaniam et al. (2007), as in Georgieva et al. (2003), used the DPX clearance rate
29 constant obtained from in vitro data instead of the assumption in Conolly et al. (2003) that all
30 DPXs cleared within 18 hours (Subramaniam et al., 2007). With this revision, weekly average
31 DPX concentrations were larger than those in Conolly et al. (2003) by essentially a constant ratio
32 equal to 4.21 (range of 4.12–4.36) when averaged over flux bin and exposure concentrations.
33 Accordingly, cancer model fits to the rat tumor incidence data using the two sets of DPX
34 concentrations (everything else remaining the same) provided very similar parameter estimates,
35 except that the parameter KMU_{rat} in equation 1 (and equation 4) was 4.23 times larger with the

1 Conolly et al. (2003) DPX concentrations. In other words, the product $KMU \times DPX$ remained
2 substantially unchanged. However, the different clearance rate does significantly impact the
3 scale-up of the two-stage clonal growth model to the human.

4 After making the above modifications, the impact of the following uncertainties, which
5 had a large impact on modeling, was examined sequentially.

7 **E.3.1. Sensitivity to Use of Historical Controls**

8 **E.3.1.1. *Use of Historical Controls***

9 Conolly et al. (2003) combined the historical controls arising from the entire NTP
10 database of bioassays. Tumor and survival rates in control groups from different NTP studies
11 are known to vary due to genetic drift in animals over time and differences in laboratory
12 procedures, such as diet, housing, and pathological procedures (Haseman, 1995; Rao et al.,
13 1987). In order to minimize extra variability when historical control data are used, the current
14 NTP practice is to limit the historical control data, as far as possible, to studies involving the
15 same route of exposure and to use historical control data from the most recent studies (Peddada
16 et al., 2007).

17 Bickis and Krewski (1989) analyzed 49 NTP long-term rodent cancer bioassays and
18 found a large difference in determinations of carcinogenicity, depending on the use of historical
19 controls with concurrent control animals. The historical controls used in the CIIT modeling
20 controls came from different rat colonies and from experiments conducted in different
21 laboratories over a wide span of years, so it is clearly problematic to assume that background
22 rates in these historical control animals are the same as those in the concurrent control group.
23 There are considerable differences among the background tumor rates of SCCs in all NTP
24 controls ($13/7,684 = 0.0017$), NTP inhalation controls ($1/4,551 = 0.0002$), and concurrent
25 controls ($0/341 = 0.0$). The rate in all NTP controls is significantly higher than that in NTP
26 inhalation controls ($p = 0.01$, Fisher's exact test). Given these differences, the inclusion of any
27 type of historical controls is problematic and is thought to have limited value if these factors are
28 not controlled for (Haseman, 1995).

30 **E.3.1.2. *Influence on Model Calibration and on Human Model***

31 To investigate the effect of including historical controls in the CIIT model, the analyses
32 in Subramaniam et al. (2007) were conducted by using the following sets of data for controls (the
33 fraction of animals with SCCs is denoted in parentheses): only concurrent controls ($0/341$),
34 concurrent controls plus all the NTP historical control data used by Conolly et al.(2003)

1 (13/8,031), and concurrent controls plus data from historical controls obtained from NTP
2 inhalation studies (1/4,949) (NTP, 2005).³

3 The results of the evaluation are shown in Table E-2. For these analyses, the same
4 normal cell replication rates and the same relationship (see eq 2) between initiated cell and
5 normal cell replication rates as used in Conolly et al. (2003) were used. In all cases, weekly
6 averaged values of DPX concentrations were used. Model fits to the tumor incidence data were
7 similar in all cases (see Figure 5-12 in Chapter 5 and Subramaniam et al. [2007] for a more
8 complete discussion). The biggest influence of the control data was seen to be on the estimated
9 basal mutation rate in rats, $\mu_{Nbasal(rat)}$, which, in turn, influences the estimated mutation effect in
10 humans through eq 4 (Appendix D). α_{max} was also seen to be a sensitive parameter and is
11 discussed later. See Subramaniam et al. (2007) for other parameters in the calibration.

12 The ratio KMU/μ_{Nbasal} is of particular interest because extrapolation to human in Conolly
13 et al. (2004) assumed its invariance as given by eq 4 (Appendix D). Now, μ_{Nbasal} in the human is
14 estimated independently by fitting a scaled-up version of the two-stage model to human baseline
15 rates of tumor incidence. Thus, a decrease in the value of μ_{Nbasal} estimated in the rat modeling
16 increases the formaldehyde-induced mutational effect in the human.

17 While the MLE of KMU/μ_{Nbasal} is zero in the CIIT animal model (Conolly et al., 2003), it
18 takes a range of values from 0 to 0.9 mm³/pmol and undefined (or infinite, when $\mu_{Nbasal} = 0$) in
19 the various cases examined in this paper. The 95% upper confidence bound on this ratio ranges
20 from 0.25–6.2 (these values would be four times larger had the Conolly et al. [2003] DPX
21 concentrations been used) to infinite. Thus, the extrapolation to human risk by using the
22 approach in Conolly et al. (2004) becomes particularly problematic when only concurrent
23 controls are used, because then the mutational contribution to formaldehyde-induced risk in
24 humans becomes unbounded. This issue will be discussed again toward the end of the
25 discussion on historical controls.

³ Three animals in the inhalation historical controls were diagnosed with nasal SCC. Of these, two of the tumors were determined to have originated in tissues other than the nasal cavity upon further review (Dr. Kevin Morgan and Ms. Betsy Gross Bermudez, personal communication). These two tumors were therefore not included on the advice of Dr. Morgan. See Subramaniam et al. (2007) for more details.

This document is a draft for review purposes only and does not constitute Agency policy.

Table E-2. Influence of control data in modeling formaldehyde-induced cancer in the F344 rat

Case	A	D	B	E	C	F
Control animals (combined with concurrent controls)	All NTP historical^a	All NTP historical^a	NTP inhalation historical^a	NTP inhalation historical^a	Concurrent only^a	Concurrent only^a
Cell replication dose response	J-shaped	Hockey stick	J-shaped	Hockey stick	J-shaped	Hockey stick
Log-likelihood	-1692.65	-1693.68	-1,493.21	-1,493.35	-1,474.29	-1,474.29
$\mu_{N_{\text{basal}}}$	1.87×10^{-6}	2.12×10^{-6}	7.32×10^{-7}	9.32×10^{-7}	0.0	0.0
KMU	1.12×10^{-7}	0.0	6.84×10^{-7}	6.18×10^{-7}	1.20×10^{-6}	1.20×10^{-6}
$KMU/\mu_{N_{\text{basal}}}$	0.06 (0.0, 0.40)	0.0 (0.0, 0.25)	0.94 (0.26, 6.20)	0.66 (0.2, 5.20)	∞ (0.42, ∞)	∞ (0.41, ∞)
α_{max}	0.045 (0.029, 0.045)	0.045 (0.029, 0.045)	0.045 (0.026, 0.045)	0.045 (0.027, 0.045)	0.045 (0.027, 0.045)	0.045 (0.027, 0.045)

^aValues in parentheses denote lower and upper 90% confidence bounds.

Source: Adapted from Subramaniam et al. (2007).

1 It may be noted, however, that absence of tumors in the limited number of concurrent
2 animals does not imply that the calculation will necessarily predict a zero background
3 probability of tumor (i.e., a parameter estimate of $\mu_{N\text{basal}} = 0$). We observed such a
4 counterexample estimate for $\mu_{N\text{basal}}$ in simulations involving the alternate dose-response curves
5 for α_N and α_I that are discussed later. Nonetheless, when $\mu_{N\text{basal}} = 0$, an upper bound for $\mu_{N\text{basal}}$
6 using the concurrent controls can be inferred. Accordingly, the 90% statistical lower confidence
7 bound on the ratio $\text{KMU}/\mu_{N\text{basal}}$ is also reported in Table E-2. Such a value would of course
8 provide a lower bound on risk by using this model and would therefore not be conservative.

9 Conolly et al. (2003) estimated KMU to be zero for both the hockey-stick and J-shape
10 cell replication models. However, the estimate for the coefficient KMU (obtained using the
11 solution of Crump et al. [2005]) is zero only for the case of the model with the hockey-stick
12 curve for cell replication and with control data as used by Conolly et al. (2003). It is positive in
13 all other cases and statistically significantly so in all cases in which either inhalation control data
14 or concurrent controls were used. With concurrent controls only and the J-shape cell replication
15 model, the MLE estimate for KMU (1.2×10^{-6}) is larger than the statistical upper bound
16 obtained by Conolly et al. (2003) (8.2×10^{-7}). It should also be kept in mind that the estimate
17 would be about 4.2 times larger still had the Conolly et al. (2003) DPX model been used.

18 19 **E.3.1.3. Influence on Dose-Response Curve**

20 Subramaniam et al. (2007) showed that inclusion of historical controls had a strong
21 impact on the tumor probability curve below the range of exposures over which tumors were
22 observed in the formaldehyde bioassays. As shown there, the MLE probabilities for occurrence
23 of a fatal tumor at exposure concentrations below 6 ppm were roughly an order of magnitude
24 higher when all the NTP historical controls were used, compared with MLE probabilities
25 predicted when historical controls were drawn only from inhalation bioassays, and many orders
26 of magnitude higher than MLE probabilities predicted when only concurrent controls were used
27 in the analysis. (Note that this comparison should not be inferred to apply to upper bound risk
28 estimates since there were many fewer concurrent than historical controls, so error bounds could
29 be much larger in the case where concurrent controls were used.)

30 However, as shown by these authors, model fits to the tumor data in the 6–15 ppm
31 exposure concentration range were qualitatively indifferent to which of these control data sets
32 was used. This observation emphasizes the statistical aspect of the CIIT modeling—that
33 significant interplay among the various adjustable parameters allows the model to achieve a
34 good fit to the tumor incidence data independent of the control data used. On the other hand, the
35 results in Subramaniam et al. (2007) show that changes in the control data affect parameter

1 KMU, resulting in significantly different tumor predictions at lower exposure concentrations.
2 Therefore, the strong influence of using all the NTP historical controls on the low-dose region of
3 the time-to-tumor curves presented in Subramaniam et al. (2007) suggests that large
4 uncertainties may arise in extrapolating to both human and rat (in the low-dose region) from
5 such considerations alone.
6

7 **E.3.1.4. Problem Including 1976 Study for Inhalation Historical Control**

8 A crucial point needs to be noted with regard to the use of inhalation NTP historical
9 controls (i.e., cases B and E) in the two-stage clonal growth modeling. The single relevant tumor
10 in the NTP inhalation studies came from the very first NTP inhalation study, dated 1976, and the
11 animals in this study were from Hazelton Laboratories, whereas the concurrent animals were all
12 from Charles River Laboratories. Similar problems arise with inclusion of several other NTP
13 inhalation studies. As mentioned before, genetic and other time-related variation can lead to
14 different tumor and survival rates, and in general it is recommended that use of historical
15 controls be restricted to the same kind of bioassays and to studies within a 5–7 year span of the
16 concurrent animals (Peddada et al., 2007). Thus, it is problematic to assume that the tumor in
17 the 1976 NTP study is representative of the risk of SCCs in the formaldehyde bioassays. Even if
18 it were appropriate to consider the 1976 study, this leads to the unstable situation in which,
19 despite all of the “upstream” mechanistic information used to construct the BBDR model, the
20 only piece of data that might keep the model predictions of human risk bounded is a single tumor
21 found among several thousand rats from NTP bioassays (Crump et al., 2008). In summary,
22 although it can be argued that the rate of SCCs among the controls in the rat bioassay is probably
23 not zero, it is also problematic to assume that this rate can be adequately represented by the
24 background rate in NTP historical controls or even in NTP inhalation historical controls.
25

26 **E.3.1.5. Inference on MOA**

27 Subramaniam et al. (2007) also examined the contribution of the DPX component (which
28 represents the directly mutagenic potential of formaldehyde in the model) to the calculated tumor
29 probability, choosing for their case study the optimized models that use the NTP inhalation
30 control data. In the range of exposures where tumors were observed (6.0–15.0 ppm), the DPX
31 term was found to be responsible for 58–74% of the added tumor probability. Below 6.0 ppm
32 the estimated DPX contribution was extremely sensitive to the shape of α_n and varied
33 between 2 and 80%.

34 The CIIT BBDR cancer modeling has contributed to the weight-of-evidence process in
35 various formaldehyde risk assessment efforts and papers by lending weight to the argument that

1 the direct mutations induced by formaldehyde are relatively irrelevant compared to the
2 importance of cytotoxicity-induced cell proliferation in explaining the observed tumorigenicity
3 in rodent bioassays and in projecting those observations to human exposures (Conolly et al.,
4 2004, 2003; Slikker et al., 2004; Bogdanffy et al., 2001, 1999; Conolly, 1995). The reanalyses in
5 Subramaniam et al. (2007) (in particular, the results in the above paragraph) indicate that, if the
6 CIIT mathematical modeling were utilized to inform this debate, it would in fact indicate the
7 contrary—that a large contribution from formaldehyde’s mutagenic potential may be needed to
8 explain formaldehyde carcinogenicity. This discussion is resumed in the context of uncertainties
9 in model specification for initiated cells.

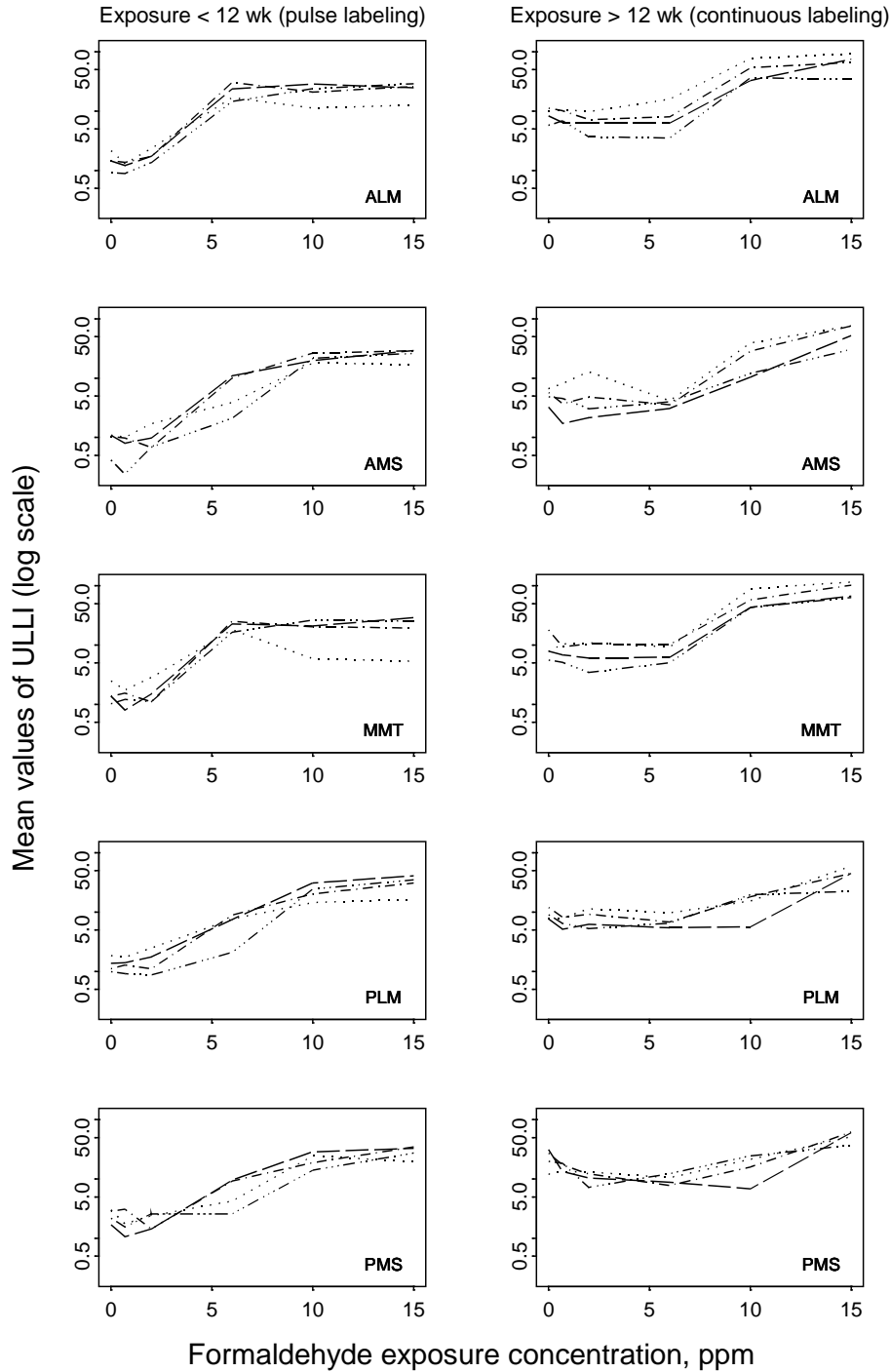
11 **E.3.2. Characterization of Uncertainty-Variability in cell Replication Rates**

12 **E.3.2.1. Dose-Response for α_N as Used in the CIIT Clonal Growth Modeling**

13 Monticello et al. (1996, 1991) used ULLI to quantify cell replication within the respiratory
14 epithelium. ULLI is a ratio between a count of labeled cells and the corresponding length (in
15 millimeters) of basal membrane examined, whereas the per-cell LI is the ratio of labeled cells to
16 all epithelial cells, in this case, along some length of basal membrane and its associated layer of
17 epithelial cells. Monticello et al. (1996, 1991) published ULLI values averaged over replicate
18 animals for each combination of exposure concentration, exposure time, and nasal site. These
19 values are plotted in Figure E-1. Conolly et al. (2003) adopted the following procedure in using
20 these values (Subramaniam et al., 2008):

- 21 1. The injection labeled ULLI data were first normalized by the ratio of the average
22 minipump ULLI for controls to the average injection labeled ULLI for controls.
- 23 2. Next, these ULLI average values were weighted by the exposure times in Monticello et
24 al. (1996, 1991) and averaged over the nasal sites. Thus, the data were combined into
25 one TWA for each exposure concentration.
- 26 3. LI was linearly related to the measured ULLI by using data from a different experiment
27 (Monticello et al., 1990) where both quantities had been measured for two sites in the
28 nose.
- 29 4. Cell replication rates of normal cells (α_N) were then calculated as $\alpha_N = (-0.5/t)\log(1 - LI)$
30 (Moolgavkar and Luebeck, 1992), where LI is the labeling index and t is the period of
31 labeling.
- 32 5. This was repeated for each exposure concentration of formaldehyde, resulting in one
33 value of α_N for each exposure concentration.
- 34 6. Correspondingly, for a given exposure concentration, the steady-state formaldehyde flux
35 into tissue, computed by CFD modeling, was averaged over all nasal sites. Thus, the
36 $\alpha_N(\text{flux})$ constructed by Conolly et al. (2003) consisted of a single α_N and a single
37 average flux for each of six exposures.

38 *This document is a draft for review purposes only and does not constitute Agency policy.*



1
2
3
4
5
6
7
8

Figure E-1. ULLI data for pulse and continuous labeling studies.

Note: Data are from pulse labeling study, left-hand side, at 1–42 days of exposure and from the continuous-labeling study, right-hand side, at 13–78 weeks of exposure for five nasal sites ALM, AMS, MMT, PLM, and posterior mid septum [PMS]). Within each graph, lines with more breaks correspond to shorter exposure times. Data source: Monticello et al. (1996, 1991).

This document is a draft for review purposes only and does not constitute Agency policy.

1 This yielded a J-shaped dose-response curve for cell replication (when viewed on a non-
2 transformed scale for α_N), as shown in Figure D-1 (Appendix D) for the full range of flux values
3 used in their modeling. The authors also considered a hockey-stick threshold representation of
4 their J-shaped curve for α_N in order to make a health-protective choice, and the differences
5 between the two can be seen from the insets in Figure D-1. In these curves, the cell replication
6 rate is less than or the same as the baseline cell replication rate at low formaldehyde flux values.
7 The shape of the dose-response curve for cell replication as characterized in Conolly et al.
8 (2003) is seen as representing regenerative cell proliferation secondary to the cytotoxicity of
9 formaldehyde (Conolly, 2002). Considerable uncertainty and variability, both quantitative and
10 qualitative, exist in the use and interpretation of these labeling data for characterizing a dose
11 response for cell replication rates. The primary issues are discussed here. Unlike the preceding
12 sections, these have largely not been published elsewhere, so more details are provided.

13 14 ***E.3.2.2. Uncertainty in the Use of Pulse Labeling Data, and Short-Time Exposure Effects on*** 15 ***Cell Replication***

16 The formula used for obtaining α_N from LI in Conolly et al. (2003) was due to
17 Moolgavkar and Luebeck (1992) who derived this formula for continuous LI, cautioning that it
18 is not applicable for pulse labeled data. However, Conolly et al. (2003) applied this formula to
19 the injection (pulse) labeled data also. Such an application is problematic because 2-hour pulse
20 labeled data represent the pool of cells in S-phase rather than the rate at which cells are recruited
21 to the pool and because the baseline values of α_N obtained in this manner from both data sets
22 differ considerably. As such, we are not aware of any reasonable manner to derive cell
23 replication rates from these pulse data without acquisition of data at additional time points.
24 Therefore, the quantitative analysis of cell replication rates is restricted in this document to the
25 continuous labeled data (Monticello et al., 1996), which does not include measurements made
26 before 13 weeks of exposure.

27 It is unfortunate that the continuous labeled data do not include any early measurements
28 because, as indicated by Figure E-1, the temporal variation in the unit-length LI (ULLI, the raw
29 data) is quite different between the “early time” (left panel) and “later time” (right panel) and
30 these early-time effects may be quite important to the cancer modeling. At the earliest times in
31 the left panel, the data show an increased trend in labeling at 2 ppm for the sites anterior lateral
32 meatus (ALM), anterior medial septum (AMS), posterior lateral meatus (PLM), and medial
33 maxilloturbinate (MMT) relative to control. (Also see the dose-response plotted as a function of
34 flux in Figure E-4 for the 13-week exposure time, where such an increase is generally indicated
35 for low flux values.)

This document is a draft for review purposes only and does not constitute Agency policy.

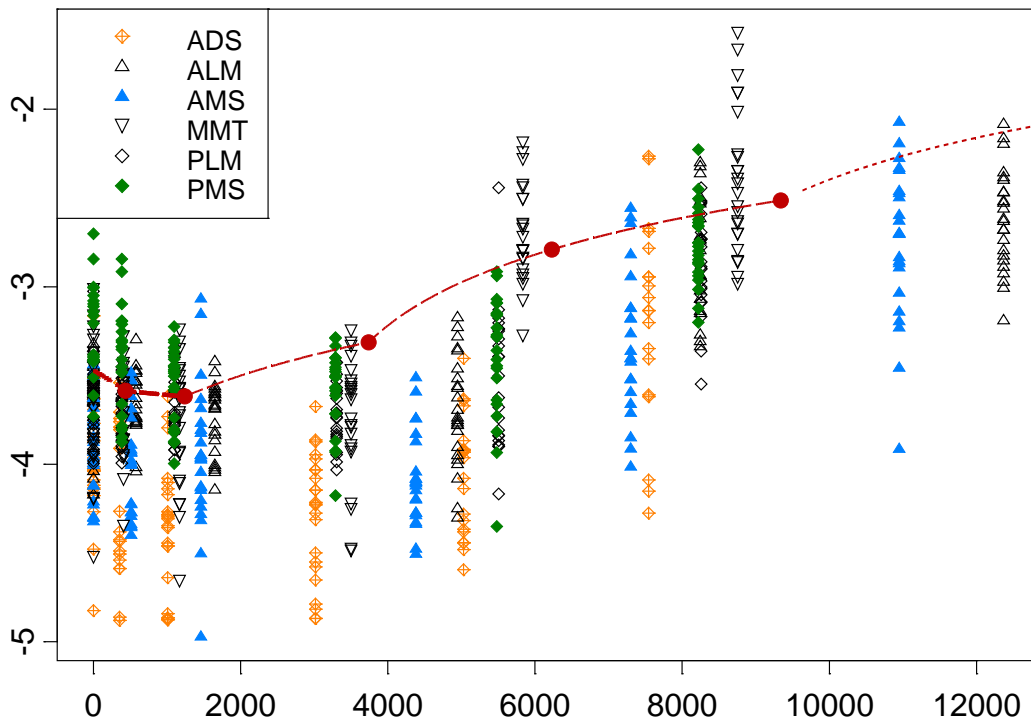
1 The early times would be important if, say, repeated episodic exposures were considered,
2 where adequate time has not elapsed for adaptive effects to take place. Such an exposure
3 scenario may be the norm in the human context. However, the contribution of the early-time
4 labeling data is minimized in the CIIT cancer modeling since the LI was weighted by exposure
5 time. Because of the problems described above in incorporating the pulse-labeled data, the
6 sensitivity analysis will be restricted to only the continuous labeling data.

7 8 **E.3.2.3. Site and Time Variability**

9 In the remainder of this section, the factors that are considered in order to represent the
10 uncertainty and variability in the cell replication data when developing alternate dose-response
11 curves for $\alpha_N(\text{flux})$ will be elaborated. Figure E-2 (from Subramaniam et al., 2008) shows the
12 variability due to replicated animals, exposure times, and nasal sites in the continuous labeled
13 data obtained by Monticello et al. (1996). The ULLI data for individual animals were provided
14 by CIIT. In this figure, $\log \alpha_N$ versus site-specific flux are plotted for six sites and four exposure
15 times for four to six replicate animals in each case. (The mean ULLI over these replicates were
16 shown in Figure E-1 for each site and time as a function of exposure concentration.) It needs to
17 be noted that these nasal sites differ considerably in the number of cells estimated at these
18 locations as shown in Table E-3. Each point in Figure E-2 represents data from a single site for a
19 single animal at a given time. For comparison, the $\alpha_N(\text{flux})$ in Conolly et al. (2003) is also
20 plotted in this figure at their averaged flux values (filled circles). For flux $>9,340 \text{ pmol/mm}^2$ -
21 hour, Conolly et al. (2003) extrapolated this empirically derived $\alpha_N(\text{flux})$ by using a scheme
22 discussed in Appendix D (section D.5) on the upward extrapolation of cell replication rate. The
23 curves shown connecting the filled circles in the figure represent their linear interpolation (long
24 dashes) between the six points. Their linear extrapolation for flux value $>9,340 \text{ pmol/mm}^2$ -hour
25 is also shown (short dashes). Note that the linear interpolation/extrapolation is shown
26 transformed to a logarithmic scale.

27 In Figures E-3, fitted dose-response curves are plotted for $\log_{10}(\alpha_N)$ versus flux with
28 simultaneous confidence limits separately for each time point for two of the largest sites in Table
29 E-3 (ALM and PLM). Note that flux levels are different at each site. Simple polynomial models
30 in flux (as a continuous predictor), with time included as a factor (i.e., a class or indicator
31 variable, τ_i representing the effect of the i^{th} time) were used as follows:

$$\log(\alpha_N) = a + b \times \text{flux} + c \times \text{flux}^2 + d \times \text{flux}^3 + \tau_i \quad (9)$$



1
2
3 **Figure E-2. Logarithm of normal cell replication rate α_N versus**
4 **formaldehyde flux (in units of $\text{pmol}/\text{mm}^2\text{-hour}$) for the F344 rat nasal**
5 **epithelium.**

6
7 Note: Values were derived from continuous unit length labeled data obtained by
8 Monticello et al. (1996) for four to six individual animals at all six nasal sites
9 (legend, sites as denoted in original paper) and four exposure durations (13, 26,
10 52, 78 weeks). Each point represents a measurement for one rat, at one nasal site,
11 and at a given exposure time. Filled red circles: $\alpha_N(\text{flux})$ used in Conolly et al.
12 (2003) plotted at their averaged flux values (see text for details). Long dashed
13 lines: their linear interpolation between points. Short dashed line: their linear
14 extrapolation for flux value $>9,340 \text{ pmol}/\text{mm}^2\text{-hour}$ (see Figure D-1 for full range
15 of extrapolation). Linear interpolation/extrapolation is shown with y-axis
16 transformed to logarithmic scale.

17
18 Source: Subramaniam et al. (2008).
19

1
2

Table E-3. Variation in number of cells across nasal sites in the F344 rat

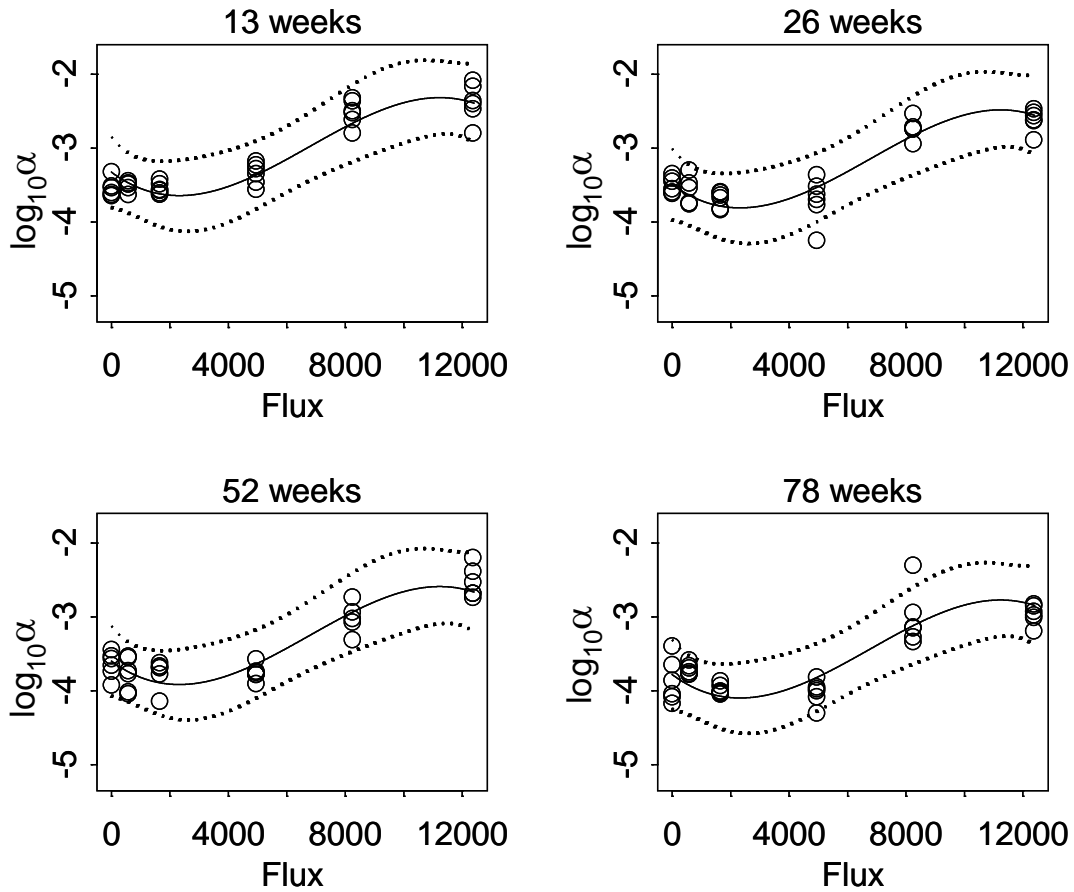
Nasal site	No. of cells
Anterior lateral meatus	976,000
Posterior lateral meatus	508,000
Anterior mid septum	184,000
Posterior mid septum	190,000
Anterior dorsal septum	128,000
Anterior medial maxilloturbinate	104,000

3
4
5
6
7

Note: Mean number of cells in each side of the nose of control animals.

Source: Monticello et al. (1996).

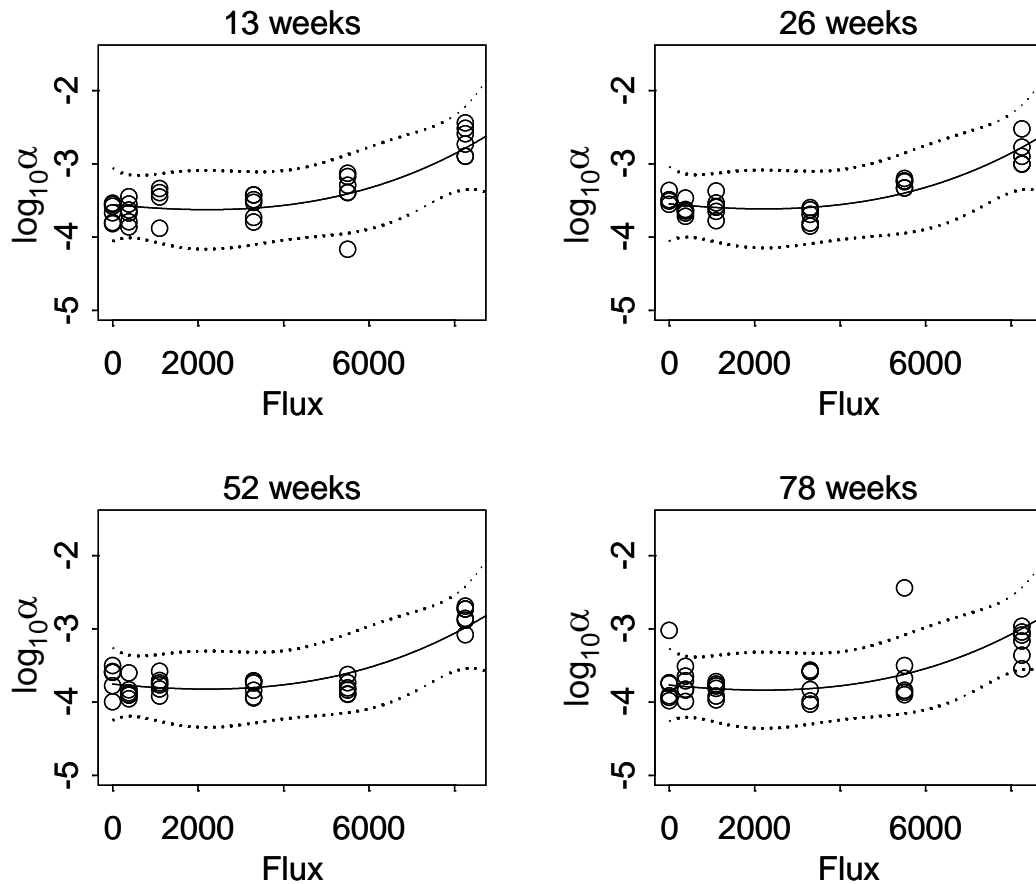
1



2
3
4
5
6
7

Figure E-3A. Logarithm of normal cell replication rate versus formaldehyde flux with simultaneous confidence limits for the ALM.

Source: Subramaniam et al. (2008).



1
2 **Figure E-3B. Logarithm of normal cell replication rate versus formaldehyde**
3 **flux with simultaneous confidence limits for the PLM.**

4
5 Source: Subramaniam et al. (2008).

6
7
8 The variability considered is that among animals and any measurement error as well as
9 any other design-related components of error. Simultaneous 95% confidence limits for $\log(\alpha_N)$
10 were produced using Scheffe's method (Snedecor and Cochran, 1980). These 95% confidence
11 limits span a range of 0.96 in $\log_{10}(\alpha_N)$, or nearly a 10-fold range in median α_N . There is
12 additional dispersion in these data that does not appear in Figures E-2 and E-3; due to variation
13 in the number of cells per mm basement membrane, the ratio of ULLI/LI had a spread of
14 approximately $\pm 25\%$ (0.45 to 0.71, mean 0.60) among the eight observations considered in
15 Monticello et al. (1990). Thus:

This document is a draft for review purposes only and does not constitute Agency policy.

- 1 1. As suggested by Table E-3, and Figures E-2 and E-3, the shape of $\alpha_N(\text{flux})$ in Conolly et
2 al. (2003) is therefore likely to be very sensitive to how α_N is weighted and averaged over
3 site and time.
- 4 2. Averaging of sites could significantly affect model calibration because of substantial
5 nonlinearity in model dependence on α_N at the 10 and 15 ppm doses associated with high
6 cancer incidence.
- 7 3. Monticello et al. (1996) found a high correlation between tumor rate and the ULLI
8 weighted by the number of cells at a site. Therefore, considering these factors while
9 regressing α_N against tissue dose would be important in the context of site differences in
10 tumor response.
- 11 4. A further complexity arises because of histologic changes and thickening that occurs in
12 the nasal epithelium over time in the higher dose groups (Morgan, 1997), factors that are
13 likely to affect estimates of local formaldehyde flux, uptake, and replication rates
14 (Subramaniam et al., 2008).

15
16 Figure E-1 indicates that the time dependence in ULLI is significant. It would also be
17 useful to examine if the time dependence affects the results of the time-to-tumor modeling and if
18 early temporal changes in replication rate are important to consider because of the generally
19 cumulative nature of cancer risk. The time window over which formaldehyde-induced cancer
20 risk is most influenced is not known, but the time weighting used by Conolly et al. (2003)
21 assigns a relatively low weight to labeling observed at early times compared with those observed
22 at later time points. Finally, initiated cells are likely to be replicating at higher rates than normal
23 cells as evidenced in several studies on premalignant lesions (Coste et al., 1996; Dragan et al.,
24 1995; Rotstein et al., 1986). Therefore, LI data as an estimator of normal cell replication rate
25 would be most reliable at early times when the mix of cells sampled include fewer preneoplastic
26 or neoplastic cells.

27 The more relevant question, therefore, is whether $\alpha_N(\text{flux})$ derived by a TWA over all
28 sites (as carried out by Conolly et al. [2003]) has an effect on low-dose risk estimates. Given the
29 above uncertainties and variability not characterized in CIIT (1999) or in Conolly et al. (2003), it
30 is important to examine whether additional dose-response curves that fit the cell replication data
31 reasonably well have an impact on estimated risk. Such sensitivity analyses are carried out in
32 the sections that follow. Clearly, a large number of alternative $\alpha_N(\text{flux})$ can be developed. In
33 conjunction with the other uncertainties, mainly the use of control data and alternative model
34 structures for initiated cell kinetics, the number of plausible clonal growth models to be
35 exercised soon require a prohibitively large investment of time. Therefore, detailed analyses

This document is a draft for review purposes only and does not constitute Agency policy.

1 were restricted to a select set of biologically plausible choices of curves for $\alpha_N(\text{flux})$, which
2 would allow the identification of a range of plausible risk estimates (MLEs and statistical
3 bounds).

4 5 **E.3.2.4. Alternate dose-response curves for cell replication.**

6 Six alternative equations for α_N were developed by regression analysis of the Monticello
7 et al. (1996) ULLI data. The replicate data corresponding to the summary data presented in this
8 paper were kindly provided to EPA by CIIT for further analyses. In each of these equations, α_N
9 is expressed as a function of formaldehyde flux to nasal tissue ($\text{pmol}/\text{mm}^2\text{-hour}$) and, in one
10 equation (eq 15) that explored time-dependence, the duration of exposure to formaldehyde in
11 weeks. All the graphs use flux/10,000 for the x-axis, and the y-axis expresses $\log_{10} \alpha_N$.

12 One source of uncertainty in the cell proliferation dose response in Conolly et al. (2003)
13 is the large value of α_{max} in the upward extrapolation (the cell replication rate corresponding to
14 the upper end of the flux range at 15 ppm exposure). The optimal value of α_{max} was found by
15 Conolly et al. (2003) to be 0.0435 hour^{-1} . As noted by the authors, an argument in support of
16 this value is that it corresponds to the inverse of the fastest cell cycle times found in the
17 literature. Since the model treats the induced replication rates as being time invariant, this means
18 that cells in the high-flux region(s) divide at the highest cell turnover rate ever observed
19 throughout most of an animal's life. This does not seem to be biologically plausible
20 (Subramaniam et al., 2008).

21 In the analysis, it was found that a 20% increase or decrease in the estimated value for
22 α_{max} degraded the fit to the tumor incidence data considerably. Because of the interplay between
23 the parameters estimated by optimization, this sensitivity of the model to α_{max} indicates that it is
24 necessary to examine if other plausible values of α_{max} are also indicated by the data and to what
25 extent low dose estimates of risk are influenced by the uncertainty in its value. The need for
26 such an analysis is also indicated by Figure E-2. The value of α_{max} ($\log_{10}\alpha_{\text{max}} = -1.37$) in the
27 modeling of Conolly et al. (2003) is roughly an order of magnitude greater than the values of
28 $\alpha_N(\text{flux})$ at the highest flux levels in this figure. If the data pooled over all sites and times are to
29 be used for $\alpha_N(\text{flux})$, then, based solely on the trend in $\alpha_N(\text{flux})$ in Figure E-2, it appears unlikely
30 that $\alpha_N(\text{flux})$ could increase up to this value of α_{max} . Visually, these empirically derived data
31 collectively suggest that α_N versus flux could be leveling off rather than increasing 10-fold.
32 Therefore, as an alternative to the approach taken in Conolly et al. (2003) of estimating α_{max} via
33 likelihood optimization against the tumor data, regressions of the empirical cell replication data
34 were used to extrapolate $\alpha_N(\text{flux})$ outside the range of observation (recognizing the uncertainty

1 and model dependence that still results from extrapolating well outside the range of observed
2 data).

3 In fitting dose-response curves to the cell replication data, a functional form was used
4 that was flexible to allow a variety of monotonic and non-monotonic shapes, with a parameter
5 that determined the asymptotic behavior of the dose-response function. This allowed the
6 extrapolation by only relying on the empirical cell replication data without using an adjustable
7 parameter estimated by fitting to the tumor data. However, the plausible asymptotes obtained
8 spanned a large range. In one case below, the asymptote suggested by the fit was judged to be
9 abnormally high. In this case, the α_N versus flux curve was followed until the biological
10 maximum of α_{\max} (as given in Conolly et al. [2003]) was reached.

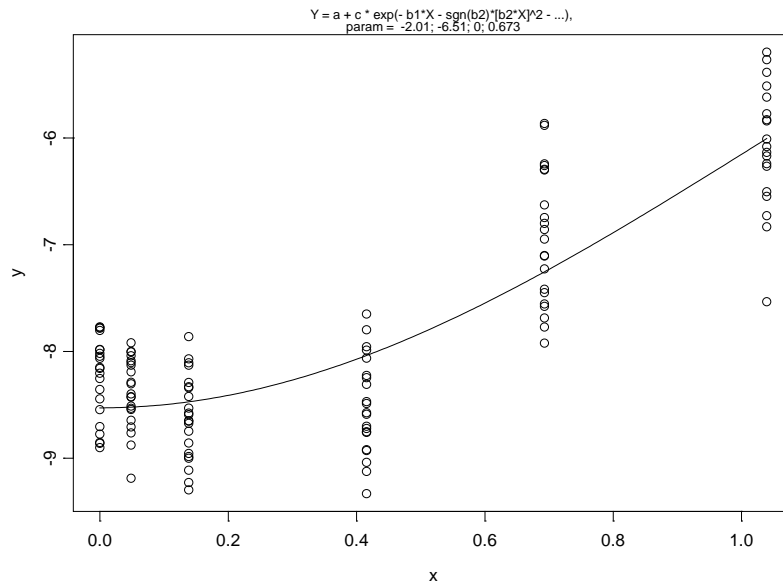
11 In three of the regression models below, the data were restricted to the earliest exposure
12 time (13 weeks) in Monticello et al. (1996) for which the cell proliferation rate (α_N) could be
13 calculated. The interest in using only the 13-week exposure time arises from observations
14 (Monticello et al., 1996, 1991) that at later times there were more frequent and severe histologic
15 changes, which may have altered formaldehyde uptake and cell proliferation response.
16 Consequently, given that the data in Monticello et al. (1991) for times earlier than 13 weeks
17 could not be utilized as explained earlier, the 13-week responses might better represent
18 proliferation rates for use in a two-stage model of the cancer process than the rest of the
19 Monticello et al.(1996) data.

20 Second, the LI data showed considerable variation among nasal sites, which may be
21 related to the variation in tumor response among sites. Since the cell replication dose-response
22 curves used in the cancer model represent all of the sites, it was attempted to include this
23 variation by weighting the regression by the relative cell populations at risk at each of the sites.
24 This was carried out for some of the models as stated below. The following models (denoted
25 N1–N6), shown in Figure E-4, have been included in addition to using the hockey stick- and J-
26 shaped curves in Conolly et al. (2003). Applicable equations are as follows:

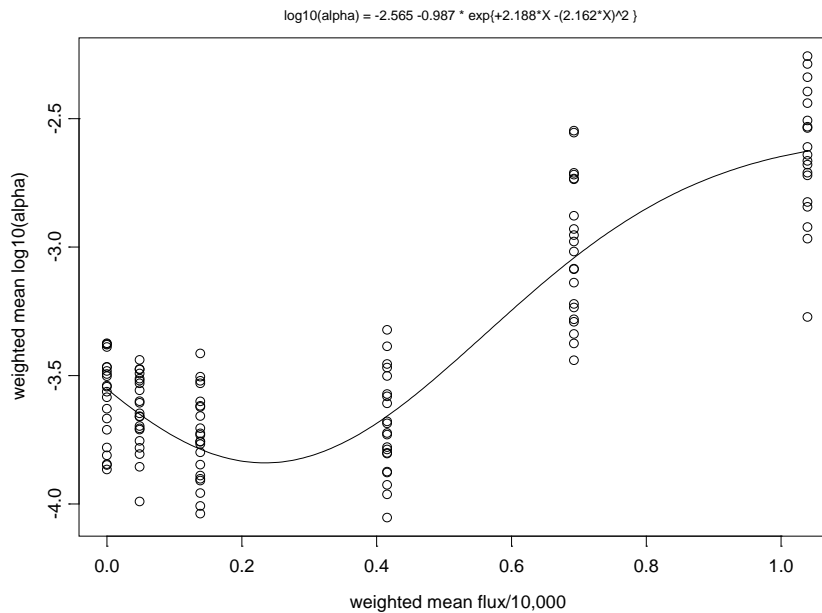
27
28 N1: Quadratic; monotone increasing in flux, derived from fit to all of the Monticello et al. (1996)
29 ULLI data.

30
31
$$\alpha_N = \text{Exp}\{-2.015 - 6.513 \times \text{Exp}[-(6.735 \times 10^{-4} \times \text{flux})^2]\} \quad (10)$$

32
33 N2: Linear-quadratic; decreasing in flux for small values of flux, derived from fit to all of the
34 Monticello et al. (1996) ULLI data.

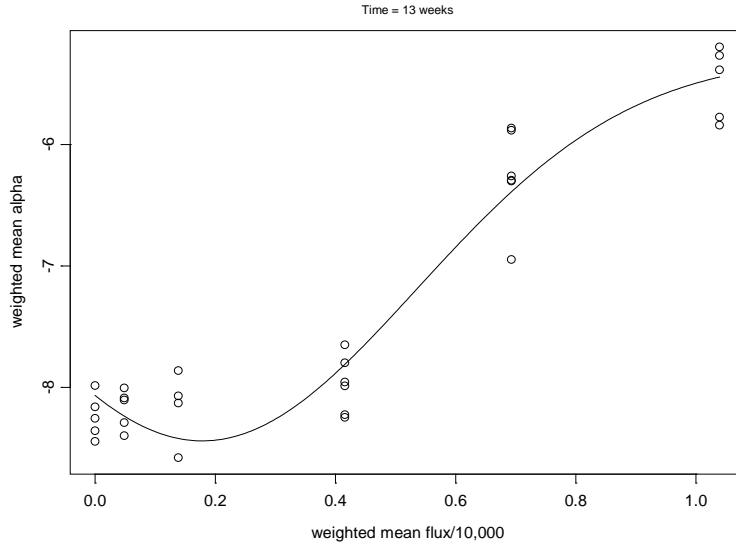


1
 2 **Figure E-4, N1. Various dose-response modeling of normal cell replication**
 3 **rate.**
 4 Note: See text for definitions of N1–N6. N1: Quadratic; monotone increasing in
 5 flux, derived from fit to all of the Monticello et al. (1996) ULLI data.



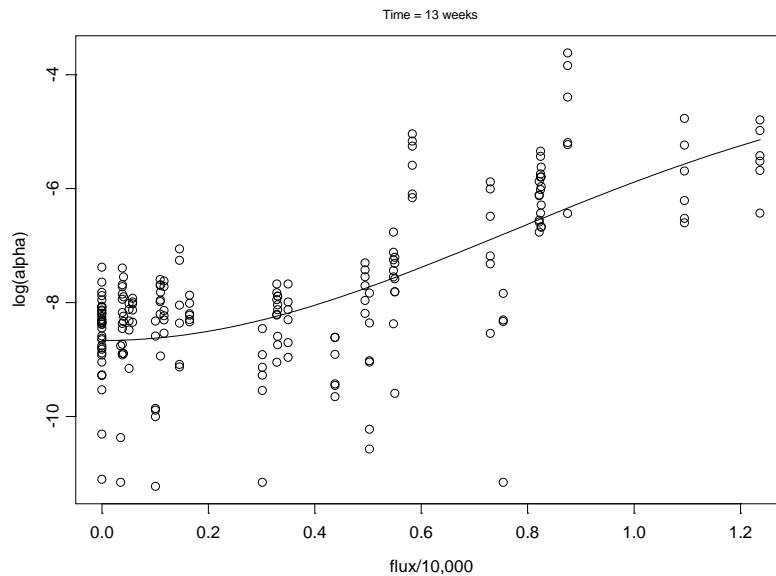
6
 7 **Figure E-4, N2: Various dose-response modeling of normal cell replication**
 8 **rate.**
 9 Note: See text for definitions of N1–N6. N2: Linear-quadratic; decreasing in flux
 10 for small values of flux, derived from fit to all of the Monticello et al. (1996)
 11 ULLI data.

This document is a draft for review purposes only and does not constitute Agency policy.



1
2 **Figure E-4, N3. Various dose-response modeling of normal cell replication**
3 **rate.**

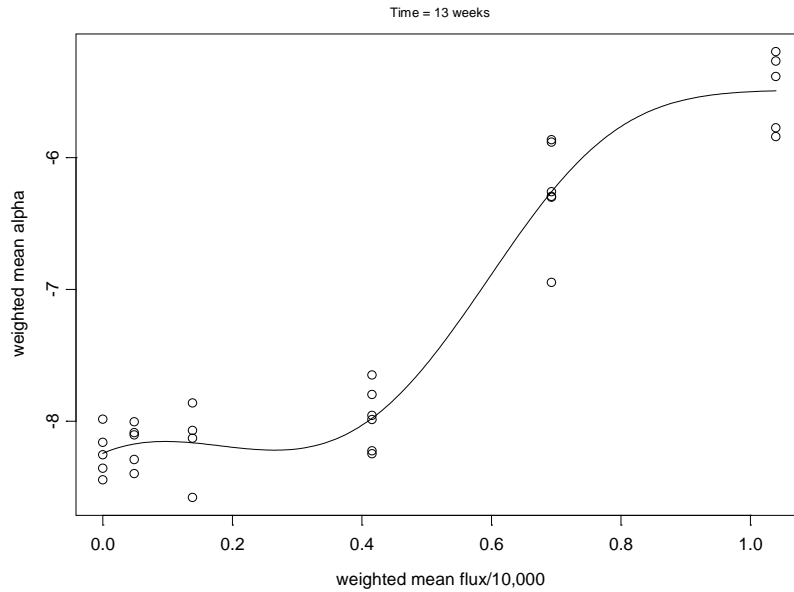
4
5 Note: See text for definitions of N1–N6. N3: Linear-quadratic; decreasing in flux
6 for small values of flux, derived from fit to the 13-week Monticello et al. (1996)
7 ULLI data, using average flux over all sites for a given ppm exposure and
8 weighting regression by estimates of the numbers of cells at each of five sites.



9
10 **Figure E-4, N4. Various dose-response modeling of normal cell replication**
11 **rate.**

12
13 Note: See text for definitions of N1–N6. N4: Quadratic; monotone increasing in
14 flux, derived from unweighted fit to 13-week Monticello et al. (1996) ULLI data.

This document is a draft for review purposes only and does not constitute Agency policy.



1
2 **Figure E-4, N5. Various dose-response modeling of normal cell replication**
3 **rate.**

4
5 Note: See text for definitions of N1–N6. N5: Linear-quadratic-cubic; initially
6 increasing slightly with increasing flux, then decreasing slightly, and finally
7 increasing, derived from fit to 13-week Monticello et al. (1996) ULLI data, using
8 average flux over all sites for a given ppm exposure and weighting regression by
9 estimates of the numbers of cells at each of five sites.

10
11

All Sites, ~ Time + 2nd order in Flux

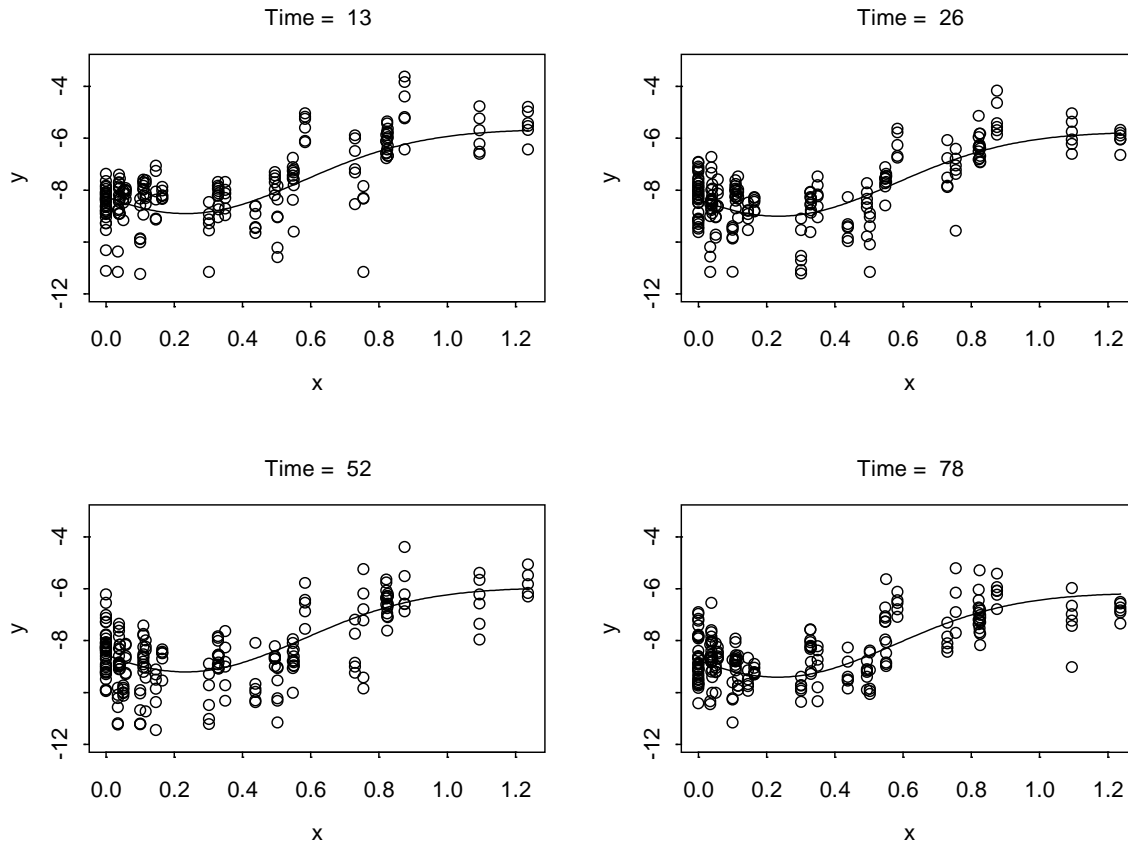


Figure E-4, N6. Various dose-response modeling of normal cell replication rate.

Note: See text for definitions of N1–N6. N6: Linear-quadratic-cubic; initially increasing slightly with increasing flux, then decreasing slightly, and finally increasing, derived from fit to all Monticello et al. (1996) ULLI data, using weeks of exposure as a covariate. In this model, time was a regression (continuous) predictor, not a class variable, and its coefficient represents the decrease in $\log_{10} \alpha_N$ per week of exposure time.

$$\alpha_N = \text{Exp}\{-5.906 - 2.272 \times \text{Exp}[2.188 \times 10^{-4} \times \text{flux} - (2.162 \times 10^{-4} \times \text{flux})^2]\} \quad (11)$$

N3: Linear-quadratic; decreasing in flux for small values of flux, derived from fit to the 13-week Monticello et al. (1996) ULLI data, using average flux over all sites for a given ppm exposure and weighting regression by estimates of the numbers of cells at each of five sites.

$$\alpha_N = \text{Exp}\{-5.274 - 2.792 \times \text{Exp}[1.407 \times 10^{-4} \times \text{flux} - (1.986 \times 10^{-4} \times \text{flux})^2]\} \quad (12)$$

This document is a draft for review purposes only and does not constitute Agency policy.

1
2 N4: Quadratic; monotone increasing in flux, derived from unweighted fit to 13-week Monticello
3 et al. (1996) ULLI data.

$$4 \quad \alpha_N = \text{Exp}\{-3.858 - 4.809 \times \text{Exp}[-(9.293 \times 10^{-5} \times \text{flux})^2]\} \quad (13)$$

6
7 N5: Linear-quadratic-cubic; initially increasing slightly with increasing flux, then decreasing
8 slightly, and finally increasing, derived from fit to 13-week Monticello et al. (1996) ULLI data,
9 using average flux over all sites for a given ppm exposure and weighting regression by estimates
10 of the numbers of cells at each of five sites.

$$11 \quad \alpha_N = \text{Exp}\{-5.488 - 2.755 \times \text{Exp}[-7.808 \times 10^{-5} \times \text{flux} + (2.349 \times 10^{-4} \times \text{flux})^2 \\ 12 \quad - (2.166 \times 10^{-4} \times \text{flux})^3]\} \quad (14)$$

14
15 N6: Linear-quadratic-cubic; initially increasing slightly with increasing flux, then decreasing
16 slightly, and finally increasing, derived from fit to all Monticello et al. (1996) ULLI data, using
17 weeks of exposure as a covariate. In this model, time was a regression (continuous) predictor,
18 not a class variable, and its coefficient represents the decrease in $\log_{10} \alpha_N$ per week of exposure
19 time.

$$20 \quad \alpha_N = \text{Exp}\{7.785 \times 10^{-3} \times (\text{weeks}) - 5.722 - 2.501 \times \text{Exp}[1.103 \times 10^{-4} \times \text{flux} \\ 21 \quad - (7.223 \times 10^{-5} \times \text{flux})^2 - (1.575 \times 10^{-4} \times \text{flux})^3]\} \quad (15)$$

23
24 Further details on the above regressions are provided in the appendix. These regressions
25 of the cell replication data as well as the hockey-stick and J-shaped curves used by Conolly et al.
26 (2003) (shown in Figure D-1, Appendix D) are used next as inputs to the clonal growth model
27 for cancer.

28 **E.3.3. Uncertainty in Model Specification of Initiated Cell Replication and Death**

29 ***E.3.3.1. Biological Inferences of Assumptions in Conolly et al. (2003)***

30 The results of a two-stage MVK model are extremely sensitive to the values for initiated
31 cell division (α_I) and death (β_I) rates, particularly in the case of a sharply rising dose-response
32 curve as in the case of formaldehyde. The pool of cells used for obtaining the available LI data
33 (Monticello et al., 1996, 1991) consists of largely normal cells with perhaps increasing numbers
34 of initiated cells at higher exposure concentrations. As such there is no way of inferring the
35

This document is a draft for review purposes only and does not constitute Agency policy.

1 division rates of initiated cells in the nasal epithelium, either spontaneous (baseline) or induced
2 by exposure to formaldehyde, from the available empirical data. Conolly et al. (2003)
3 considered $\alpha_I(\text{flux})$ as a function of $\alpha_N(\text{flux})$ as given by eq 2 in Appendix D. As shown in
4 Figure D-1 (Appendix D), α_I is estimated in Conolly et al. (2003) to be very similar to α_N . That
5 is, with eq 2 assumed to relate $\alpha_I(\text{flux})$ to $\alpha_N(\text{flux})$, a J- or hockey-shaped dose-response curve
6 for $\alpha_N(\text{flux})$ results in a J or hockey shape for $\alpha_I(\text{flux})$.

7 The J shape for the TWA $\alpha_N(\text{flux})$ in Conolly et al. (2003) could plausibly be explained,
8 as suggested by the examples in Conolly and Lutz (2004), by a mathematical superposition of
9 dose-response curves describing the effects of the inhibition of cell replication by the formation
10 of DPXs (Heck and Casanova, 1999) and cytotoxicity-induced regenerative replication (Conolly,
11 2002). However, as explained earlier, there is considerable uncertainty and variability, both
12 qualitative and quantitative, in the interpretation of the LI data and in the derivation of *normal*
13 cell replication rates from the ULLI data. While the TWA values of ULLI indicate a J-shaped
14 dose response for some sites, as also concluded by Gaylor et al. (2004), this is not consistently
15 the case for all exposure times and sites as discussed earlier. Notwithstanding this uncertainty
16 variability, and in the absence of data, the following essential questions have a significant impact
17 on risk predictions and need resolution if the model structure in eq 2 is to be used in a
18 biologically based (or motivated) sense to predict risk outside observable data:

- 19
- 20 • Should mechanisms that might explain a J-shaped dose response for normal cell
21 replication or a cytotoxicity-driven threshold in dose response (as indicated by a hockey-
22 stick-shaped curve) be expected to prevail also for initiated cells?
- 23 • Would the formaldehyde flux at which the cell replication dose-response curve rises
24 above its baseline be similar in value for both normal and initiated cells as inferred by the
25 CIIT model in Figure D-1?
- 26

27 The next critical assumption was that made for β_I (the death rate of initiated cells),
28 namely, $\beta_I(\text{flux}) = \alpha_N(\text{flux})$ (eq 3). In Subramaniam et al. (2008), the rationale for this
29 assumption in Conolly et al. (2003) is explained by assuming formaldehyde to be equally
30 cytotoxic to initiated and normal cells (since the mechanism is presumed to be via its general
31 chemical reactivity). In essence, this assumption brings the cytotoxic action of formaldehyde to
32 bear strongly on the parameterization of the CIIT model.

33 There are no data to evaluate the strength of these assumptions, so Subramaniam et al.
34 (2008) studied the plausibility of various inferences that arise as a result of these assumptions.
35 These inferences are only briefly listed here (see the paper for further discussion).

This document is a draft for review purposes only and does not constitute Agency policy.

- 1
- 2
- For flux $<27,975$ pmol/mm²-hour, $\alpha_I > \alpha_N$ (Figures D-1 & D-2 of Appendix D).
3 Qualitatively, this is in line with data on epithelial and other tissue types with or without
4 exposure to specific chemicals.
 - For higher flux levels, however, the model indicates $\alpha_I < \alpha_N$ (Figure D-2). There are no
5 data to shed further light on this inference.
6
 - At these higher flux levels, initiated cells in the model die at a faster rate than they
7 divide, indicating the extinction of initiated cell clones in regions subject to these flux
8 levels. There are no data indicating formaldehyde to have this effect.
9
- 10

11 In evaluating these inferences, Subramaniam et al. (2008) point to various data that
12 indicate that initiated cells represent distinctly different cell populations (from that of normal
13 cells) with regard to proliferation response (Ceder et al., 2007; Bull, 2000; Schulte-Hermann et
14 al., 1997; Coste et al., 1996; Dragan et al., 1995), have excess capacity to clear formaldehyde
15 and, in general, are considerably more resistant to cytotoxicity (such a resistance is manifested
16 variably as decreased ability of the toxicant to induce cell death or to inhibit cell proliferation
17 compared to corresponding effects in normal cells), and may already have altered cell cycle
18 control; thus, the influence of formaldehyde on apoptosis likely differs between normal and
19 initiated cells.

20 As concluded in Subramaniam et al. (2008), taken together, there is much data to suggest
21 that inferring $\alpha_I < \alpha_N$ at cytotoxic formaldehyde flux levels is problematic and that death rates of
22 initiated cells are likely to be very different from those of normal cells. In the absence of data to
23 indicate that eq 2 and eq 3 (in Appendix D) are biologically reasonable approaches to link the
24 kinetics of initiated cells with those of normal cells, alternate model structures other than those
25 represented by these relationships considered by Conolly et al. (2003) need to be explored, given
26 that the two-stage model is extremely sensitive to α_I and β_I . Such an evaluation needs to
27 primarily explore if the assumptions in eq 2 and eq 3 significantly impact the intended use of the
28 model, namely extrapolation to low-dose human cancer risk and the calculation of an upper
29 bound on human risk. Any such alternate model structure needs to provide a good fit to the
30 time-to-tumor data.

31

1 **E.3.3.2. Plausible Alternative Assumptions for α_I and β_I**

2 Therefore, in the additional sensitivity analysis presented here, initiated cell kinetics are
3 considered to be independent of normal cells, and initiated cell proliferation cannot take a J
4 shape (motivated by the consideration that lower-than-baseline turnover rate represents an
5 increased amount of DNA repair taking place, which may not be consistent with impaired DNA
6 repair in initiated cells).

7 Thus, two alternatives were considered to eq 2 for α_I (flux):

8

9 I1:
$$\alpha_I = \gamma_1 \times [1 + \exp(\gamma_2 / \gamma_3)] / \{1 + \exp[-(\text{flux} - \gamma_2) / \gamma_3]\}$$
 (16)

10

11 I2:
$$\alpha_I = \max[\alpha_I(\text{eq. I1}), \alpha_{N\text{Basal}}]$$
 (17)

12

13 Here γ_1, γ_2 , and γ_3 are parameters estimated by fitting the cancer model to the rat bioassay
14 data. In eq 16, α_I increases monotonically with flux from a background level of γ_1 asymptotically
15 up to a maximum value of $\gamma_1 \times [1 + \text{Exp}(\gamma_2 / \gamma_3)]$. The choice of this functional form in eq 16
16 and eq 17 was considered in order to be parsimonious while at the same time allowing for a
17 flexible shape to the dose-response curve. The sigmoidal curve allows for the possibility of a
18 slow rise in the curve at low dose and an asymptote.

19 Equation 17 is a modification of equation 16 that restricts the rate of division of initiated
20 cells to be at least as large as the spontaneous division rate of unexposed normal cells. There is
21 evidence to suggest (e.g., in the case of liver foci) that initiated cells have a growth advantage
22 over normal cells, with or without exposure to specific chemicals (Ceder et al., 2007; Grasl-
23 Kraupp et al., 2000; Schulte-Hermann et al., 1999; Coste et al., 1996; Dragan et al., 1995).

24 In addition, in most runs, an upper bound (α_{high}) is selected for both α_N and α_I . This value
25 is assumed to represent the largest biologically plausible rate of cell division. Following Conolly
26 et al. (2003), in most cases α_{high} is set equal to 0.045 hours⁻¹. If a value of α_I or α_N computed
27 using one of the above formulas exceeded α_{high} , the value of α_{high} was used in the computation
28 rather than the value obtained by using the formula.

29 As noted above, Conolly et al. (2003) set the rate of death for intermediate cells, β_I , equal
30 to the division rate of normal cells, $\beta_I = \alpha_N$. On the other hand, apoptotic rates and cell
31 proliferation rates are thought to be coupled (Schulte-Hermann, 1999; Moolgavkar, 1994), so
32 that death rates of initiated cells would rise concomitantly with an increase in their division rates
33 (Grasl-Kraupp et al., 2000; Schulte-Hermann et al., 1999). Therefore, as an alternative to the
34 Conolly et al. (2003) formulation, it is assumed that the death rate of intermediate cells is
35 proportional to the division rate of intermediate cells.

This document is a draft for review purposes only and does not constitute Agency policy.

1
$$\beta_I = K_\beta \times \alpha_I$$
 (18)

2
3 where the constant of proportionality, K_β , is an additional parameter to be estimated by
4 optimization against the tumor incidence data. Such an assumption has also been made by other
5 authors (Luebeck et al., 2000, 1995; Moolgavkar et al., 1993).

6 Since most of the SCCs in the rat bioassays occurred in rats exposed to the highest
7 formaldehyde concentration (15 ppm), the data from this exposure level have a big impact on the
8 estimated model parameters. In most runs that incorporated the 15 ppm data, the model
9 appeared, based on inspection of the KM plots, to fit the 15 ppm data quite well but to fit the
10 lower exposure data less well. Because of the high level of necrosis occurring at 15 ppm, it is
11 possible that the data at this exposure may not be particularly relevant to modeling the sharp
12 upward rise in the dose response at 6 ppm. Furthermore, the principal interest is in the
13 predictions of the model at lower levels to which human populations may be exposed.
14 Consequently, in order to improve the fit of the model at lower exposures, some of the
15 alternative models were constructed with the 15 ppm data omitted.

16
17 **E.3.4. Results of Sensitivity Analyses on α_N , α_I , and β_I**

18 **E.3.4.1. Further Constraints**

19 The number of models that might be constructed if all the possibilities listed above for
20 α_N , α_I , and β_I are to be tried in a systematic manner clearly become exponential and daunting.
21 (Optimally, it would have been desirable to elucidate the role of a specific modification while
22 keeping others unchanged to determine risk.) Therefore, in order to carry out a viable sensitivity
23 analysis while at the same time examining the plausible range of risks resulting from variations
24 in parameters and model structures, various uncertainties were combined in any given
25 simulation. By using the constraints described above (eq 10–17 and associated text) for α_I , β_I ,
26 and α_N , 19 models were obtained that provided similarly good fits to the time-to-tumor data
27 (which in some cases contained only five dose groups).

28 However, for many of these models, the optimal α_I (flux) displayed a threshold in flux
29 even when the model utilized for α_N (flux) was a monotonic increasing curve without a threshold
30 (i.e., model N4 for α_N in Figure E-4). Indeed, if a thresholded dose-response curve was
31 plausible for α_I based on arguments of cytotoxicity, then a threshold is all the more plausible for
32 α_N , and such models are removed from consideration.

33 Secondly, the basal value of α_I was required to be at least as large as the basal value of
34 α_N . Another constraint was placed on the baseline initiated cell replication rate. In the absence

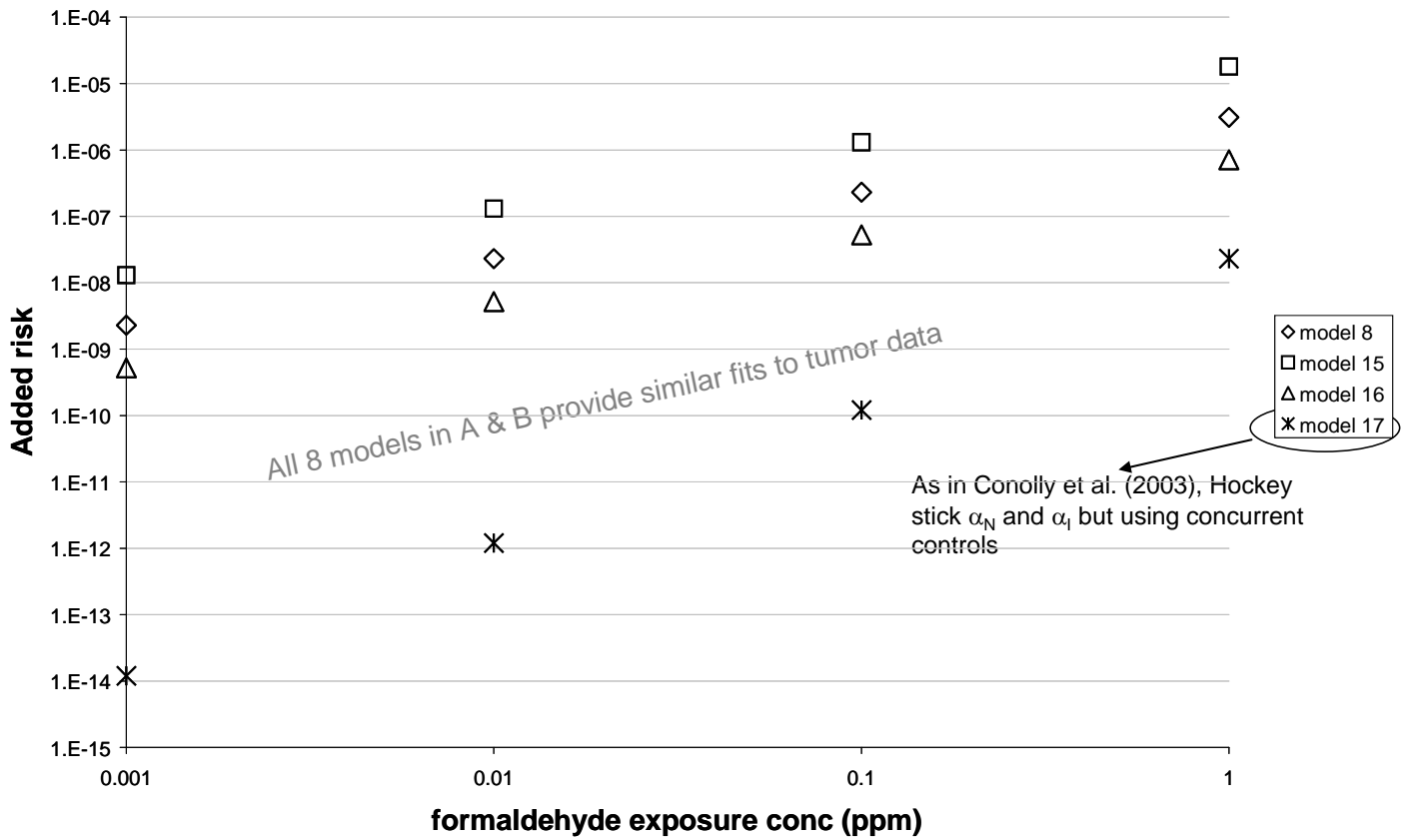
1 of formaldehyde exposure, α_I was not allowed to be greater than two or four times α_N , even if
2 such models described the tumor data, including the control data, very well. There are some data
3 that suggest that baseline initiated cells have a small growth advantage over normal cells, so a
4 huge advantage was thought to be biologically less plausible.

6 **E.3.4.2. Sensitivity of Risk Estimates for the F344 Rat**

7 Figure E-5 contains plots of the MLE of additional risk computed for the F344 rat at
8 formaldehyde exposures of 0.001, 0.01, 0.1, and 1 ppm for eight models. Two log-log plots are
9 provided. For those models for which the estimates of additional risk are all positive, the
10 additional risks are plotted (panel A), and, for those for which estimates of additional risk are
11 negative, the negatives of additional risks are plotted (panel B). Only five dose groups were
12 considered (i.e., 15 ppm data omitted) for models 8, 5, 15, and 16. Figure E-6 shows the dose-
13 response curves for α_N and α_I for these eight cases (panels A and B corresponding to those in
14 Figure E-5). The primary results are as follows:

- 16 1. Among the models considered, negative values for additional risk can arise only in
17 models in which the dose response for normal cells is J shaped. Thus, all of the models
18 with negative dose responses for risk have J-shaped dose responses for normal cells.
19 However, the converse is not necessarily true as may be noted from model 8. This model
20 has both a positive dose response for risk and a J-shaped dose response for normal cells.
21 In this case, the strong positive increase in response of initiated cells at low dose was
22 sufficient to counteract the negative response of normal cells.
- 23 2. The risk estimates predicted by the different models span a very large range for doses
24 below which no tumors were observed. This result points to large uncertainties in model
25 specification (how to relate the kinetics of normal and initiated cells) as well as in
26 parameter values. As mentioned above, the analysis does not attempt to separate the
27 influence of the different sources of uncertainty, so this range also incorporates the
28 uncertainty arising from the use of different control data and that due to α_{max} .
- 29 3. At the 10 ppb (0.01 ppm) concentration, MLE risks range from -4.0×10^{-6} to $+1.3 \times 10^{-7}$.
30 At this dose, models that gave only positive risks resulted in a five orders of magnitude
31 risk range from 1.2×10^{-12} to 1.3×10^{-7} , while narrowing to a four orders of magnitude
32 risk range from 1.2×10^{-10} to 1.3×10^{-6} at the 0.1 ppm level. This narrowing continues as
33 exposure concentration increases, and the curves coalesce to substantially similar values
34 at 6 ppm and above (not shown).

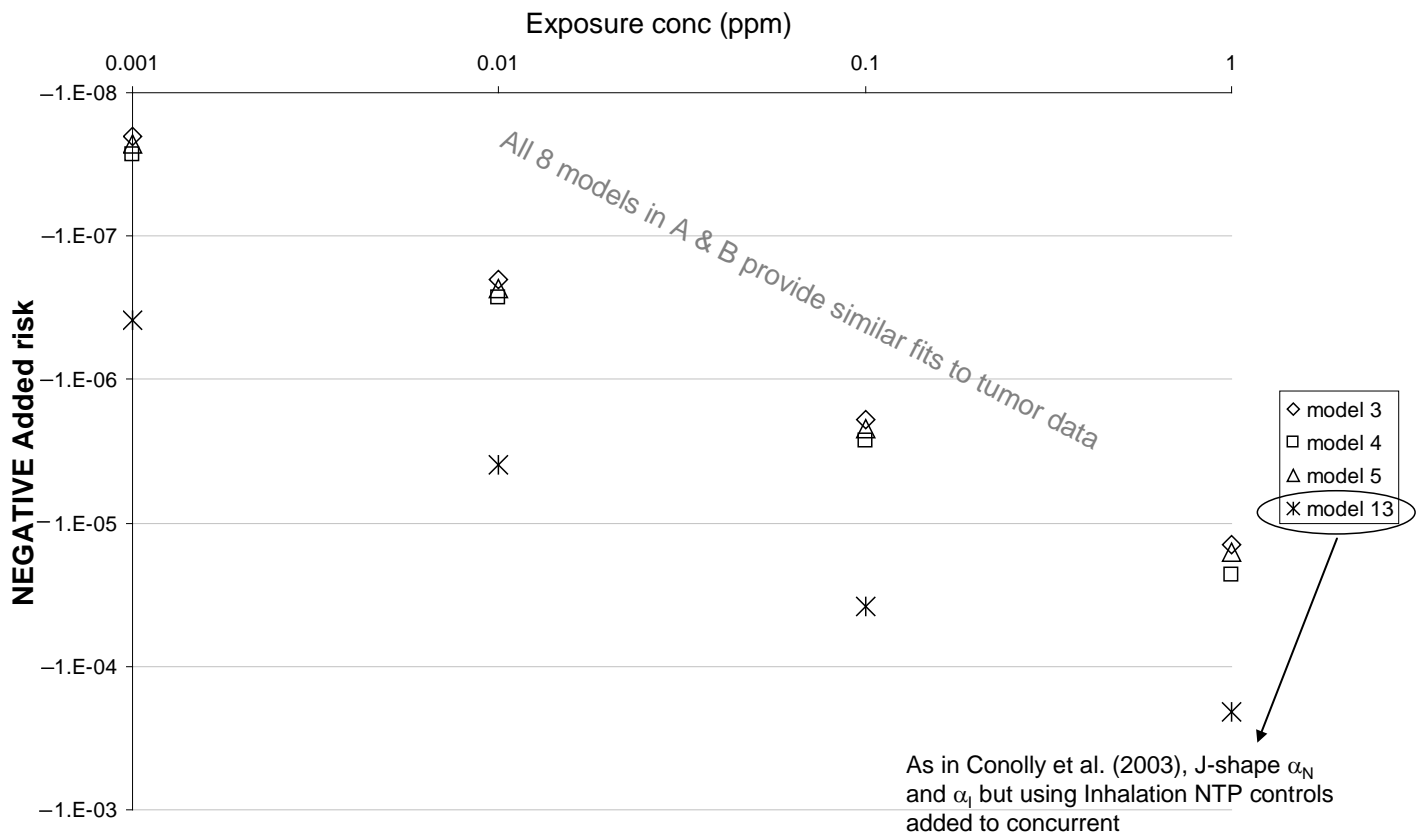
This document is a draft for review purposes only and does not constitute Agency policy.



1
2
3
4
5

Figure E-5A. BBDR models for the rat—models with positive added risk.

Note: All four models provide “similar” fits to tumor data (see text).

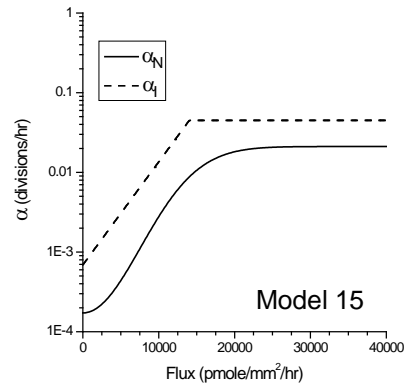
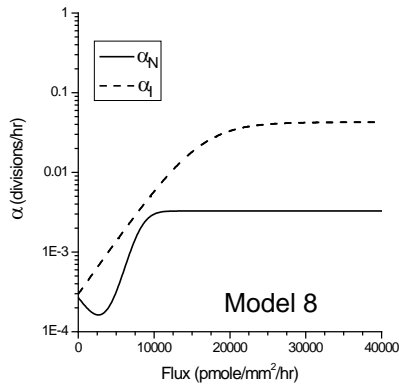


1
2
3
4
5
6

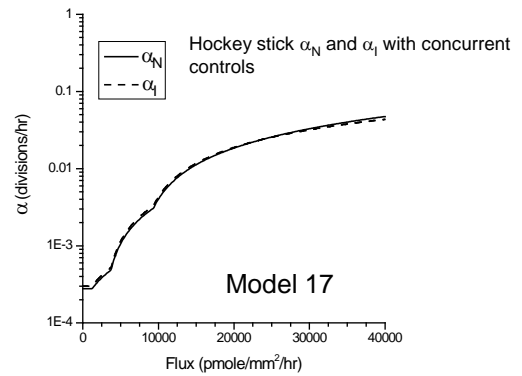
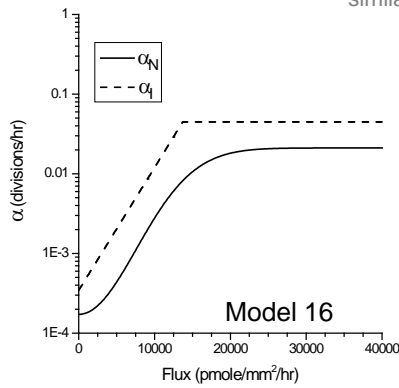
Figure E-5B. BBDR rat models resulting in negative added risk.

Note: All four models provide “similar” fits to tumor data (see text).

1

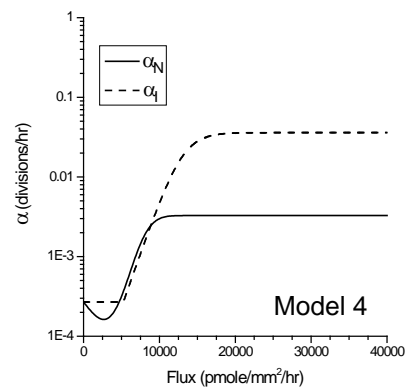
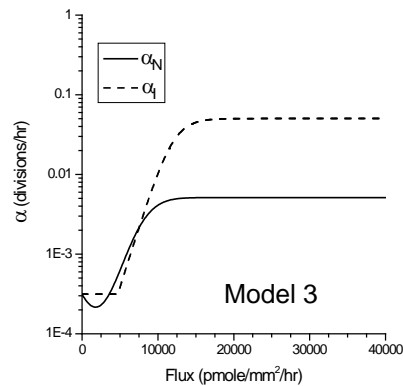


All 8 models in A & B provide similar fits to tumor data

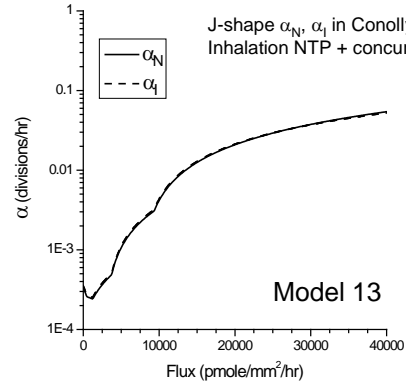
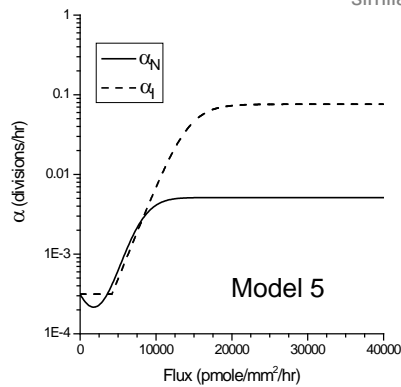


2
3
4
5
6

Figure E-6A. Models resulting in positive added rat risk: Dose-response for normal and initiated cell replication



All 8 models in A & B provide similar fits to tumor data



2
3
4
5
6

Figure E-6B. Models resulting in negative added rat risk: Dose-response for normal and initiated cell replication

- 7
8
9
10
11
12
13
4. There does not seem to be any systematic effect on additional risk that depends on whether the 15 ppm data are included in the analysis.
 5. For all of the models except models 13 and 17 in Figures E-5 & E-6, the additional risk varies substantially linearly with exposure at low exposures between 0.001 and 1.0 ppm (departing only to a small extent from linearity between 0.1 and 1.0 ppm). Models 13 and 17 (the models in Conolly et al. [2003] except for different control data being used) show a quadratic dependence.

14
15
16

The various model choices presented in Figure E-5 all provided equally good fits to the time-to-tumor data although within the context of a significant qualification. It was not possible

This document is a draft for review purposes only and does not constitute Agency policy.

1 to simply use the log-likelihood values as a means of comparing the goodness-of-fit to the tumor
2 incidence data across these model choices. This is because many of the model choices differed
3 in the number of doses or in the number of control animals that were used, so the fits were
4 compared across such models only visually. Within model choices where such a comparison did
5 not pose a problem, the log-likelihood values did not differ statistically significantly.

6 Wherever results from the BBDR modeling are discussed, values of added risk, as
7 opposed to extra risk, are reported. This is purely for convenience in interpretation. Because of
8 the low background incidence, these values are only negligibly different from the corresponding
9 extra risk estimate. The final risk (or unit risk) estimates provided in this document are based on
10 extra risk estimates.

11 12 **E.3.4.3. MOA Inferences Revisited**

13 The ratio $KMU/\mu_{N_{\text{basal}}}$ represents the added fractional probability of mutation per cell
14 generation $(\mu_N - \mu_{N_{\text{basal}}})/\mu_{N_{\text{basal}}}$ due to unit concentration of DPXs. As discussed earlier, this
15 parameter has a critical impact on the extrapolation as well as on inferring whether the
16 mutagenic action of formaldehyde is relevant to the quantitative risk characterization. In that
17 prior discussion, this ratio was found to be extremely sensitive to the choice of historical control
18 data. The analysis indicates that, for a given set of control data that is used, uncertainties
19 associated with α_N and α_I also have a large impact on this ratio. In that discussion, this ratio was
20 infinite when concurrent controls were used because the MLE value for $\mu_{N_{\text{basal}}}$ was found to be
21 zero. The use of these concurrent controls, however, does not necessarily imply that $\mu_{N_{\text{basal}}}$ will
22 be determined to be zero. In one of the scenarios examined in the sensitivity analysis, where
23 concurrent controls were used along with the combination of dose-response curves eq 13 for α_N
24 (Figure E-4) and eq 17 for α_I , the optimal value of the ratio $KMU/\mu_{N_{\text{basal}}}$ was equal to 0.25. For
25 the models in Figure 5-13A, this ratio was 0 for all except model 17 for which it was infinite.
26 For the models in Figure 5-13B with negative added risk, the ratio ranged from 0–4.5. For some
27 of those models where $KMU/\mu_{N_{\text{basal}}}$ was finite, the upper confidence bound on this ratio was
28 found to increase by an order of magnitude from the MLE value. Thus, we conclude that the
29 modeling does not help resolve the debate as to the relevance of formaldehyde’s mutagenic
30 potential to its carcinogenicity.

31 32 **E.3.4.4. Confidence Bounds: Model Uncertainty Versus Statistical Uncertainty**

33 For models 15 and 17 in Figures E-5A and E-6A, 90% CIs for additional risk were
34 calculated by using the profile likelihood method. Table E-4 compares the lower and upper
35 confidence bounds for these models for 0.001 ppm, 0.1 ppm (doses well below the range where

This document is a draft for review purposes only and does not constitute Agency policy.

tumors were observed), and 6 ppm (the lowest dose where tumors were observed) with the MLE risk estimates at these doses. In both cases, these intervals were quite narrow compared with the differences in risk predicted by different models in Figure E-5. This suggests that model uncertainty is of more consequence in the formaldehyde animal model than is statistical uncertainty. We also estimated confidence bounds using the bootstrap method for select models, and determined that these estimates were in agreement with the bounds calculated using the profile likelihood method. These results are not presented here. We return to the calculation of confidence limits when determining points of departure (PODs).

Table E-4. Comparison of statistical confidence bounds on added risk for two models

Dose (ppm)	Model	Lower bound	MLE	Upper bound
0.001	Model 15	4.4×10^{-9}	1.3×10^{-8}	1.6×10^{-8}
	Model 17	1.2×10^{-14}	1.2×10^{-14}	1.3×10^{-14}
0.1	Model 15	4.5×10^{-7}	1.3×10^{-6}	1.7×10^{-6}
	Model 17	1.2×10^{-10}	1.2×10^{-10}	1.3×10^{-10}
6	Model 15	1.8×10^{-2}	2.1×10^{-2}	2.3×10^{-2}
	Model 17	1.3×10^{-2}	1.8×10^{-2}	3.0×10^{-2}

In conclusion, it is demonstrated that the different formaldehyde clonal growth models can fit the data about equally well and still produce considerable variation in additional risk and biological inferences at low exposures. However, even with these large variations, the highest MLE added risk for the F344 rat is only of the order of 10^{-6} at 0.1 ppm. Thus, with regard to calculating a reasonable upper bound that includes model and statistical uncertainty, the relevant question is whether the range arising out of uncertainties in the rat model amplifies when extrapolated to the human. Thus, in Appendix F, the human model in Conolly et al. (2004) will be examined.

This page intentionally left blank.

Appendix F

1 **APPENDIX F**

2
3 **SENSITIVITY ANALYSIS OF BBDR MODEL FOR FORMALDEHYDE INDUCED**
4 **RESPIRATORY CANCER IN HUMANS**
5

6 **F.1. MAJOR UNCERTAINTIES IN THE FORMALDEHYDE HUMAN BBDR MODEL**

7 Subsequent to the BBDR model for modeling rat cancer, Conolly et al. (2004) developed
8 a corresponding model for humans for the purpose of extrapolating the risk to humans estimated
9 by the rat model. Also, rather than considering only nasal tumors, it is used to predict the risk of
10 all human respiratory tumors. The human model for formaldehyde carcinogenicity (Conolly et
11 al., 2004) is conceptually very similar to the rat model and follows the schematic in Figure 5-11
12 in Chapter 5. The model structure, notations, and calibration are described in Appendix D.
13 Unlike the sensitivity analysis of the rat modeling where a number of issues were examined, a
14 much more restricted analysis will be presented here for the sake of brevity. A more extensive
15 analysis was carried out initially that carried forward several of the rat models to the human, and
16 the lessons learned from those exercises are in agreement with the more restricted presentation
17 that follows. Table F-1 lists the major uncertainties and assumptions in the human extrapolation
18 model in Conolly et al. (2004).

Table F-1. Summary of evaluation of major uncertainties in CIIT human BBDR model

Assumptions, approach, and characterization of input data^a	Rationale in Conolly et al. (2003) or CIIT (1999)	EPA uncertainty evaluation	Further elaboration
Cell division rates derived from rat labeling data assumed applicable for human (except for assuming different fraction of cells with replicative potential).	No equivalent LI data for human or guidance in extrapolating cell division rate across species.	Enzymatic metabolism plays a role in mitosis. Therefore, we expect interspecies difference in cell division rate. Basal cell division rates in humans expected to be much more variable than in laboratory animals.	Subramaniam et al. (2008)
Development of PBPK model for DPX concentration in human respiratory lining.	See text (Chap 3)	See text (Chap 3)	Chap 3; Conolly et al. (2000); Subramaniam et al. (2008); Klein et al. (2009)
Anatomically realistic representation of nasal passages.	Reduces uncertainty (over default calculation carried out by averaging dose over entire nasal surface).	Computer representation pertains to that of one individual (Caucasian male adult). Considerable interindividual variability in nasal anatomy. Susceptible individuals even more variable.	Kimbell et al. (2001a, b); Subramaniam et al. (2008, 1998)
KMU/ $\mu_{N_{\text{basal}}}$ is species invariant (used to estimate human).	Human cells are more difficult to transform than rodent, both spontaneously and by exposure to formaldehyde.	$\mu_{N_{\text{basal}}}$ is 0 when concurrent controls or inhalation NTP controls in time frame of concurrent bioassays are used. Leads to infinitely large KMU for human.	Subramaniam et al. (2007); Crump et al. (2009, 2008).
Conservative assumptions were made. Results are conservative in the face of model uncertainties.	<ol style="list-style-type: none"> 1) Hockey-stick dose-response for α_N was included even though TWA indicated J-shape. 2) Overall respiratory tract cancer incidence data for human baseline rates were used. 3) Risk was evaluated at statistical upper bound of the proportionality parameter relating DPXs to the probability of mutation. 	CIIT result cannot be characterized as conservative in the face of model uncertainties and as a plausible upper bound on human risk. Human model is unstable.	Conolly et al. (2004); Subramaniam et al. (2007); Crump et al. (2009, 2008).

^aAssumptions in this table are in addition to those listed for the BBDR model for the F344 rat.

1 **F.2. SENSITIVITY ANALYSIS OF HUMAN BBDR MODELING**

2 Crump et al. (2008) carried out a limited sensitivity analysis of the Conolly et al. (2004)
3 human model. This analysis was limited to evaluating the effect on the human model of the
4 following. These evaluations have been the subject of some debate in the literature and in
5 various conferences (Conolly, 2009; Conolly et al., 2009, 2008; Crump et al. 2009).

- 6
- 7 1. The use of the alternative sets of control data for the rat bioassay data that were
8 considered in the sensitivity analysis of the rat model (Subramaniam et al., 2007).
- 9 2. Minor perturbations in model assumptions regarding the effect of formaldehyde on the
10 division and death rates of initiated cells (α_I , β_I). Now, recall from the description of the
11 structure of the human model that one (of the two) adjustable parameter in the expression
12 for the human α_I was determined from the model fit to the rat tumor incidence data while
13 the second parameter was determined from background rates of cancer incidence in the
14 human. Therefore, variations considered in α_I were constrained to only those that (a) did
15 not meaningfully degrade the fit of the model to the rat tumor incidence data and (b) were
16 in concordance with background rates in the human. Crump et al. (2008) also evaluated
17 these variations with respect to their biological plausibility. The sensitivity analysis on
18 assumed initiated cell kinetics was thought to be particularly important since there were
19 no data to even crudely inform the kinetics of initiated cells for use in the models, even in
20 rats, and the two-stage clonal expansion model is very sensitive to initiated cell kinetics
21 (Gaylor and Zheng, 1996; Crump, 1994a, b).
- 22

23 Crump et al. (2008) note that, since the purpose of their analysis was to carry out a
24 sensitivity analysis, in order to illustrate certain points, only risks to the general U.S. population
25 from constant lifetime exposure to various levels of formaldehyde under the Conolly et al.
26 (2004) environmental scenario (8 hours/day sleeping, 8 hours/day sitting, and 8 hours/day
27 engaged in light activity) are considered. Fits based on the hockey-stick and J-shape models
28 were identical, and, of the three estimated parameters (μ_{basal} , μ_{ltb} , and D), only the estimate
29 of μ_{basal} differed between the two models.

30

31 **F.2.1. *Effect of background Rates of Nasal Tumors in Rats on Human Risk Estimates***

32 Crump et al. (2008) quantitatively evaluated the impact of different control groups on
33 estimates of additional human risk as follows:

- 1 1. Concurrent controls plus all NTP controls:, the same as used by Conolly et al. (2004);
- 2 2. Concurrent controls plus controls from NTP inhalation studies;
- 3 3. Only concurrent controls;
- 4 4. Each set of control data was applied with both the J shape and hockey-stick models in
- 5 Conolly et al. (2004) for $\alpha_N(\text{flux})$ and $\alpha_I(\text{flux})$ for a total of six analyses,;
- 6 5. Uncertainties associated with α_N or α_I are not addressed. Parameters α_{max} , multfc, and
- 7 KMU were estimated in exactly the same manner as in Conolly et al. (2004).

8
9 Crump et al. (2008) present the following dose-response predictions of additional risk in
10 humans from constant lifetime exposure to various levels of formaldehyde arising from
11 exercising the above six cases. Their plots are reproduced in Figure F-1, where the
12 corresponding curves based on Conolly et al. (2004) are also shown for comparison.

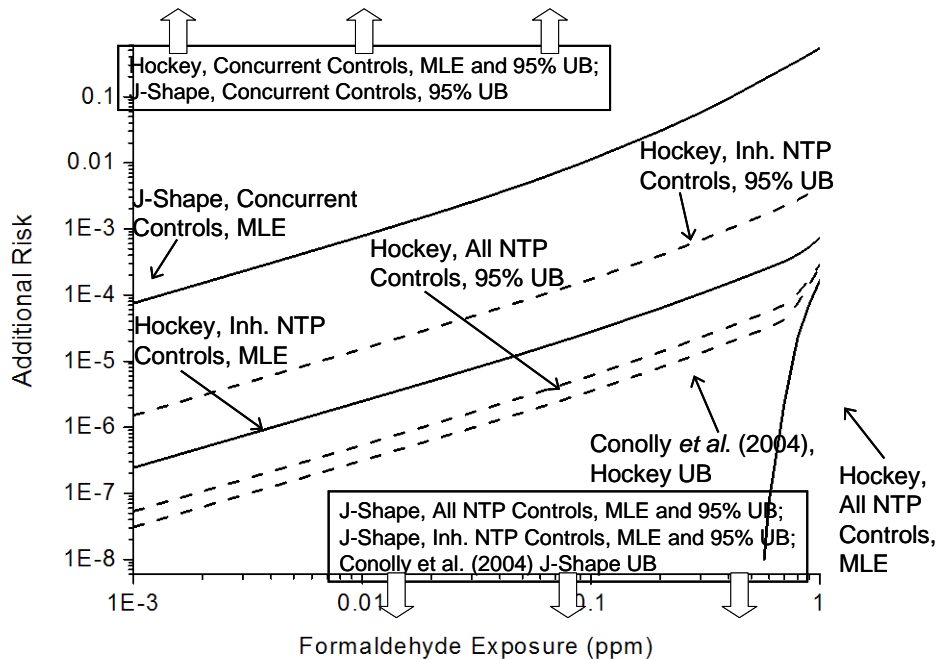
13 The lowest dotted curve in Figure F-1 represents the highest estimates of human risk
14 developed by Conolly et al. (2004). This resulted from use of the hockey-stick model for cell
15 division rates in conjunction with the statistical upper bound for the parameter KMU. As
16 indicated by the downward block arrows in the figure, their corresponding estimates based on
17 the J-shape model were all negative for exposures below 1 ppm.

18 Consider next the solid curves in the figure, which show predicted MLE added risks that
19 were positive and less than 0.5. Crump et al. (2008) next examined the added risk obtained
20 when the MLE estimate of (KMU/μ_{basal}) in these cases is replaced by the 95% upper bound of
21 this parameter ratio. The upper bound risk estimates in Conolly et al. (2004) were calculated in a
22 similar manner (but using all NTP historical controls). Except for minor differences, risk
23 estimates corresponding to such an upper bound and using all NTP controls were very similar in
24 the two efforts (Crump et al., 2008; Conolly et al., 2004).

25 Figure F-1 shows that the choice of controls to include in the rat model can make an
26 enormous difference in estimates of additional human risk. For the J-shaped model for cell
27 replication rate both estimates based on the MLE and those based on the 95% upper bound on
28 KMU/μ_{basal} are negative for formaldehyde exposures below 1 ppm. However, when only
29 concurrent controls are used in the model in Crump et al. (2008), the MLE from the J-shape
30 model is positive and is more than three orders of magnitude higher than the highest estimates
31 obtained by Conolly et al. (2004). Using only concurrent controls, estimates based on the 95%
32 upper bound on KMU/μ_{basal} are unboundedly large (block arrows at the top of the figure). For
33 the hockey-stick shaped model for cell replication rate, when all NTP controls are used, the
34 estimates based on the MLEs are zero for exposures less than about 0.5 ppm. If only inhalation
35 controls are added, the MLEs are about seven times larger than the Conolly et al. (2004) upper

This document is a draft for review purposes only and does not constitute Agency policy.

1 bound estimates, and the estimates based on the 95% upper bound on KMU/μ_{basal} are about 50
 2 times larger than the Conolly et al. (2004) estimates. If only concurrent controls are used, both
 3 the MLE estimates and those based on the 95% upper bound on KMU/μ_{basal} are unboundedly
 4 large.
 5



6
7
8
9
10
11
12
13
14
15
16
17

Figure F-1. Effect of choice of NTP bioassays for historical controls on human risk.

Note: Estimates of additional human risk of respiratory cancer by age 80 from lifetime exposure to formaldehyde are obtained by using different control groups of rats.

Source: Crump et al. (2008).

F.2.2. Alternative Assumptions Regarding the Rate of Replication of Initiated Cells

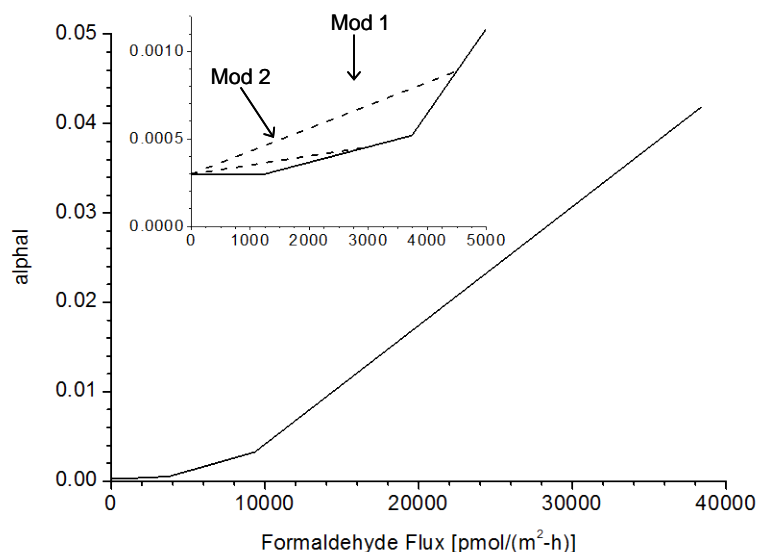
For the human model, Conolly et al. (2004) made the same assumptions for relating $\alpha_I(\text{flux})$ and $\beta_I(\text{flux})$ to $\alpha_N(\text{flux})$ as in their rat model (Conolly et al., 2003). That is, these quantities were related by using eq 2 and eq 3. As discussed in the context of the rat modeling, by extending the shape of these curves to humans, the authors' model brings the cytotoxic action of formaldehyde to bear strongly on the parameterization of the human model as well.

This document is a draft for review purposes only and does not constitute Agency policy.

1 In the sensitivity analyses of the rat modeling, it was concluded that other biologically
2 plausible assumptions for α_I and β_I resulted in several orders of magnitude variations in the low
3 dose risk relative to those obtained by models based on the assumptions in Conolly et al. (2003)
4 but that the highest risks were nonetheless of the order of 10^{-6} at the 10 ppb level. This section
5 examines how these uncertainties in the rat model propagate to the human model.

6 Crump et al. (2008) made minor modifications to the assumed division rates of initiated
7 cells in Conolly et al. (2004), while all other aspects of the model and input data were kept
8 unchanged. Two alternatives were considered for each of the J-shape and hockey-stick models.
9 Figure F-2 shows the hockey-stick model for initiated cells in rats. In the first modification to
10 the hockey-stick model (hockey-stick Mod 1), rather than having a threshold at a flux of
11 1,240 $\text{pmol}/\text{m}^2\text{-hour}$, the division rate increases linearly with increasing flux until the graph
12 intersects the original curve at 4,500 $\text{pmol}/\text{m}^2\text{-hour}$, where it then assumes the same value as in
13 the original curve for larger values of flux. The second modification (hockey-stick Mod 2) is
14 similar, except the modified curve intersects the original curve at a flux of 3,000 $\text{pmol}/\text{m}^2\text{-hour}$.

15



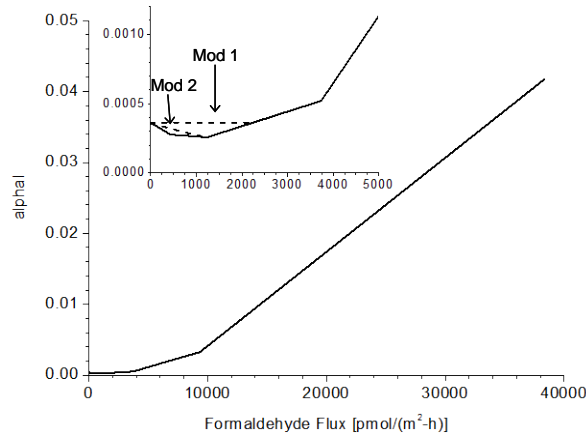
16
17 **Figure F-2. Conolly et al. (2003) hockey-stick model for division rates of**
18 **initiated cells in rats and two modified models.**

19
20 Source: Crump et al. (2008).

21
22
23 Figure F-3 shows the rat J-shape model for initiated cells. In the first modification to this
24 dose response (J-shape Mod 1), rather than having a J shape, the division rate of initiated cells
25 remains constant at the basal value until the original curve rises above the basal value and has

This document is a draft for review purposes only and does not constitute Agency policy.

1 the same value as the original curve for larger values of flux. In the second modification
2 (J-shape Mod 2), the J shape is retained but somewhat mitigated. In this modification, the
3 division rate initially decreases in a linear manner similar to that of the original model but with a
4 less negative slope until it intersects the original curve at a flux of 1,240 $\mu\text{m}^2\text{-hour}$, where it
5 then follows the original curve for higher values of flux.
6

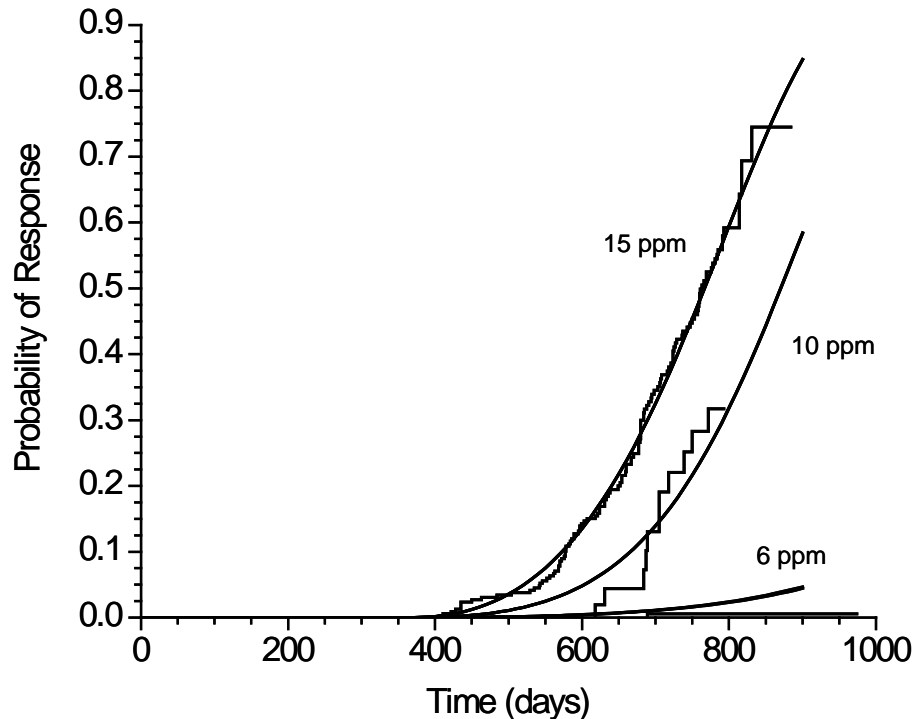


7
8
9 **Figure F-3. Conolly et al. (2003) J-shape model for division rates of initiated**
10 **cells in rats and two modified models.**

11
12 Source: Crump et al. (2008).

13
14
15 Since the first constraint on the variation in α_1 was in concordance with the rat time-to-
16 tumor incidence data, Crump et al. (2008) applied each of the modified models in Figures F-2
17 and F-3 to the version of the formaldehyde models in Subramaniam et al. (2007) that employed
18 all NTP controls and the hockey-stick curve for α_N . These authors restricted their analysis to
19 this case since their stated purpose was only a sensitivity analysis as opposed to developing
20 alternate credible risk estimates. Figure F-4 reproduces (from Crump et al. [2008]) curves of the
21 cumulative probability of a rat dying from a nasal SCC by a given age for bioassay exposure
22 groups of 6, 10, and 15 ppm. For comparison purposes, the corresponding KM (nonparametric)
23 estimates of the probability of death from a nasal tumor are also shown. Three sets of
24 probabilities are graphed: the original unmodified one and the ones obtained by using hockey-
25 stick Mod 1 and Mod 2. Crump et al. (2008) state that the changes in the tumor probability
26 resulting from these modifications are so slight that the three models cannot be readily

1 distinguished in this graph.⁴ Thus, the modifications considered to the models for the division
2 rates of initiated cells caused an inconsequential change in the fit of the model-predicted tumor
3 incidence to the animal tumor data.
4



5
6
7 **Figure F-4. Very similar model estimates of probability of fatal tumor in**
8 **rats for three models in Figure F-2.**
9

10 Note: The differences are visually indistinguishable. Models were derived from
11 the implementation of Conolly et al. (2003) with the hockey-stick curves for
12 $\alpha_I(\text{flux})$ and $\alpha_N(\text{flux})$ and variants derived from modifications (Mod 1 and Mod 2,
13 Figure F-2) to $\alpha_I(\text{flux})$. Model probabilities are compared to KM estimates. The
14 three sets of model estimates are so similar that they cannot be distinguished on
15 this graph.
16

17 Source: Crump et al. (2008).
18

⁴ The largest change in the tumor probability resulting from this modification for any dose group and any age up through 900 days was found to be less than 0.002, a change so small that it would be impossible to detect, even in the largest bioassays ever conducted. The changes in tumor probability resulting from the other modifications described earlier were found to be even smaller. These comparisons were made in Crump et al. (2008) without re-optimizing the likelihood. The authors note that re-optimization of the model subsequent to the variations would have made the fit of modified models even better.

This document is a draft for review purposes only and does not constitute Agency policy.

1 The above modifications did not affect the basal rate of cell division in the model and
2 likewise had no effect on the fit to the human background data (Crump et al., 2008).

3 Crump et al. (2008) noted that, although the threshold model for initiated cells in Conolly
4 et al. (2003) was replaced with a model that had a small positive slope at the origin, the resulting
5 curves, hockey-stick Mod 1 and hockey-stick Mod 2, could have been shifted slightly to the right
6 along the flux axis in order to introduce a threshold for α_I without materially affecting the risk
7 estimates resulting from these modified curves. Thus, “the assumption of a linear no-threshold
8 response is not an essential feature of the modifications to the hockey-stick model; clearly
9 threshold models exist that would produce essentially the same effect” (Crump et al. 2008).

10 **F.2.3. Biological Plausibility of Alternate Assumptions**

11 These very small variations made to the α_I in Conolly et al. (2003) are seen to be
12 consistent with the tumor-incidence data (just demonstrated above); small compared with the
13 variability and uncertainty in the cell replication rates characterized from the available empirical
14 data (at the formaldehyde flux where α_I was varied); supported (qualitatively) by limited data,
15 suggesting increased cell proliferation at doses below cytotoxic; perturbations that one should
16 expect on any dose response derived from laboratory animal data because of human population
17 variability in cell replication; and biologically plausible because cell cycle control in initiated
18 cells is likely to be disrupted.

19 The averaged cell replication rate constants as tabulated in Table 1 of Conolly et al.
20 (2003) and shown by the red curve in Figure E-2 of Appendix E (for various exposure
21 concentrations and corresponding average formaldehyde flux values in the F344 rat nose)
22 demonstrate an increase over baseline values only at exposure concentrations of 6 ppm and
23 higher. Increased cell proliferation at these concentrations of formaldehyde, whether transient or
24 sustained, have been associated in the literature with epithelial response to the cytotoxic
25 properties of formaldehyde (Conolly, 2002; Monticello and Morgan, 1997; Monticello et al.,
26 1996, 1991). The labeling data are considered to show a lack of cytotoxicity and regenerative
27 cell proliferation in the F344 rat at exposures of 2 ppm and below (Conolly, 2002). In the
28 Conolly et al. (2003) modeling, it is further assumed that the formaldehyde flux levels at which
29 cell replication exceeds baseline rates remain essentially unchanged when extrapolated to the
30 human and for initiated cells for the rat as well as the human. These assumptions need to be first
31 viewed in the context of the uncertainty and variability in the data on normal cells discussed
32 earlier.

33
34 Arguments for a hockey-stick or J shape over the background have been made in the
35 literature for sustained and chronic cell replication rates; the analyses of the cell replication data

This document is a draft for review purposes only and does not constitute Agency policy.

1 show that the data are not consistently (over each site and time) indicative of a hockey-stick or
2 J shape as the best representation of the data. This uncertainty is particularly prominent when
3 examining the cell replication data at the 13-week exposure time and the pooled data from the
4 PLM nasal site from Monticello et al. (1996) (Figures E-1 [dotted curve], E-3B, E-4 of Appendix
5 E). The earliest exposure time in this experiment was at 13 weeks, and the 13-week cell
6 replication data appear to be more representative of a monotonic increasing dose response
7 without a threshold. It is possible that early times are of more relevance to the carcinogenesis as
8 well as for considering typical (short duration) human exposures.

9 For initiated cells, there are no data on which to evaluate the modifications made to these
10 rates. However, some perspective can be gained by comparing them to the variability in the
11 division rates obtained from the data on normal cells used to construct the formaldehyde model.
12 As shown in Figure E-2 and discussed further in Subramaniam et al. (2008), these data show
13 roughly an order of magnitude variation in the cell replication rate at a given flux. As part of a
14 statistical evaluation of these data, a standard deviation of 0.32 was calculated for the log-
15 transforms of individual measurements of division rates of normal cells. By comparison, the
16 maximum change in the log-transform division rate of initiated cells resulting from hockey-stick
17 Mod 2 was only 0.20, and the average change would be considerably smaller. Thus, although
18 there are no data for initiated cells, it can be said that the modifications introduced in Crump et
19 al. (2008) for initiated cells are extremely small in comparison to the dispersion in the data for
20 normal cells.

21 Subramaniam et al. (2008) also point to some additional, albeit limited, data, suggesting
22 that exposure to formaldehyde could result in increased cell replication at doses far below those
23 that are considered to be cytotoxic. Tyihak et al. (2001) treated different human cell lines in
24 culture to various doses (0.1–10 mM) of formaldehyde and found that the mitotic index
25 increased at the lowest dose of 0.1 mM. These findings considered along with human population
26 variability and susceptibility (for example, polymorphisms in ADH3 [Hedberg et al., 2001])
27 indicate that it is necessary to consider the possibility of small increases in the human α_I over
28 baseline levels at exposures well below those at which cytotoxicity-driven proliferative response
29 is thought to occur.

30 Heck and Casanova (1999) have provided arguments to explain that the formation of
31 DPXs by formaldehyde leads to inhibition of cell replication (i.e., if this effect alone is
32 considered, normal cell replication rate of the exposed cells would be less than the baseline rate).
33 However, this hypothesis was posed for normal cells. Subramaniam et al. (2008) argue that if an
34 initiated cell is created by a specific mutation that impairs cell cycle control, the effect would be
35 to mitigate the DPX-induced inhibition in cell replication, either partially or fully, depending on

1 the extent to which the cell cycle control has been disrupted. In the absence of data on initiated
2 cells, the above argument provided biological motivation to the modification applied to the
3 J-shape model for cell division (Crump et al. 2008).

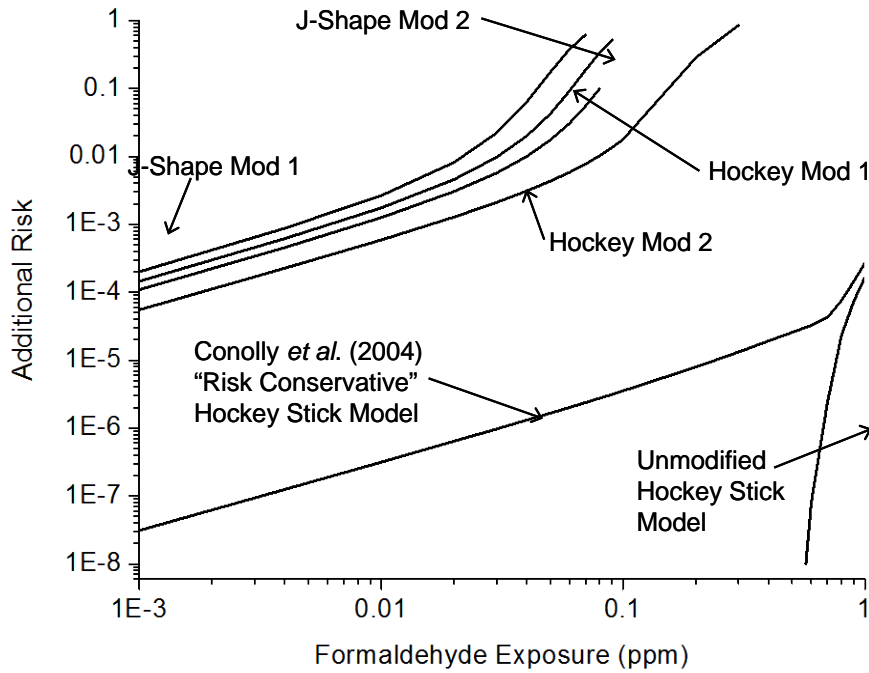
4 Thus, the previous paragraphs suggest that the changes made in the analysis in Crump et
5 al. (2008) to the assumption by Conolly et al. (2003) regarding the dose response for the division
6 rate of initiated cells are not implausible.

7 8 **F.2.4. Effect of Alternate Assumptions for Initiated Cell Kinetics on Human Risk Estimates**

9 Figure F-5 contains graphs of the additional human risks estimated (in Crump et al.
10 [2008]) by applying these modified models for α_I and using all NTP controls, compared with
11 those obtained by using the original Conolly et al. (2004) model. Each of the four modified
12 models presents a very different picture from that of Conolly et al. (2004). At low exposures,
13 these risks are three to four orders of magnitude larger than the largest estimates obtained by
14 Conolly et al. (2004).

15 These results have been criticized by Conolly et al. (2009) as being unrealistically large
16 and above the realm of any epidemiologic estimate for formaldehyde SCC. Thus, they argue that
17 the parameter adjustments made in Crump et al. (2008) are inappropriate. Crump et al. (2009)
18 rebutted these points by arguing that the purpose of their work was not to provide a more reliable
19 or plausible model but to carry out a sensitivity analysis. They argued that the changes made to
20 the model (in their analyses) were reasonable since they did not violate any biological
21 constraints or the available data. Further, they pointed out that “by appropriately mitigating the
22 small modifications [they] made to the division rates of initiated cells, the model [would]
23 provide any desired risk ranging from that estimated by the original model up to risks 1,000-fold
24 larger than the conservative estimate in Conolly et al. (2004).”

25 Crump et al. (2008) also evaluated the assumption in eq 3 of the CIIT modeling
26 pertaining to initiated cell death rates (β_I) by making small changes to β_I . They report that they
27 obtained similarly large values for estimates of additional human risk at low exposures.
28 Obtaining reliable data on cell death rates in the nasal epithelium appears to be an unusually
29 difficult proposition (Hester et al., 2003; Monticello and Morgan, 1997), and, even if data are
30 obtained, they are likely to be extremely variable.



1
2
3
4
5
6
7

Figure F-5. Graphs of the additional human risks estimated by applying these modified models for α_I , using all NTP controls, compared to those obtained using the original Conolly et al. (2004) model.

Source: Crump et al. (2008).

This page intentionally left blank.

Appendix G

1
2
3
4
5
6
7
8
9
10
11
12
13
14
15
16
17
18
19
20
21
22
23
24
25
26
27
28
29
30
31
32
33
34
35
36

APPENDIX G

EVALUATION OF THE CANCER DOSE-RESPONSE MODELING OF GENOMIC DATA FOR FORMALDEHYDE RISK ASSESSMENT

G.1. MAJOR CONCLUSIONS IN ANDERSEN ET AL. (2008)

In Chapter 4, the gene microarray data from animal studies on formaldehyde (Andersen et al., 2008; Thomas et al., 2007) were described. The analysis of these animal high throughput data and the conclusions reached in these two groundbreaking papers were closely examined for use in this assessment. Studies on high throughput animal data provide a wealth of information that helps further understanding of the relevant mechanisms. However, such studies have generally not made quantitative bottom-line inferences that inform low dose human risk. The above-mentioned studies are a notable exception due to the breadth of their conclusions on low dose MOAs, their pioneering application of the benchmark dose (BMD) methodology to genomic data, their use of BMD-response analysis that identified dose estimates at which specific cellular processes were significantly altered, the fact that they were accompanied by recommendation in the literature urging use of these results in setting exposure standards for formaldehyde (Daston, 2008).

We focus here on the conclusions in these papers with regard to modeling the cancer dose-response for formaldehyde. In addition to supporting our disposition of these analyses for this assessment, this write-up serves the purpose of exemplifying critical issues that need to be considered for the future.

The overall BMD determined in Andersen et al. (2008) for all genes with significant dose-response averaged 6.4 ppm. These analyses indicated a general progression with the lowest BMD values (i.e., the most sensitive epithelial responses) for extracellular and cell membrane components and higher BMD values for intracellular processes. Overall, these authors concluded that

- Genomic changes, including those suggestive of mutagenic effects, did not temporally precede or occur at lower doses than phenotypic changes in the tissue
- Genomic changes were no more sensitive than tissue responses
- Formaldehyde, being an endogenous chemical, is well handled until some threshold is achieved. Above these doses, toxicity rapidly ensues with concomitant genomic and histologic changes.
- Linear extrapolations, or extrapolations that specify similar MOAs at high and low doses would be inappropriate.

This document is a draft for review purposes only and does not constitute Agency policy.

1 These findings were judged to have significant implications on the debated MOA for
2 formaldehyde carcinogenicity, confirming results from earlier bioassays and dose-response
3 modeling that the mutagenicity of formaldehyde was too weak to be of relevance to its
4 carcinogenicity. Daston (2008) judged the method in these efforts to be extremely sensitive and
5 therefore suited to examining whether responses at the molecular level take place at doses below
6 which frank adverse effects occur. Daston (2008) argued that "... if there are pleiotropic effects
7 at lower exposure levels that would elicit a different profile of gene expression, those genes
8 would not go unnoticed" and thus concluded that "the gene expression data confirm that the
9 responses are not linear at low doses."

10 In the analyses that follow, we point to some significant quantitative factors that impact
11 on these conclusions.

12 13 **G.2. USE OF MULTIPLE FILTERS ON THE DATA**

14 The analyses in these papers involved the following sequence of data filters.

- 15
16 1. Gene probe sets that differed in expression in response to treatment were identified by
17 one-way analysis of variance. Probability values were adjusted for multiple comparisons
18 by using a false discovery rate of 5%.
- 19 2. Next, in addition to the above statistical filter, the output was further screened by
20 selecting only those genes that exhibited a change from the control group that was greater
21 than or equal to 1.5-fold (logarithmic).
- 22 3. The gene probe sets that demonstrated significant dose-response behavior were then
23 matched to their corresponding biological process and molecular function gene ontology
24 (GO) categories (considering only those involving more than three genes) and grouped
25 into process categories such as cell division, DNA repair, cellular proliferation,
26 apoptosis, and related molecular function categories.

27
28 A large number of genes are expressed in these studies; therefore, clearly some
29 appropriate filter needs to be used for meaningful interpretation of the vast database. Tissue
30 pathology served as a phenotypic anchor for the interpretation of microarray results, and the
31 genomic study confirmed (and improved on) the qualitative and quantitative understanding
32 derived from the histopathology and observation of frank effects. It is possible that the
33 combination of filters used by these authors is adequate for an inquiry into some mechanisms
34 associated with the specific phenotypic effects. However, the studies reached bottom-line
35 conclusions with regard to the low-dose MOA and approach to be considered for quantitative

This document is a draft for review purposes only and does not constitute Agency policy.

1 extrapolation. These conclusions necessarily involve questions as to whether there were gene
2 expression changes at low dose and at early exposure times that may be relevant to initiating
3 carcinogenesis and finally as to whether there is a threshold in dose associated with
4 formaldehyde carcinogenesis. However, collectively, the three filters employed in these studies
5 likely constitute overly stringent criteria, taking away the resolution needed to observe critical
6 gene changes needed to delineate low dose effects. An indication that this may indeed be the
7 case can be seen by examining the correlations in their findings with the observed trend in the
8 data on DPXs formed by formaldehyde. This is detailed in the following section.

9 10 **G.3. DATA FOR LOW-DOSE CANCER RESPONSE**

11 A significant finding in Thomas et al. (2007) is that BMD estimates for the GO
12 categories applicable to cell proliferation and DNA damage were similar to values obtained for
13 cell labeling indices and DPXs in earlier studies and to BMD estimates obtained for the onset of
14 nasal tumors. The mean BMD for the GO category of “positive regulation of cell proliferation”
15 was 5.7 ppm; in comparison, Schlosser et al. (2003) obtained a 10% BMD of 4.9 ppm for the cell
16 labeling index. The GO category associated with “response to DNA damage stimulus,” seen as a
17 genomic correlate to a mutagenic effect, had a mean BMD of 6.31 ppm. Thomas et al. (2007)
18 compare this finding with significant increase at 6 ppm of DPXs following a 3-hour exposure in
19 the study by Casanova et al. (1994). The formation and repair of DPXs have been considered to
20 be one of the potential mechanisms associated with the genotoxic action of formaldehyde
21 (Conolly et al., 2003, 2000). Based on earlier work in the same laboratory (Conolly et al., 2004,
22 2003; Conolly, 2002), Slikker et al. (2004) concluded that there is a dose threshold (at about
23 6 ppm) to formaldehyde carcinogenicity and that the putative mutagenic action of formaldehyde
24 is not relevant to its carcinogenicity. Therefore, the finding that a significant genomic response
25 (e.g., induction of DNA repair genes) is not observed at doses lower than those that induce
26 tumors in rodent bioassays is seen by these authors (Andersen et al., 2008; Daston, 2008;
27 Thomas et al., 2007) to further buttress the above conclusions related to the mode of action for
28 formaldehyde-induced respiratory cancer.

29 However, phenotypic anchoring to the DPX data drawn only from Casanova et al. (1994)
30 misses critical low-dose data that informs mode of action. In an earlier study, Casanova et al.
31 (1989) observed statistically significantly elevated (over controls) levels of DPXs at 2 ppm and a
32 trend towards elevated DPXs at 0.7 ppm. In analysis of low-dose data, the trend in the dose-
33 response is critically important because data inherently lack the power to establish statistical
34 significance. Furthermore, the two studies by Casanova and coworkers are different in some
35 respects. The earlier study was a 6-hour exposure, while the later study was a 3-hour study; thus,

This document is a draft for review purposes only and does not constitute Agency policy.

1 on this account alone, it appears more relevant to compare with the older study. Exposures in
2 the earlier study were additionally at 0.3 and 10 ppm, thus affording a lower exposure
3 concentration. In the earlier study, tissue from the whole nose was analyzed, whereas in the later
4 study tissue from two specific regions was obtained from the “high” tumor (Level II) and “low”
5 tumor regions. Together, these data suggest that DPXs occur at exposure concentrations
6 considerably lower than those that elicited transcriptional changes. One possible explanation is
7 that the increase in DPXs was not sufficient to induce DNA repair genes. Alternatively, these
8 discrepancies may be due to the stringent filters and the low statistical power of the Andersen et
9 al. (2008) study. These disparities between the gene array study and the DPXs question the
10 ability of the studies in Andersen et al. (2008) and Thomas et al. (2007) to inform the presence or
11 absence of a mutational MOA for formaldehyde, and in essence, to inform the low-dose response
12 curve for formaldehyde-induced cancer.

13 In another instance, Andersen et al. (2008) clearly stated that no genes were significantly
14 altered by exposure to 0.7 ppm, yet they state that there was “a trend toward altered expression at
15 0.7 ppm” in some genes with U and inverted U shape dose-responses (Figures 4 and 5 of their
16 paper). While these changes may not be statistically significant, they could be biologically
17 significant.

18

19 **G.4. DIFFICULTIES IN INTERPRETING THE BENCHMARK MODELING**

20 The benchmark analyses are summarized in Thomas et al. (2007) as average BMD
21 estimates for genes in a given GO that were statistically significantly dose related. The
22 benchmark modeling was then used by the authors to identify that the dose below individual
23 cellular processes was judged to be “not altered.”

24 The BMD definition used by these authors is quite stringent: it defines an effect so that
25 only 0.005 of controls will be considered affected and sets the BMR corresponding to this dose
26 at 0.105. The net effect is that the BMD is the air level, such that the increase in the mean
27 response is $1.349 \times$ standard deviation. This is essentially an arbitrary definition. For
28 comparison, if 0.05 of controls are considered affected and the BMR is set at 0.1 (common
29 values that are applied to whole animal data), the BMD is the air level such that the increase in
30 the mean response is $0.608 \times$ standard deviation. Thus, if this definition had been used (as is
31 traditionally the case), the BMD estimates would all be 2.2 times smaller than those obtained by
32 Schlosser et al. (2003). Furthermore, the analysis assumes equal variance in all dose groups.
33 Thus, further consideration of these issues with regard to interpretation of the BMR obtained
34 from these studies is needed before it can be used in regulatory exposure setting. Secondly,
35 lower confidence limits on the BMDs need to be derived for the data in Andersen et al. (2008).

This document is a draft for review purposes only and does not constitute Agency policy.

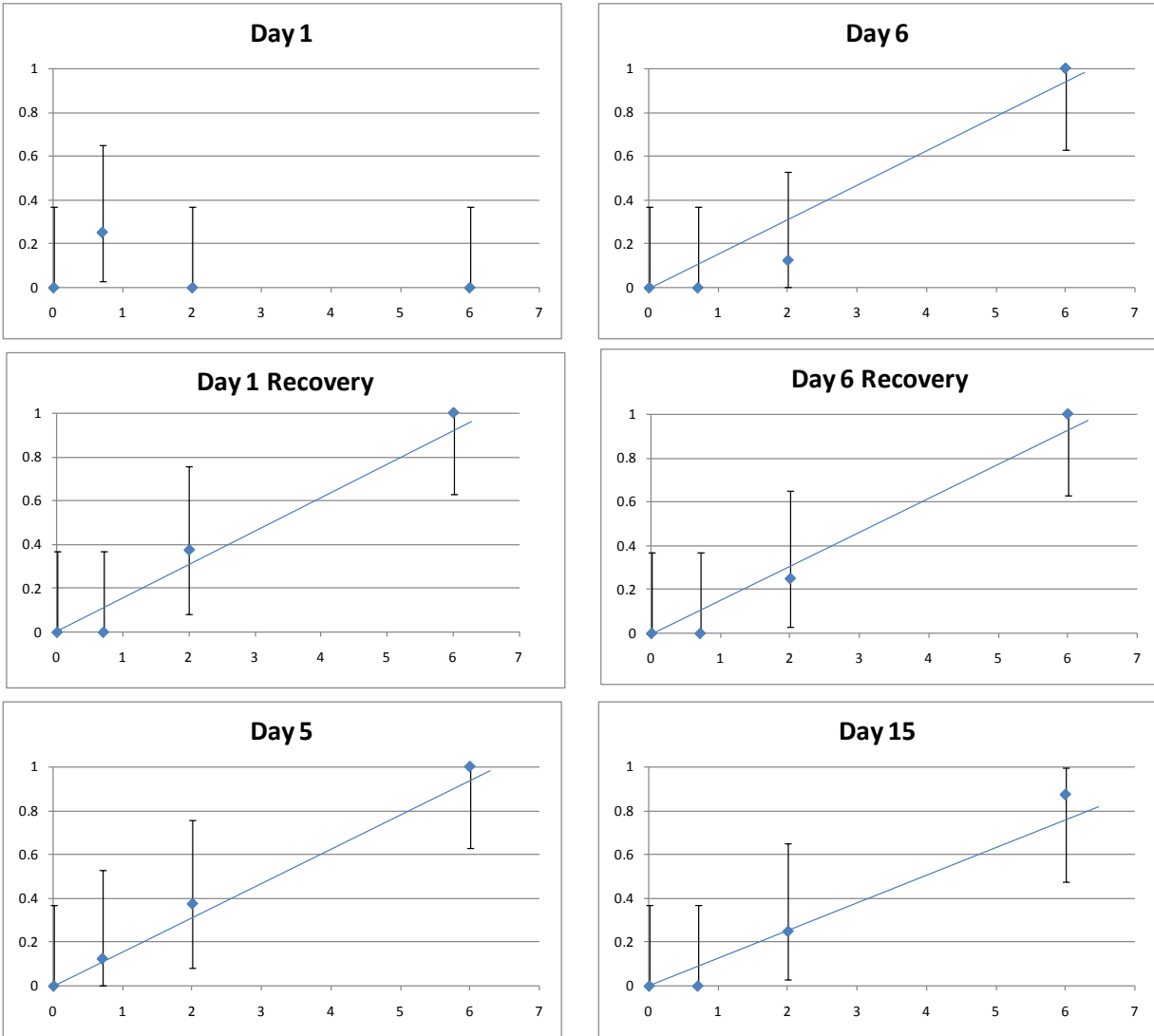
1 **G.5. STATISTICAL SENSITIVITY OF THE DATA FOR DOSE-RESPONSE**

2 Another cautionary note pertains to the qualification of gene array studies as being
3 extremely sensitive. Such a qualification should actually refer to the fact that only tiny amounts
4 of mRNA are needed, that is, the sensitivity of the assay per se for measuring gene expression.
5 However, this should not be confused with the sensitivity needed to identify the very small dose-
6 related changes at low dose. Andersen et al. (2008) reports on results of studies that involve
7 small numbers of animals in each dose group (five or eight). Despite the limited power in such
8 studies, the paper equates the absence of a statistically significant effect with no effect. This
9 limitation is generally true of studies of the dose responses of changes in gene expression
10 conducted to date; they have generally relied on very few animals (≤ 10 per dose group). Since
11 there will likely always be background amounts of gene expression, quantifying the dose
12 response requires statistically significant changes in gene expression as a function of dose. If the
13 genomic data involve even fewer animals per group than the histopathological data, they have
14 even less power to delineate the dose response; in particular, whether there is a threshold at low
15 exposures. This is illustrated by the example in Figure G-1 of the dose responses for epithelial
16 hyperplasia (Andersen et al. 2008, lesion 2). These appear equally consistent with both a
17 threshold at around 1 ppm and a linear response down to zero.

18
19 **G.6. LENGTH OF THE STUDY AND STOCHASTIC EVENTS**

20 Another significant consideration with regard to MOA conclusions that are pertinent to
21 the disease process is the length of the study, 15 days. If formaldehyde-induced tumor formation
22 is a stochastic process (e.g., genotoxicity), then exposure of a small number of animals to low
23 concentrations for 15 days may not be long enough to detect changes that might occur under
24 long-term exposure scenarios.

25 Relatedly, it has been suggested that gene (and protein) expression is a stochastic process
26 whereby steady state gene expression obeys Poisson statistics (i.e. distribution of rare events),
27 and that events of interest may occur in a single cell or small number of cells in which larger
28 tissue samples can average out such stochastic events and prevent the detection of non-average
29 behavior (Quakenbush, 2007). Given the implied difficulty in such an analysis, duration of
30 exposure may be one of the most tenable ways of addressing whether a chemical increases the
31 probability of an adverse response.



1
2
3
4
5
6
7
8
9
10
11
12

Figure G-1: Graphs of epithelial hyperplasia (Lesion 2) versus formaldehyde concentration (ppm) with 95% confidence intervals (with linear fit by eye)

G.7. OVERALL CONCLUSION

We believe our analyses of the presentations in Andersen et al. (2008) and Daston (2008) are generally useful with regard to future developments in quantitative analyses of genomic data if they are to be of relevance to risk assessment. For risk assessment, rather than focusing on what responses are statistically significant, an analysis should focus on 1) what range of values of critical parameters (e.g., gene expression) are consistent with the data, and 2) what these values imply for whole animal risk. This is of course, an extremely difficult proposition because

This document is a draft for review purposes only and does not constitute Agency policy.

- 1 we do not know nearly enough about how changes in genes quantitatively affect whole animal
- 2 risk, or even which genes are important.

Appendix H

1 **APPENDIX H**

2
3 **EXPERT PANEL CONSULTATION ON QUANTITATIVE EVALUATION OF ANIMAL**
4 **TOXICOLOGY DATA FOR ANALYZING CANCER RISK DUE TO INHALED**
5 **FORMALDEHYDE**
6

7 The National Center for Environmental Assessment convened an expert panel of
8 scientists for advice on evaluating available approaches for incorporating biological information
9 in analyzing animal tumor data for assessing cancer risk due to inhaled formaldehyde. This
10 Appendix pertains to the major deliberations and results of that meeting and is divided into three
11 sections.

- 12
- 13 A. Scope and Agenda of Meeting on Quantitative Evaluation of Animal Toxicology Data for
14 Analyzing Cancer Risk due to Inhaled Formaldehyde. October 28 & 29, 2004.
 - 15
 - 16 B. Summary of Consultative Meeting on CIIT Formaldehyde Model. October 28 & 29,
17 2004.
 - 18
 - 19 C. Meeting Report from Dr. Rory B. Conolly

1 **A. Scope and Agenda of Meeting on Quantitative Evaluation of Animal Toxicology**
2 **Data for Analyzing Cancer Risk due to Inhaled Formaldehyde**
3 **October 28 & 29, 2004. Washington, DC.**

4
5 This meeting is to assist EPA in evaluating available approaches for incorporating biological
6 information in analyzing animal tumor data for assessing cancer risk due to inhaled
7 formaldehyde. The CIIT Centers for Health Research (CIIT) has published a novel risk
8 assessment that links site-specific predictions of flux using computational fluid dynamics (CFD)
9 modeling with a two-stage clonal growth model of cancer to analyze nasal tumor incidence in
10 two rodent bioassays. The rodent models are used with corresponding human models for low-
11 dose extrapolation of cancer risk to people.

12
13 Key predictions of the CIIT effort are a zero maximum likelihood estimate of the probability of
14 formaldehyde-induced mutation per cell generation in the rat and a *de minimus* additional
15 lifetime risk in non-smokers due to continuous environmental exposure below 0.2 ppm. The
16 National Center for Environmental Assessment is carrying out sensitivity analyses and
17 examining variations of the CIIT model in order to understand the implications of the model
18 structure and parameters on model predictions. In this meeting, we wish to focus on the
19 strengths and key uncertainties of this model, the extent to which assumptions in the CIIT model
20 are supported by biological data, and examine the impact of uncertainty and variability on the
21 overall quantitative risk characterization.

22
23 Broadly, the discussions will focus on the following areas:

- 24
25 • Impact of uncertainties in dosimetry on human risk estimates
26 • Uncertainties in the use of experimental data on labeling index
27 • The model structure related to initiated cells and DNA protein cross-links
28 • Considerations of time-to-tumor in the clonal growth modeling
29 • Inferences and information on the role of mutation and cytotoxicity in estimating human risk
30 • Relative merits of benchmark dose modeling vs. the 2-stage clonal growth model

31
32 Discussions on Mode of Action are expected to be an integral part of several of the sessions.
33 Therefore a specific time-slot is not set aside for this purpose.

34
35 The meeting will have a panel discussion format. There will be no formal presentations unless
36 necessary to elucidate an issue. Various attachments referred to in the Agenda below, as well as
37 the relevant manuscripts will be sent separately.

38
39 Specifically, we suggest the following issues upon which to focus the discussion in the above
40 areas, and approximate time frames and discussion leads, although discussants should feel free to
41 bring up other critical issues.

1 **I. Introduction and purpose of discussion**

2 Peter Preuss.

3 9:00 AM, Oct 28

4
5 **II. Impact of uncertainties in dosimetry on risk estimates**

6 *Lead discussant: Linda Hanna*

7 9:15 - 11 AM Oct 28

8
9 ***Boundary conditions***

10 The CFD modeling specified a mass transfer coefficient as a boundary condition on the
11 nasal lining, adjusting the value of this coefficient on the “absorbing” portion of the
12 lining so as to match simulated overall uptake in the rat nose to the experimentally
13 determined average overall uptake. This value was then used for the corresponding
14 human nasal lining. Are these boundary conditions appropriate surrogates for the
15 underlying pharmacokinetics, including saturation in metabolism and mucociliary
16 clearance, particularly with reference to humans?
17

18 ***Turbulence***

19 Turbulent flow has been seen to occur in experimental models of the human nose at some
20 of the higher flow rates at which the CFD models were used in CIIT=s assessment. It is
21 not likely that the CIIT CFD model can reliably identify signatures of transition to
22 turbulent behavior. Turbulent flow can significantly alter regional uptake patterns.
23 Additionally, significant mass balance errors were seen at the higher flow rates in the
24 human flow models. Discuss if these are likely to impact significantly on risk estimates.
25

26 ***Interindividual variability***

27 The CIIT assessment has focused on the nasal anatomy of a single individual. Discuss
28 the implications of interindividual variations in nasal anatomy on the population
29 distribution in risk.
30

31 **III. Uncertainties in the use of experimental data on labeling index**

32 *Lead discussant: George Lucier*

33 11AM – 11:45 AM, 1:00 - 3:15 PM Oct 28

34
35 Cell-replication rate and its relationship to flux is a critical determinant of risk. Therefore
36 uncertainties and variability in measurement of the unit length labeling index and its use in the
37 CIIT clonal growth modeling need to be characterized.
38

- 39 1. Discuss the strengths, uncertainties and limitations associated with estimating cell
40 replication rates from the unit length labeling index (ULLI).
41 a. For example, a constant ratio of the measured ULLI to the labeling index (LI) that
42 is used in the model is assumed. Is it valid to assume this ratio to be constant
43 across nasal sites, dose and exposure time.
44 b. How uncertain is this ratio?
45

This document is a draft for review purposes only and does not constitute Agency policy.

- 1 2. Considering the large patterns of variability in the ULLI data, discuss the validity of
2 using ULLI averaged over site and exposure times.
3 a. The averaging loses information on the sequential effect of change with
4 time, and on significant differences among sites.
5 b. How sensitive is the clonal growth modeling result to these variations in the dose-
6 response function for cell replication rates vs. flux to the tissue? A discussion of
7 this question in this session is intended to serve as input to later deliberations on
8 the issue.
9
- 10 3. Discuss the validity of combining data collected in different experiments using different
11 labeling methods, and the validity of estimating cell replication rates from LI or ULLI
12 measured in a single pulse labeling experiment.
13

14 *See attachment C: "ULLI Dose-Response Modeling and Statistical Analysis" for a*
15 *discussion of these issues, and Moolgavkar and Luebeck (1992).*
16

17 **IV. Model Structure: Birth and death rates for Initiated cells, Role of DPX**

18 *Lead discussant: Kenny Crump*

19 *3:30 - 6:00 PM Oct 28.*
20

21 ***Parameters for initiated cells***

22

- 23 1. The CIIT analysis of ULLI data allows for a virtual threshold in dose in the replication
24 rate of normal cells. Discuss the validity of ascribing such a behavior to initiated cells
25 considering the sensitivity of 2-stage model results to the initiated cell replication rates.
26
- 27 2. Discuss the treatment of death rate for initiated cells in the model (set equal to birth rate
28 of normal cells in Conolly et al., 2003) and implications for confidence in model
29 predictions.
30

31 *Also see Attachment A (memo from Rory Conolly) and Attachment D (EPA discussion of*
32 *CIIT clonal growth modeling and some sensitivity analyses. . .)*
33

34 ***Treatment of DNA protein cross-links (DPX) in clonal expansion model***

35

- 36 3. FORMALDEHDYE-INDUCED MUTATION IS MODELED AS TAKING
37 PLACE ONLY WHILE DPX ARE IN PLACE WITH DPX UNDERGOING
38 RAPID REPAIR. DISCUSS THE POSSIBILITY OF PERSISTENT GENETIC
39 DAMAGE THAT EXTENDS BEYOND THE DPX HALF-LIFE AND
40 ENHANCES MUTATION. HOW MIGHT THIS ISSUE BE INCLUDED IN
41 THE MODEL STRUCTURE?
42
43

This document is a draft for review purposes only and does not constitute Agency policy.

1 **V. Considerations of time-to-tumor in the CIIT clonal growth modeling**

2 *Lead discussant: Christopher Portier*

3 *8:30 – 11:00 AM, Oct 29.*

- 4
- 5 1. A number of issues affect likelihood values and the model fit to the time-to-tumor data.
- 6 Discuss assumptions in the treatment of time-to-tumor in the CIIT clonal expansion
- 7 model, and their impact on parameter estimates. For example,
- 8
- 9 a. Results in Conolly et al. (2003, 2004) are derived considering all tumors to be
- 10 fatal. Note in this context that serially sacrificed animals have been combined
- 11 with those experiencing mortality. The effect of this is visible as irregularities in
- 12 the time-to-tumor curve.
- 13
- 14 b. How is the time variability in ULLI likely to impact on the time-to-
- 15 tumor predictions?
- 16
- 17 2. Long delay times are predicted by the model for observation of detectable tumor. Is this
- 18 compatible with the assumption of rapidly fatal tumors?
- 19
- 20 3. Discuss the weight to be given to differences in likelihood when comparing with
- 21 variations on the Conolly et al (2003) model structure such as in Attachment A or D.
- 22

23 **VI. Inferences on the role of formaldehyde-induced mutation and cell proliferation**

24 *Lead discussant: Dale Hattis*

25 *11:15 – 12:00 PM, 1:00 – 4:00 PM, Oct 29.*

- 26
- 27 1. The model structure in Conolly et al. (2003) predicts a zero maximum likelihood estimate
- 28 for the constant of proportionality (KMU) linking DPX to the probability of
- 29 formaldehyde-induced mutation per cell generation. Examine the strength of this
- 30 conclusion, and the extent to which an insignificant probability of formaldehyde-induced
- 31 mutation per cell generation is supported by data.
- 32
- 33 2. Discuss the biological relevance and validity of model-estimated parameters, particularly
- 34 in the context of low-dose predictions.
- 35 a. Discuss possible avenues to validate CIIT cancer model predictions.
- 36
- 37 3. Discuss the validity of using cell replication rates determined for the rat to predict human
- 38 risk in a population.
- 39
- 40 4. In the face of uncertainties, are the results in Conolly et al. (2003, 2004) conservative in
- 41 the sense of overpredicting risk?
- 42 a. Discuss the extent to which sensitivity analyses have addressed this issue and the
- 43 extent to which sensitivity analyses can speak to the strength of the model. [*See*
- 44 *Attachments A: Memo from Conolly, and D: EPA discussion of CIIT clonal*
- 45 *growth modeling and some sensitivity analyses . . .].*
- 46

This document is a draft for review purposes only and does not constitute Agency policy.

1 **VII. Benchmark Dose Modeling**

2 *Lead discussant: Kenny Crump*

3 *4:15 – 5:30 PM, Oct 29.*

4

5 Discuss the relative merits of using a benchmark dose approach that incorporates
6 biological modeling (such as estimating flux to tissue or DPX levels) as compared with
7 the CIIT 2-stage model for cancer. (*See attachment E and Schlosser et al., 2003.*)

8

9

1 **B. Summary of Consultative Meeting on CIIT Formaldehyde Model**
2 **October 28 & 29 2004, NCEA, Washington, DC**

3
4 Date: November 10, 2004

5 Ravi P. Subramaniam, Ph.D.

6 Quantitative Risk Methods Group

7 National Center for Environmental Assessment, ORD, US EPA

8
9 This is a broad summary of the most important issues at the formaldehyde meeting.

10 It was generally felt by consultants that the broad framework of the approach adopted by
11 CIIT, namely the use of a two-stage model for cancer, the linking of localized flux to cell
12 replication rates and DPX concentration, and the expression of formaldehyde-induced mutation
13 as a linear function of DPX, was reasonable.

14 Potential errors in the dosimetry modeling were seen not to have a significant effect on
15 risk estimates. The boundary conditions used were discussed to be a reasonable representation
16 of the pharmacokinetics for both rats and humans. The discussion on the impact of
17 interindividual variability of nasal anatomy was not particularly conclusive. It was determined
18 that there was likely to be much less variability in reactive gas uptake than that seen in
19 particulates.

20 Crucial errors were however identified on several fronts in the manner in which the
21 clonal growth model had been implemented in the CIIT effort. Dr. Portier felt that the
22 calculation of probability was seriously flawed on account of lumping serially-sacrificed animals
23 and animals that died of tumor together, while at the same time assuming rapid fatality of all
24 tumors. This was seen to significantly alter the calculation of tumor probability (the shape of the
25 dose-response curve), and his insight was that a correction was likely to allow for a substantially
26 higher value for the probability of formaldehyde-induced mutation at low-dose. The best
27 estimate for this probability is now zero in the model. Drs. Crump, Portier and Hattis argued that
28 replacing this estimate by an upper confidence bound on KMU (the coefficient determining the
29 role of DPX in the probability of mutation per cell generation), keeping other structural problems
30 in the model unexplored, or other parameters fixed, would not be enough. There was a
31 discussion on the need to provide confidence bounds on risk determined by allowing all the
32 parameters to vary. Drs. Crump and Hattis (and Portier?) felt such an estimate would be very
33 different from that calculated based on individual parameters.

34 Drs. Crump, Hattis and Portier urged us not to be constrained by the optimal likelihood
35 values of a single plausible model, and underscored the need to explore a variety of biologically
36 reasonable model structures as a requisite for utilizing such a model in risk assessment.

This document is a draft for review purposes only and does not constitute Agency policy.

1 Likelihood was seen to be an inadequate expression of what is to be considered an optimal
2 model (okay only for comparing models that were nested, etc.). These models should allow the
3 expression of variability and uncertainty in the data, as well as in underlying assumptions in
4 model specification. Dr. Crump (and Hattis also?) felt that alternate model structures, if
5 explored, could potentially lead to risk estimates, for the range below the observed data, that
6 were higher by several thousands.

7 Dr. Crump cautioned that extrapolating to human using the hockey or J-shaped cell
8 replication curve used in the rodent carried with it a large uncertainty that had not been
9 characterized in the Conolly modeling.

10 Dr. Portier expressed concern over the manner in which historical and concurrent
11 controls were lumped together. The thrust of Portier's comments was that such a combination of
12 controls was generally not done. The large number of historical controls was likely to
13 significantly bias the impact of the bioassay data in determining the time-to-tumor fits.

14 There were various discussions about the pros and cons of constructing a joint likelihood
15 of the cell replication data and the tumor data, and the weights to be assigned to the separate
16 likelihoods. This was considered to be problematic by Dr. Portier.

17 Dr. Crump's opinion was that the Conolly model, and those explored by EPA, fit the
18 tumor data poorly, and that an improved description of the tumor data was needed before the
19 model could be used for low-dose and inter-species extrapolation.

20 Drs. Lucier and Hattis placed emphasis on including the early-time cell replication data
21 instead of constructing a time-weighted average. It was felt that the two Monticello experiments
22 could not be combined together as in Conolly et al. Dr. Lucier felt that the early-time data would
23 have a greater impact in the progression of carcinogenesis. In general, the effect of "time" was
24 considered to have significant effects on the time-to-tumor modeling, and they urged us to
25 incorporate time-dependent terms in the modeling. CIIT expressed willingness to provide the
26 original cell replication data to us for further analysis. (Further discussion on this matter did not
27 take place in the open forum.)

28 Preliminary indications are, particularly based on Dr. Portier's insight, that the currently-
29 held "de-minimus" picture of low-dose risk, as expressed in Conolly et al. (2004), is not likely to
30 be the case if these various suggestions are incorporated in the modeling.
31

1 **C. Meeting Report from Dr. Rory B. Conolly**

2
3 Rory B. Conolly, Sc.D., D.A.B.T.
4 106 Michael's Way
5 Chapel Hill, NC 27516
6 Voice: 919.929.2258
7

8 July 24, 2005
9

10 Dr. Bobette Norse
11 ORAU Procurement - MS-04
12 P.O. Box 117
13 Oak Ridge, TN 37831-0117
14 Phone: 865-576-3051
15 Fax: 865-576-9385
16

17 Dear Dr. Nourse,
18

19 The following is my final written report on the formaldehyde review meeting held at the
20 U.S. EPA in Washington, D.C. on 28-29 October, 2004.

21 EPA provided no guiding philosophical statement about the criteria being used to
22 evaluate the CIIT assessment. The new Guidelines for Carcinogen Assessment state that the
23 preferred default approach is to use a biologically based model. Since the key components of the
24 CIIT assessment have been published in the peer-reviewed literature and have undergone several
25 peer reviews other than the current NCEA effort, one has to wonder just how high the bar is set
26 for acceptance of biologically based assessments. Given the time and resources expended on the
27 CIIT assessment and the richness of the supporting data base, I find it difficult to imagine what
28 an acceptable biologically-based assessment might look like if in the end the CIIT assessment is
29 deemed not acceptable by NCEA. If this is in fact the outcome it will have major implications
30 for the likelihood that anyone will be willing to commit the significant resources needed to
31 develop of these kinds of risk assessment models.

32 The documents provided in advance of the October 2004 review meeting were
33 collectively a discussion of uncertainty about the CIIT work. With respect to the clonal growth
34 model, however, no new risk predictions were provided, so there was no way to judge how the
35 uncertainties that NCEA identified might impact predicted risk. Evaluation of the significance
36 of "uncertainties" when the impact of the uncertainties on the predicted risk is not known is itself
37 an uncertain process.

38 A related concern is that there did not seem to be any consideration of the historical
39 context of the CIIT assessment. EPA developed formaldehyde assessments in 1987 and 1991.
40 The 1987 assessment used ppm as the input and the LMS model for the dose-response
41 prediction. The 1991 assessment used DPX as a dosimeter and the LMS model. BMD
42 assessments have since become available from other sources such as Paul Schlosser's work. The
43 risk predictions of the BMD models are similar to the 1991 LMS assessment. Both the DPX-
44 LMS and BMD assessments predicted somewhat less risk than the 1987 assessment, establishing
45 the trend of less risk with increased incorporation of relevant data. I have always argued

This document is a draft for review purposes only and does not constitute Agency policy.

1 (probably initially at the 1998 Ottawa review) that the historical context is the appropriate
2 context for evaluating the CIIT clonal growth model. For a "level playing field" the
3 uncertainties of the 1987 and 1991 assessments, and of the more recent BMD models, should be
4 analyzed to the same degree as the clonal growth model. Does NCEA think that, because the
5 LMS and BMD approaches used structurally simpler dose-response models and much more
6 limited data inputs, they are less uncertain? The NCEA analysis seemed to be implying that use
7 of more data and of a biologically more realistic model structure actually makes the CIIT
8 approach more uncertain than the LMS and BMD approaches. I encourage NCEA to consider
9 how uncertainties that can be evaluated explicitly in the structurally rich CIIT model compare to
10 hidden uncertainties in the simpler models, where the hidden uncertainties encompass, for
11 example:

- 12
- 13 1. Missing or incomplete descriptions of the regional dosimetry of formaldehyde.
- 14 2. Lack of simultaneous incorporation of the directly mutagenic and
15 cytolethal/regenerative proliferation modes of action.
- 16 3. Lack of explicit consideration of the multistage nature of cancer.
- 17 4. Lack of consideration of the growth kinetics of initiated cell populations
- 18 5. Lack of evaluation of the measured J-shaped dose response for regenerative cellular
19 proliferation.
- 20

21 A careful, balanced comparison of the CIIT assessment with the previous assessments along
22 these lines would be informative with respect to the suitability of the CIIT assessment as the
23 basis for a new IRIS listing for formaldehyde.

24 A further concern involves the peer-review of the CIIT formaldehyde assessment held in
25 Ottawa in 1998. This review was sponsored by the U.S. EPA and Health Canada and involved
26 what was arguably a world-class review panel. The CIIT assessment was not in its final form at
27 that time, though we did provide a detailed description of the overall approach and the specific
28 methods we were using to generate dose-response predictions. The 1999 CIIT document and the
29 subsequent peer-reviewed publications are responsive to the comments and suggestions raised by
30 the reviewers. My concern is that no information was provided on the role that Ottawa review
31 plays in the ongoing review of the CIIT formaldehyde assessment by NCEA. Should the
32 October 2004 review be viewed as standing on the shoulders of the 1998 review or as being in
33 parallel to it? It was not at all clear to me that the October 2004 review in any way utilized the
34 judgments of the 1998 review. It seems that the 2004 review was more of a parallel effort and
35 that the 1998 review was ignored and was effectively a waste of time and money. I would like to
36 have some clear understanding of how the 2004 review effort should be viewed relative to that of
37 1998.

38 In closing, let me reiterate that while the detailed examination of the CIIT formaldehyde
39 assessment is laudable, this examination should be conducted with an eye to the historical context
40 of formaldehyde risk assessment on the one hand and, on the other hand, to a concern for
41 encouraging, and not discouraging, development of biologically based risk assessment models.

42
43 Sincerely yours,

44
45 Rory B. Conolly, Sc.D., D.A.B.T.

This document is a draft for review purposes only and does not constitute Agency policy.

- End of Volume IV -

This document is a draft for review purposes only and does not constitute Agency policy.

H-12 DRAFT—DO NOT CITE OR QUOTE